Universidade de Aveiro
Ano 2021

CATARINA MARÇAL CORREIA

(*E*)-2-ESTIRILCROMONAS – SÍNTESE E AVALIAÇÃO DOS EFEITOS INIBITÓRIOS NO *BURST* OXIDATIVO PRODUZIDO POR MONÓCITOS HUMANOS

(*E*)-2-STYRYLCHROMONES – SYNTHESIS AND EVALUATION OF THE INHIBITORY EFFECTS ON THE OXIDATIVE BURST PRODUCED BY HUMAN MONOCYTES

2021

Universidade de Aveiro
Ano 2021

CATARINA MARÇAL CORREIA

(*E*)-2-ESTIRILCROMONAS – SÍNTESE E AVALIAÇÃO DOS EFEITOS INIBITÓRIOS NO *BURST* OXIDATIVO PRODUZIDO POR MONÓCITOS HUMANOS

(*E*)-2-STYRYLCHROMONES – SYNTHESIS AND EVALUATION OF THE INHIBITORY EFFECTS ON THE OXIDATIVE BURST PRODUCED BY HUMAN MONOCYTES

Dissertação apresentada à Universidade de Aveiro para cumprimento dos requisitos necessários à obtenção do grau de Mestre em Bioquímica, com especialização em Bioquímica Clínica, realizada sob a orientação científica da Doutora Vera Lúcia Marques da Silva, Professora Auxiliar do Departamento de Química da Universidade de Aveiro e coorientação científica do Professor Doutor Artur Manuel Soares da Silva, Professor Catedrático do Departamento de Química da Universidade de Aveiro

Dedico esta dissertação aos meus pais, ao meu irmão, à minha tia, aos meus avós e a quem sempre acreditou em mim.

o júri

presidente

Professora Doutora Ana Maria Pissarra Coelho Gil
professora associada c/ agregação da Universidade de Aveiro

Doutora Marisa Andreia Carvalho de Freitas
investigadora auxiliar do Departamento de Ciências Químicas da Universidade do Porto

Professora Doutora Vera Lúcia Marques da Silva
professora auxiliar em regime laboral da Universidade de Aveiro

agradecimentos

À Doutora Vera L. M. Silva, orientadora desta dissertação, agradeço todo o apoio, dedicação e atenção prestados e acima de tudo, toda a compreensão e disponibilidade demonstrada ao longo deste percurso. Agradeço também por todos os ensinamentos, quer práticos quer teóricos, que me transmitiu ao longo deste tempo todo. Agradeço a confiança depositada em mim para o sucesso desta dissertação. Foi, sem dúvida, o apoio mais importante durante este percurso.

Ao Professor Doutor Artur M. S. Silva, coorientador desta dissertação, agradeço também o apoio, dedicação e orientação científica.

À Professora Eduarda Fernandes, à Doutora Marisa Freitas e a todos os colegas da Faculdade de Farmácia da Universidade do Porto, agradeço todo o apoio e disponibilidade prestados nos estudos biológicos apresentados nesta dissertação.

Ao Doutor Hilário Tavares e à Doutora Cristina Barros, agradeço por todo o contributo prestado na obtenção dos espetros de RMN e espetros de massa, respetivamente.

À Cátia, à Mónica, à Sónia, à Mariana e à Rita, agradeço toda a paciência e o incentivo que sempre me deram. Agradeço todas as palavras, todo o apoio e amizade. Foram um dos meus pilares neste percurso.

Agradeço ainda à Patrícia, à Sara, à Cláudia ao Ricardo, à Andreia, à Catarina, ao Luís e a todos os outros colegas do grupo de Química Orgânica com quem privei e que sempre foram prestáveis.

À Fundação para a Ciência e a Tecnologia, agradeço a bolsa de Investigação (PTDC/MED-QUI/29253/2017) que permitiu a realização deste trabalho.

À Universidade de Aveiro, agradeço a oportunidade de integrar esta academia, onde fui feliz durante estes 6 anos e da qual vou levar muitas aprendizagens.

Por fim, agradeço aos maiores pilares da minha vida: aos meus pais, ao meu irmão, à minha tia e aos meus avós por acreditarem sempre em mim, por todo o apoio, incentivo, disponibilidade e valores que me passaram e que fizeram com que chegasse até aqui; ao Pedro por ter estado sempre ao meu lado e nunca me deixar desistir.

palavras-chave

Stress oxidativo, inflamação, monócitos humanos, polifenóis, (*E*)-2-estirilcromonas, atividade antioxidante, atividade anti-inflamatória, *burst* oxidativo, citometria de fluxo

resumo

O aparecimento e progressão de várias doenças, incluindo doenças neurodegenerativas, cardiovasculares, envelhecimento celular e cancro, têm sido associados à produção de radicais livres assim como a processos inflamatórios, de acordo com vários estudos realizados. Por conseguinte, têm sido realizadas diversas investigações com a finalidade de encontrar novos fármacos com potencial antioxidante e anti-inflamatório, mais eficazes e seguros, e de compreender os seus mecanismos de ação. Atualmente, a avaliação da atividade antioxidante e/ou antirradicalar e anti-inflamatória de compostos polifenólicos, classe de compostos onde se incluem as 2-estirilcromonas, quer de origem natural quer sintéticos, é uma área de estudo de grande interesse.

Neste trabalho apresenta-se uma breve introdução sobre o stress oxidativo e a origem das espécies reativas de oxigénio e nitrogénio e sobre a inflamação e as células intervenientes neste processo, mais especificamente, acerca dos monócitos. Aborda-se a relação entre o processo inflamatório e o *burst* oxidativo produzido por monócitos humanos.

Os polifenóis, metabolitos secundários de várias plantas, são reconhecidos como uma fonte importante de flavonóides, incluindo 2-estirilcromonas, que têm demonstrado importantes atividades biológicas. Seguidamente são apresentados vários exemplos de (*E*)-2-estirilcromonas de origem natural e sintética e as atividades biológicas que lhes estão associadas, destacando-se as atividades antioxidantes e anti-inflamatórias. O grande foco deste trabalho reside no desenho e síntese de um painel de nove (*E*)-2-estirilcromonas e o seu efeito inibitório no burst oxidativo produzido por monócitos humanos e ainda o estudo da relação estrutura-atividade (SARS). Por fim, são descritos os métodos mais utilizados para a síntese de (*E*)-2-estirilcromonas contendo grupos substituintes relevantes para a sua atividade antioxidante e anti-inflamatória, nomeadamente grupos hidroxilo e halogéneos, assim como os métodos utilizados nos ensaios *in chemico* e *in vitro*.

keywords

Oxidative stress, inflammation, human monocytes, polyphenols, (*E*)-2-styrylchromones, antioxidant activity, anti-inflammatory activity, oxidative burst, flow cytometry

abstract

Several studies have attributed the onset and progression of several diseases, including degenerative and cardiovascular diseases, cell aging and cancer, to the production of free radicals and inflammatory processes. Consequently, a large number of investigations have been carried out in order to find new, safer and potent antioxidant and anti-inflammatory drugs, and to elucidate their corresponding mechanisms of action. The evaluation of antioxidant vs antiradicalar and anti-inflammatory activity of phenolic compounds, either of natural or synthetic origin, is nowadays an important area of research in the field of medicinal chemistry.

This work presents a brief introduction about oxidative stress and the origin of reactive oxygen and nitrogen species, and about inflammation and the cells involved in this process, specifically monocytes. The relationship between the inflammatory process and the oxidative burst produced by human monocytes is addressed.

Polyphenols, secondary metabolites of several plants, are recognized as an important source of flavonoids, including 2-styrylchromones, which have demonstrated important biological activities. Thus, several examples of (*E*)-2-styrylchromones of natural and synthetic origin and the biological activities associated with them are presented herein, with emphasis on antioxidant and anti-inflammatory activities. The major goal of this work relies on the design and synthesis of a library of nine (*E*)-2-styrylchromones and their inhibitory effects on the oxidative burst produced by human monocytes and the establishment of structure-activity relationship studies (SARS). At last, the most used methods for the synthesis of (*E*)-2-styrylchromones containing relevant substituent groups to their antioxidant and anti-inflammatory activity, namely hydroxyl and halogen groups, as well as the procedures for the *in chemico* and *in vitro* biological assays, are described.

Index

Abbreviations

δ	Chemical shift (ppm)
μ	Micro
μM	Micromolar
λ	Wavelength (nm)
η	Yield (%)
^{1}H NMR	Nuclear magnetic resonance spectroscopy of proton
4-PPy	4-Pyrrolidinopyridine
^{13}C NMR	Nuclear magnetic resonance spectroscopy of carbon-13
ABTS	2,2'-Azino-bis(3-ethylbenzothiazoline-6-sulfonic acid)
ATP	Adenosine triphosphate
CD14	Cluster of differentiation 14
CD16	Cluster of differentiation 16
d	Doublet
DAG	Diacylglycerol
DCC	*N,N'*-Dicyclohexylcarbodiimide
DCM	Dichloromethane
dd	Doublet of doublets
ddd	Doublet of doublets of doublets
ddt	Doublet of doublets of triplets
DHR	Dihydrorhodamine
DMSO	Dimethyl sulfoxide
DNA	Deoxyribonucleic acid
DPI	Diphenyleneiodonium chloride
DPPH	2,2-Diphenyl-1-picrylhydrazyl
EDTA	Ethylenediamine tetraacetic acid K3
equiv	Molar equivalent
Fc	Fragment crystallizable
FcγR	Fragment crystallizable gamma-receptor
FITC	Fluorescein isothiocyanate
FSC-A	Forward scatter
HIV	Human Immunodeficiency Virus
GI_{50}	Concentration causing 50 % cell growth inhibition
GPI	Glycosylphosphatidylinositol
IC_{50}	Half-maximal inhibitory concentration
IFNγ	Interferon-gamma
IgG	Immunoglobulin G

IUPAC	International Union of Pure and Applied Chemistry
J	Coupling constant (Hz)
M	Molar
m	Multiplet
MAPK	Mitogen-activated protein kinases
Me	Methyl
mM	Millimolar
MS	Mass Spectrometry
m.p	Melting point
m/z	Mass/charge ratio (mass spectrometry)
NADPH	Reduced nicotinamide adenine dinucleotide phosphate
NF-kB	Nuclear factor kappa-light-chain-enhancer of activated B cells
NMR	Nuclear Magnetic Resonance
NSAIDS	Non-steroidal anti-inflammatory drugs
NOS	Nitric oxide synthase
NOX	Nitric oxide oxidase
p-	*para*-
PBS	Dulbecco's phosphate buffer saline without calcium and magnesium ions
phox	Phagocytic oxidase
PI	Propidium iodine
PKC	Protein kinase C
PMA	Phorbol 12-myristate 13-acetate
PMNL	Polymorphonuclear leukocytes
ppm	Parts per million
PS	Phosphatidylserine
p-TSA	*p*-Toluenesulfonic acid
Rac1	Ras-related C3 botulinum toxic substrate 1
RCS	Reactive copper species
RIS	Reactive iron species
RNS	Reactive nitrogen species
ROS	Reactive oxygen species
RS	Reactive species
RSS	Reactive sulfur species
r.t	Room temperature
s	Singlet
SARS	Structure-activity relationship studies
SEM	Standard error of the mean

SNP	Sodium nitroprusside
SOD	Superoxide dismutase
SSC-A	Side scatter
t	Triplet
TLC	Thin-layer chromatography
TMS	Tetramethylsilane
UV	Ultraviolet
VIS	Visible
XO	Xanthine oxidase

General considerations

Structure of the dissertation

This dissertation is divided into six chapters. The first chapter, **Introduction**, describes the inflammatory process and the cells involved in it, highlighting monocytes, due to the aim of this work. The second chapter, **Synthesis and Structural Characterization of Target Compounds**, presents the description of the synthetic methods adopted to prepare the target compounds, their respective names according to the IUPAC nomenclature and their structural characterization with both 1D and 2D spectra. The third chapter, **Evaluation of the Biological Activity**, presents the methods used for the evaluation of the free radicals scavenging activity of the target compounds, in order to assess their potential as antioxidants. The results obtained in these studies are also presented and discussed. The fourth chapter, **Discussion and Conclusions**, presents the main conclusions of this work and future perspectives. The fifth chapter, **Experimental Section**, contains the detailed experimental procedures followed for the synthesis of the target compounds and the data of their structural characterization, as well as for the evaluation of their biological activities. The sixth chapter, **References**, includes all the references cited in this dissertation.

After the introduction, in **Chapter 1**, the numbering of compounds will start over at number 1 for sake of simplicity.

Chapter 1 - Introduction

1.1 Inflammation

Over the years, there have been several studies concerning the relationship between oxidative stress and inflammation. Both pathological conditions are related with several chronic diseases such as rheumatoid arthritis, cancer, diabetes mellitus, multiple sclerosis and Alzheimer's disease.[1,2]

Most authors defend that diseases which are linked to an increase of reactive oxygen species (ROS) production lead to oxidative stress and protein oxidation, initiating intracellular signaling cascades that promote proinflammatory gene expression and release of inflammatory signals, such as proinflammatory cytokines.[3–6] When it comes to neurological disorders, oxidative stress causes glycated products and lipid peroxidation, leading to neuroinflammation and cell death and, ultimately, neurodegeneration and memory loss, like in Alzheimer's disease.[1] However, the opposite process can also occur, since inflammation can lead to oxidative stress. When there is an inflammation in the body, several inflammatory cells are recruited to the inflammation site which can release different enzymes, reactive species and chemical mediators, for example lipases, superoxide anion radical and cytokines respectively, causing tissue damage and inducing oxidative stress.[7]

1.1.1 Historical perspective and definition

Along the time, different definitions have been suggested to explain the concept of inflammation. Celsus was the first person to list *rubor* (redness), *tumor* (swelling), *calor* (heat), and *dolor* (pain) as the first four main signals of this disease.[8–10] A fifth signal (loss of function) was yet considered in the nineteenth century however, there has never been a consensus on who has discovered this fact (**Figure 1**).[10,11] Also, during this time, a new definition was proposed for inflammation: a nonspecific physiological response of the body to an unknown damage in any tissue as a consequence of a harmful stimuli such as wounds, bacterial infections or pathogens, burns, damaged cells, toxic compounds or irradiation. In other words, inflammation has been understood as a biological process instead of a disease.[8,9,12,13] Later on, between the 1840s and 1860s, Augustus Waller and Julius Cohnheim observed a phenomena's cascade - i) vasodilation, which means the vascular permeability changes, leading to ii) leakage of plasma followed by iii) migration of leukocytes out of blood vessels into the surrounding tissue of the damage and release of some anti-inflammatory mediators, which was crucial to explain the physiological basis of all the signals previously detected.[9,14] In 1892, the discovery of the phagocytosis mechanism and phagocytic cells as well as the development of the Theory of Cellular Immunity, both by Elie Metchnikoff, were a turning point in the understanding of the inflammatory process.[15]

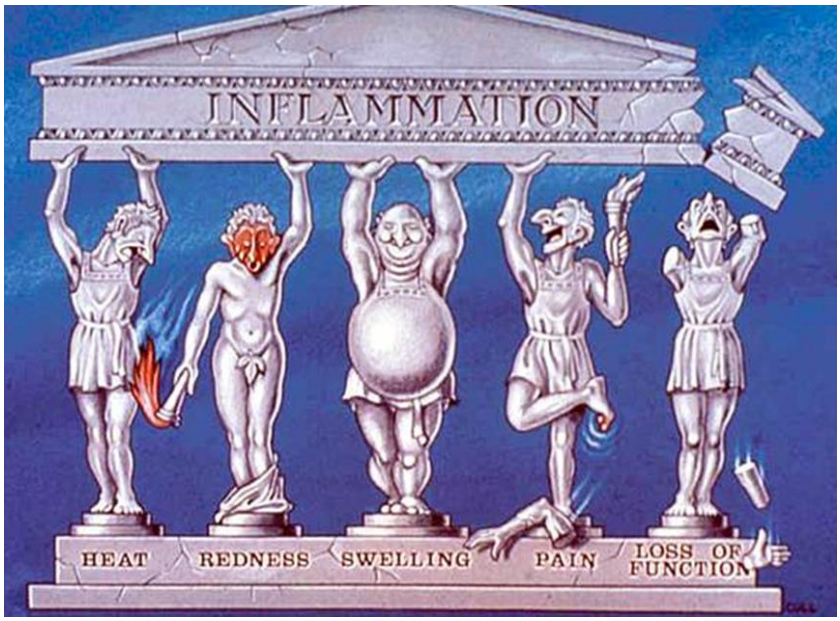

***Figure 1**. Schematic cartoon illustrative of the five cardinal signs of inflammation. Adapted from Laurence et al.*[10]

1.1.2 The inflammatory process

A certain type of white blood cells designated neutrophils, specifically macrophages and microphages, was found to play a major role both in defending the damaged organism and in maintaining the tissue homeostasis, considering their migration to the site of infection and the ability to phagocytize the foreign bacteria or bodies.[16,17] The process aforementioned is considered to be the physiological response to acute inflammation. The concept of chronic inflammation is used when the inflammation lasts for more than a few days, which can occur after an acute inflammation or associated with chronic diseases, such as rheumatoid arthritis. During this type of inflammation, the tissue damage and the processes to repair it coexist.[12] A handful of stimuli can lead to inflammation, including obesity, alcohol and chronic diseases and free radicals (**Figure 2**).[13]

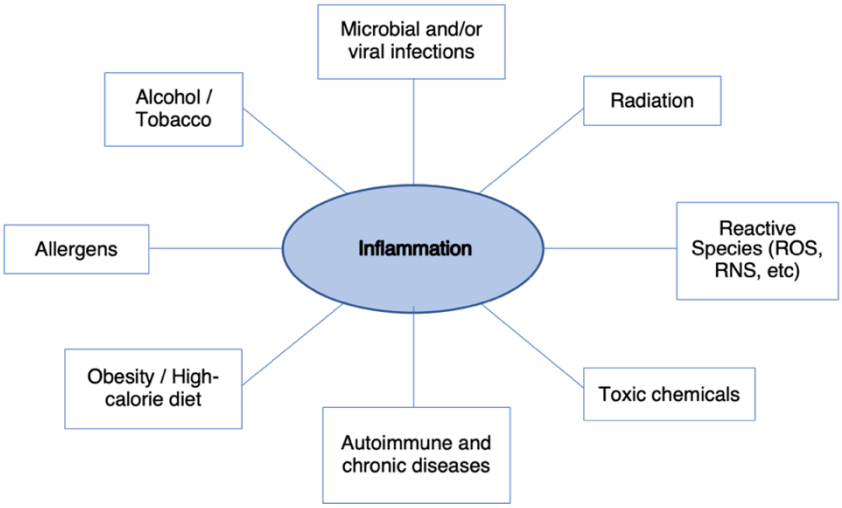

***Figure 2**. Stimuli that can lead to inflammation.*

1.1.3 Cells involved in the inflammatory process

During an inflammatory process, the activation and release of several mediators (**Figure 3**) is required to fight the inflammation and respond to the needs of the body. The first step requires mast cells, fibroblasts, and endothelial cells, promoting changes of the local adhesion molecules' profile, which leads to a chemotactic gradient.[12]

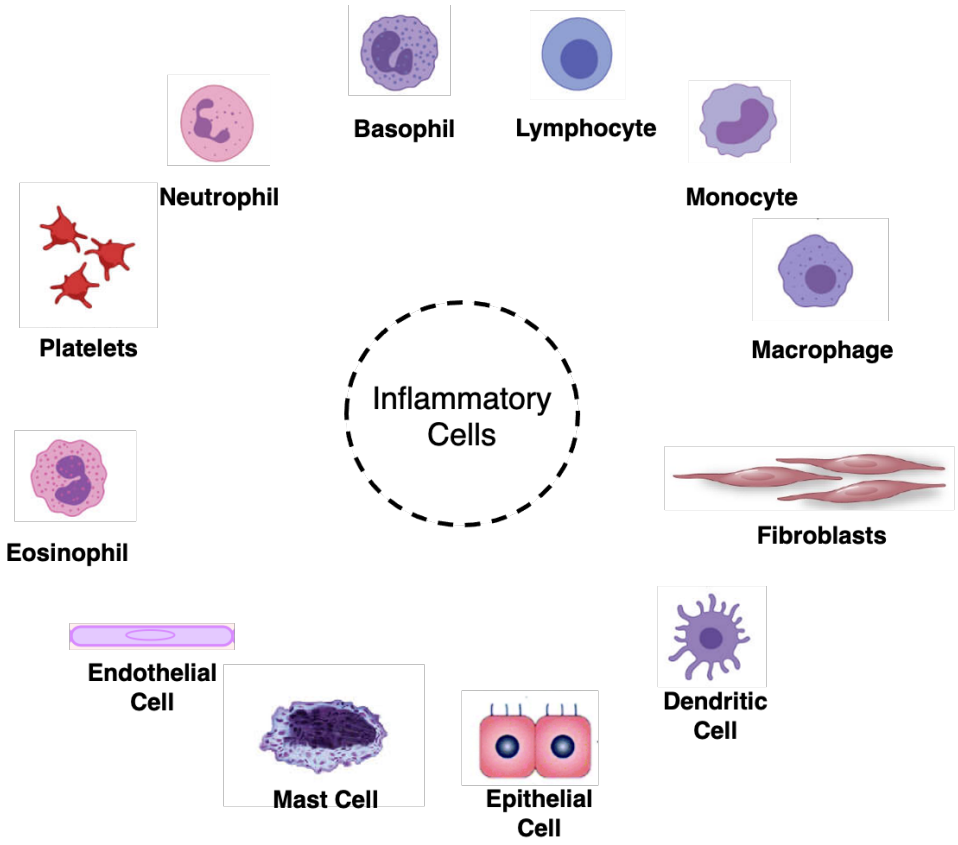

***Figure 3**. Cells involved in the inflammatory response. Adapted from Ribeiro et al.[12]*

Once this gradient is promoted, a large number of cells, namely leukocytes, are recruited from the blood stream. Leukocytes, commonly known as white blood cells, are divided into two groups, based on the presence or absence of granules inside the cell. As such, the group designated as granulocytes includes leukocytes with granules, such as neutrophils, eosinophils, and basophils. Contrariwise, the absence of granules leads to a group named agranulocytes in which lymphocytes and monocytes can be found. Furthermore, monocytes can differentiate into macrophages and dendritic cells, two major mediators in the inflammatory process as well (**Figure 4**).[12,18]

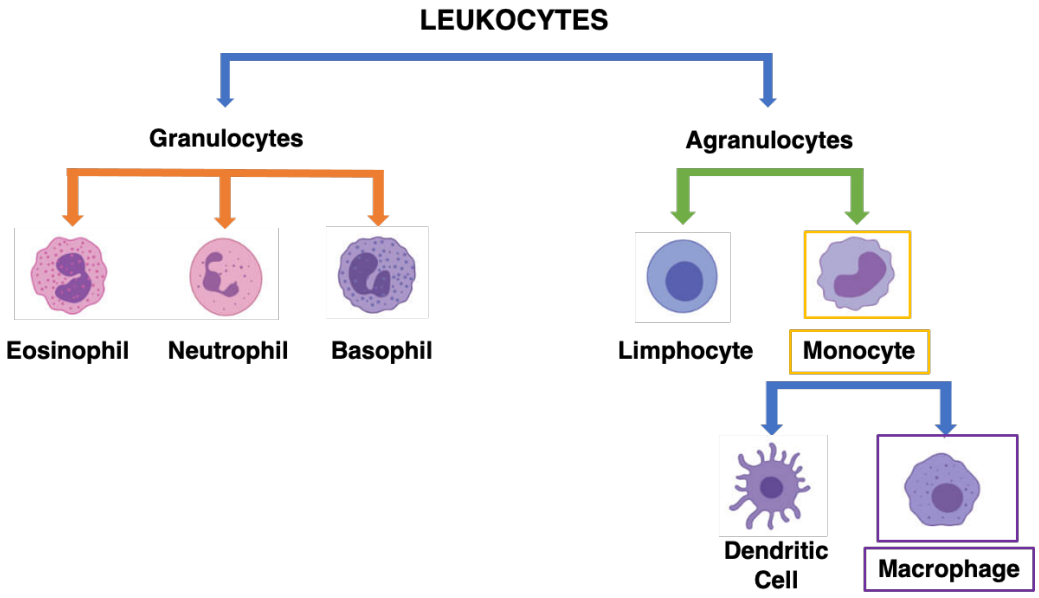

***Figure 4**. Types of leukocytes and differentiated cells from monocytes.*

Considering that monocytes are a huge part of this work, a deeper characterization of this type of cells will be done, as well as their role in inflammation.

1.2 Monocytes

Monocytes are heterogenous cells originated from hematopoietic progenitors in the bone marrow, specifically from promonocytes which in turn derive from the monoblast, a pluripotent stem cell (**Figure 5**).[19,20] These innate immune cells are a subtype of circulating leukocytes in the blood stream, being a crucial group of cells not only in the immune response during the invasion of pathogens and/or inflammation, but also in the maintenance of homeostasis and tissue repair.[21]

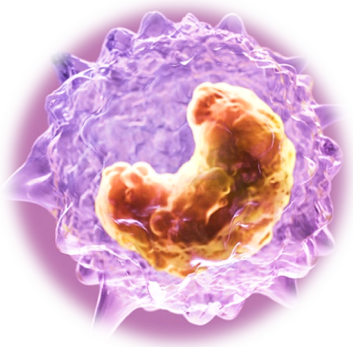

***Figure 5**. Tridimensional illustration of a monocyte.*

According to several studies, the identification of distinct populations of monocytes is based on CD14 and CD16 IFNγ expression.[20,22,23] CD14 is a lipopolysaccharide-binding protein, anchored to the cell surface by linkage to glycosylphosphatidylinositol (GPI), highly expressed (or positive) on

monocytes and most tissue macrophages but weakly expressed (or negative) in their precursors, monoblasts and promonocytes, while CD16 is a glycoprotein receptor expressed on the membrane of immune cells, designated fragment crystallizable receptor (FcγR) due to the fragment crystallizable (Fc) portion of IgG antibody molecules.[24,25] CD16 is a particular type of FcγR, since it is a GPI-linked receptor, lacking a cytoplasmic tail (FcγRIIIb/CD16b).[26–29] Regarding the human monocytes, these are classified into three subsets: classical monocytes ($CD14^{++}CD16^{-}$) without CD16 expression, intermediate monocytes ($CD14^{++}CD16^{+}$) considered as a transition from classical to non-classical, beginning to express low levels of CD16 marker, and non-classical monocytes ($CD14^{+}CD16^{++}$) with CD16 being highly expressed but also a small percentage of expression of the CD14 marker.[20,30] In addition, classical monocytes are called inflammatory monocytes because of their ability to infiltrate tissues and produce inflammatory cytokines.[31] Ziegler-Heitbrock *et al.* showed a relation between the populations of monocytes and their development during an infection, due to the observation of a first increase of intermediate monocytes, followed by an increase of non-classical monocytes.[20] Although it is not specified, it appears that the increase of CD16 marker's levels is linked to an inflammatory process, since intermediate and non-classical monocytes are the two populations where this glycoprotein receptor is expressed.

Monocytes' resting condition in the blood stream is altered in response to an activating stimulus, promoting monocytes' adherence to activated endothelial cells on the blood vessel wall and consequently the extravasation into the adjacent tissue. Once in the tissue, they differentiate into monocyte-derived macrophages, one more reason why the classical monocytes are known as the inflammatory population.[32,33] The process described above is known as the leukocyte recruitment cascade (**Figure 6**), which includes different steps: capture, rolling, adhesion, transmigration and macrophage differentiation.[34]

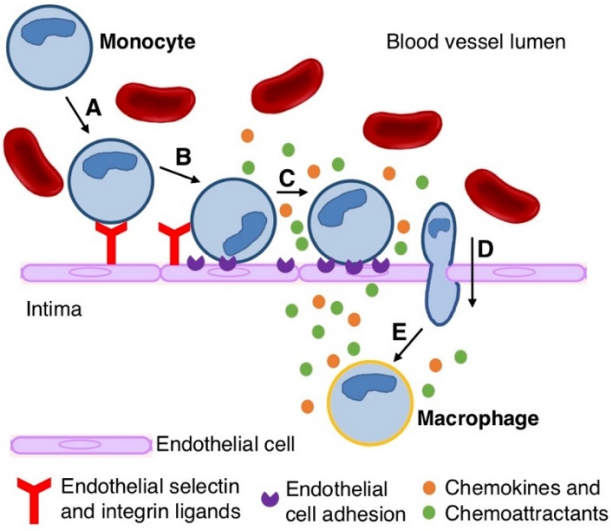

***Figure 6**. Schematic illustration of the leukocyte recruitment cascade. A) Capture, B) Rolling, C) Adhesion, D) Transmigration and E) Macrophage Differentiation. Adapted from Jones et al.[35]*

1.2.1 Production of reactive species by monocytes

Monocytes are key cells regarding the immune response of the body against pathogens, causing an oxidative burst when activated, a major feature in their action.[36] During this process and at the same time due to the oxidative phosphorylation of ATP in the mitochondria, large amounts of O_2 are consumed, leading to the formation of a very well-known reactive species, the superoxide anion radical ($O_2^{\bullet -}$). Among these highly unstable compounds, reactive oxygen species and reactive nitrogen species (RNS) are the most common types but there are also known some reactive iron species (RIS), reactive copper species (RCS) and reactive sulfur species (RSS), considering that there are radicalar and non-radicalar species with one or more unpaired valence electrons that oxidize cellular machinery (**Table 1**).[37–40]

Table 1. *ROS and RNS: examples of radicalar and non-radicalar species.*

	Radicalar	**Non-Radicalar**
Reactive oxygen species	Superoxide anion ($O_2^{\bullet -}$)	Hydrogen peroxide (H_2O_2)
	Hydroxyl ($^{\bullet}OH$)	Singlet oxygen ($^1O_2$)
	Peroxyl ($ROO^{\bullet}$)	Hypochlorous acid (HOCl)
Reactive nitrogen species	Nitric oxide ($^{\bullet}NO$)	Peroxynitrite anion ($ONOO^-$)
	Nitrogen dioxide ($^{\bullet}NO_2$)	Peroxynitrous acid (ONOOH)

ROS and RNS are a large group of key molecules in cell growth, cell signaling, smooth muscle relaxation, immune responses, synthesis of biological molecules and blood pressure modulation, derived from both enzymatic and non-enzymatic processes in cells.[41–44] Although these species play an important role as aforementioned, an abnormal increase in their production, which can occur during an inflammatory response, creates an imbalance in the pro-oxidant/antioxidant homeostasis, a physiological condition known as oxidative stress (**Figure 7**).[45] Furthermore, this imbalance can also result from a deficient antioxidant defense in the cellular system, a scenario also very likely to occur during inflammation. Oxidative stress causes modifications and damages in several biomolecules, for example proteins, lipids, DNA, and sugars and has also been found to play a major role in the development of diverse chronic diseases linked to chronic inflammation, such as cancer, neurodegenerative diseases (Alzheimer's and Parkinson's diseases), diabetes, chronic obstructive pulmonary disease, rheumatoid arthritis and cardiovascular diseases.[2,46–54]

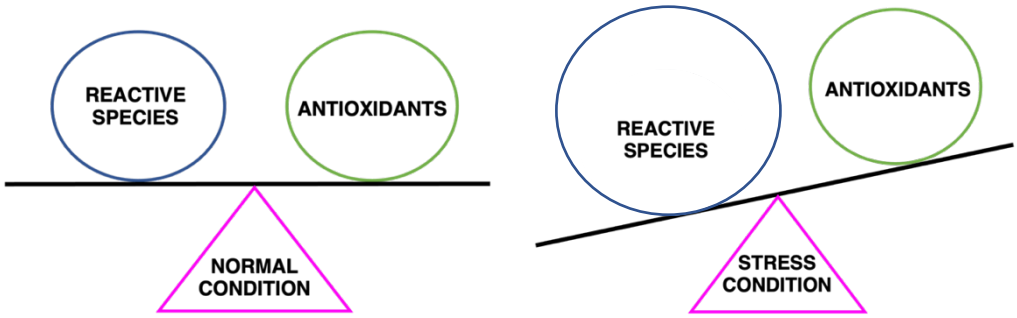

***Figure 7**. Schematic representation of normal and oxidative stress conditions.*

Although being a relatively unreactive radical, the superoxide radical anion can also be potentially dangerous, and it is the main precursor of many other ROS.

Singlet oxygen ($^1O_2$), a highly reactive form of O_2, can be produced *in vivo* by a range of peroxidase enzymes, for example lactoperoxidase.[55] The peroxyl radical ($HOO^\bullet$) is the protonated form of $O_2^{\bullet-}$ and has a role in fatty acid peroxidation.[56] $O_2^{\bullet-}$ can be converted into hydrogen peroxide (H_2O_2) by some enzymes such as superoxide dismutase (SOD) and xanthine oxide reductase.[57] Although H_2O_2 is not a free radical, this molecule can diffuse through the membranes and is crucial for the formation of the hydroxyl radical ($^\bullet OH$), the most reactive species of all.[37,58]

The production of $^\bullet OH$ from H_2O_2 can occur by the Haber–Weiss reaction, which combines the reduction of Fe^{3+} by $O_2^{\bullet-}$ and a Fenton reaction (**Scheme 1**).[37]

Haber-Weiss Reaction

$$O_2^{\bullet-} + Fe^{3+} \longrightarrow Fe^{2+} + O_2 \quad \text{(Reduction of iron)}$$

$$H_2O_2 + Fe^{2+} \longrightarrow Fe^{3+} + OH^- + {}^\bullet OH \quad \text{(Fenton reaction)}$$

$$\text{Net reaction: } H_2O_2 + O_2^{\bullet-} \longrightarrow O_2 + OH^- + {}^\bullet OH$$

***Scheme 1**. Production of hydroxyl radicals by the Haber-Weiss reaction.*

When it comes to RNS, the most known is nitric oxide ($NO^\bullet$), produced by nitric oxide synthase (NOS) in tissues, and it has a “double effect”. When its concentration increases, it promotes enzyme function inhibition, DNA damage and can react with $O_2^{\bullet-}$ to produce the peroxynitrite anion ($ONOO^-$), a strong oxidant, leading to more damages caused by oxidative stress (**Scheme 2**).[37,59] However, when there is a redox balance, it plays a crucial role on different processes like vascular permeability and inhibition of platelet adhesion, being even considered as anti-inflammatory.[59]

$$NO^\bullet + O_2^{\bullet-} \longrightarrow ONOO^-$$

***Scheme 2**. Production of peroxynitrite anion.*

Considering that most of the aforementioned RS are produced by the superoxide anion, it is important to understand how these reactions work, especially in monocytes.

The superoxide anion is produced through a reaction mediated by the NADPH oxidase complex, which is unassembled in resting human monocytes.[60] This enzymatic complex is constituted by several subunits: a Ras-related C3 botulinum toxic substrate 1 (Rac1) and three phagocytic oxidases (phox) subunits, namely polypeptides $p40^{phox}$, $p47^{phox}$, $p67^{phox}$, which are located in the cytoplasm, whereas in the membrane there is only the cytochrome *b*558, constituted by a glycoprotein ($gp91^{phox}$) and another polypeptide designated $p22^{phox}$. Upon activation of monocytes by a stimulus, the cytosolic components $p40^{phox}$, $p47^{phox}$, $p67^{phox}$ and Rac1 translocate to the membrane where the association with the cytochrome *b*558 occurs (**Figure 8**).[33,61] The activation and consequent assembling of the NADPH oxidase complex occurs through a major three-step process, involving different proteins, enzymes and other factors, as follows:

1) **phosphorylation of NADPH subunits**: the stimulation of phospholipases induces the production of diacylglycerol (DAG), which consequently activates protein kinase C (PKC). Then, PKC is responsible for the phosphorylation of the NADPH enzyme, which leads to the first interaction between p47phox subunit with cytochrome b558;

2) **translocation of the other cytosolic subunits to the membrane**: once the first step occurs, the cytosolic subunits move to the membrane, where they bind to cytochrome b558, forming a single membrane-associated complex;

3) **activation of Rac1**: the activation of Rac1 and its consequent translocation to the previously assembled complex, forming at last a functional complex responsible for the production of RS (**Figure 8**).[12,33]

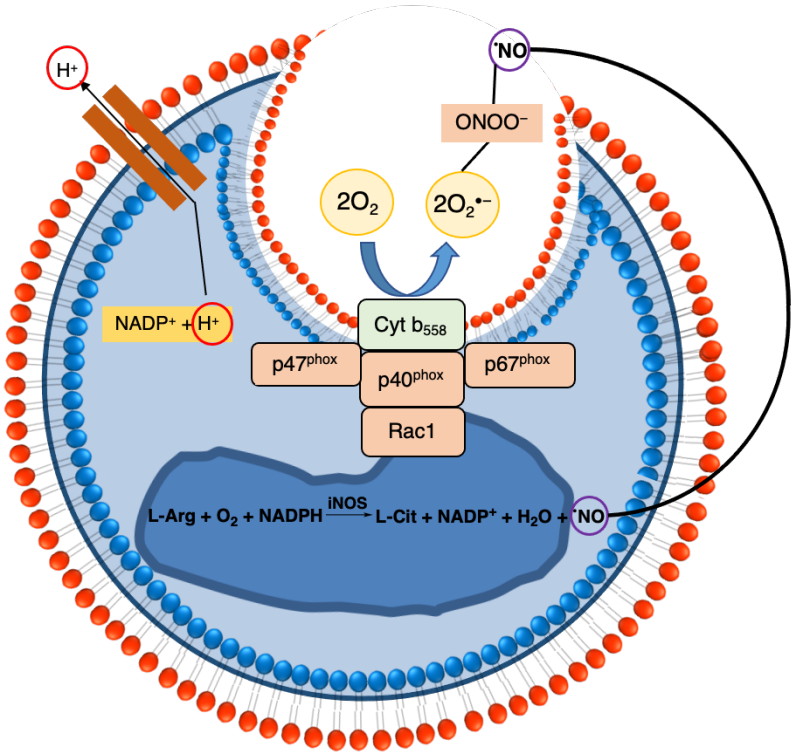

***Figure 8**. Activation and assembling of NADPH oxidase complex in the cell membrane.*

1.3 Drugs for prevention of oxidative stress and inflammation

Based on the cellular and molecular pathways involved in the progression of oxidative stress and inflammation, these pathological conditions can be ameliorated and eventually treated with pure compounds.

Currently, several therapeutic drugs with antioxidant and anti-inflammatory potential are used to lighten some symptoms or even for the treatment of some pathological conditions. The most used drug is Aspirin, which the active principle is acetylsalicylic acid, is a very well-known anti-inflammatory drug which inhibits COX-1 and COX-2, enzymes responsible for the production of prostaglandins and thromboxane, both inflammatory mediators.[62] Also, for the inhibition of COX-2 and, consequently, of prostaglandins, the use of immunosuppressors and non-steroidal anti-inflammatory drugs (NSAIDS) such as Sulfasalazine is very common.[62,63] This drug can also reduce oxidative stress in some conditions.[64] The therapeutic agents aforementioned are considered to be safe and effective however, there are also drugs with more side effects, which is the case of glucocorticoids.[62] Daflon is also an anti-inflammatory drug, which has the ability to scavenge free radicals, and just like Sulfasalazine, is a polyphenolic compound.[65] (**Figure 9**).

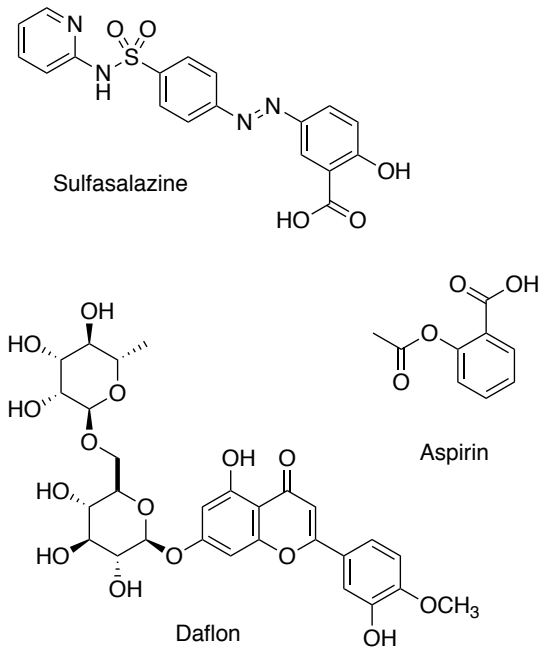

***Figure 9**. Commercially available anti-inflammatory drugs.*

Nevertheless, the search and development of new, safer, and more effective therapeutic drugs with antioxidant and anti-inflammatory properties is ongoing

These commercially available drugs and their main targets brings to our attention that some inflammatory pathways have not been deeply studied as they should, which is a great encouragement for the understanding of the monocyte-related pathways and all the RS and factors involved in it.

1.4 Polyphenols

Polyphenols are naturally occurring secondary metabolites which are present not only in vegetables and fruits, like grapes and apples, but also in cereals, beverages and even chocolate.[66,67] These polyphenolic compounds are divided into four main groups, being one of them flavonoids. Some well-known flavonoids such as quercetin, apigenin, kaempferol and luteolin have shown to have diverse biological activities like anticancer and antiviral activities. Furthermore, it has been reported that polyphenols are good antioxidant and anti-inflammatory agents, since they have demonstrated strong ability as free radicals scavengers and ability to modulate the inflammatory processes.[68]

In this line of thought, the search for new flavonoid-type compounds with antioxidant and anti-inflammatory activities as well as their mechanisms of action has been a major field of study.

1.4.1 Chromones and (*E*)-2-styrylchromones

Chromones (**A**), also known as 4*H*-chromen-4-ones or 1,4-benzopyrones, are oxygen-containing heterocyclic compounds widespread in nature. The interest in this type of compounds has been increasing due to their well-known biological activities and pharmacological properties.[69–71]

Although scarce in nature, (*E*)-2-styrylchromones [(*E*)-2-styryl-4*H*-chromen-4-ones, according to the IUPAC nomenclature] are a well-recognized class of chromones, whose major structural feature is the presence of a styryl group appended at C-2 of the chromone core structure (**Figure 10**).[72–75] The styryl group (**B**) improves molecular stability and consequently increases these derivatives' antiradical activity. Moreover, the distinct double bond system makes these vinylogues of flavones a very reactive group of molecules.[72,76,77]

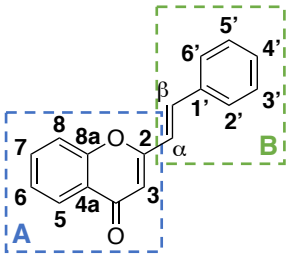

***Figure 10**. Structure of (E)-2-styrylchromone, the chromone core (**A**) and the styryl group (**B**).*

As mentioned before, (*E*)-2-styrylchromones are scarce in nature. Since the first one, hormothamnione (**1**), was discovered in 1986, eight others were found to occur naturally in plants or algae. These nine natural (*E*)-2-styrylchromones (**1**-**9**), which present mostly methoxy and hydroxy groups on their structures, are represented in **Figure 11**.

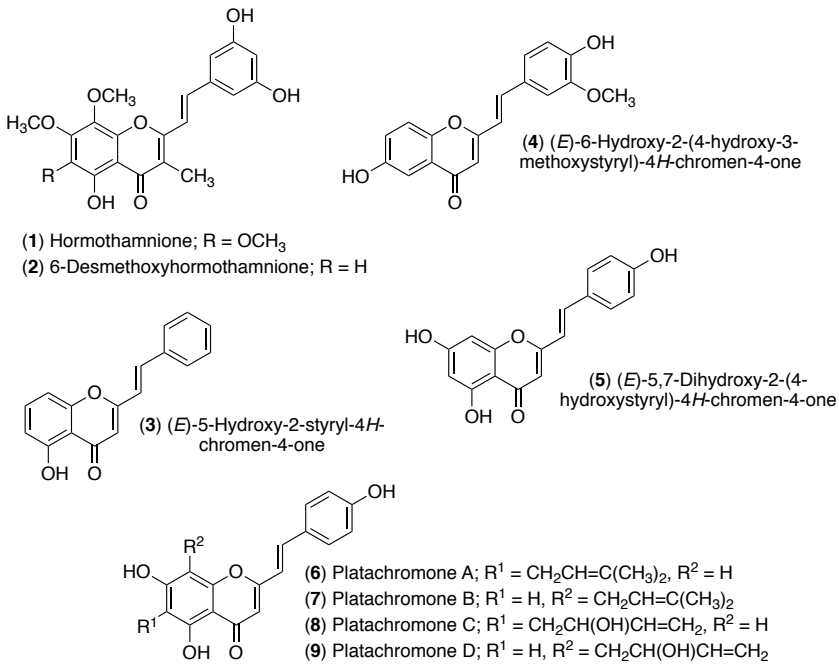

***Figure 11**. Structures and respective nomenclature of natural (E)-2-styrylchromones **1**-**9**.*

The interest in (*E*)-2-styrylchromones has been increasing in the last years due to their biological activities and the therapeutic benefits they have demonstrated, particularly in chronic and neurodegenerative diseases, which led to the synthesis of new (*E*)-2-styrylchromones (**Figure 12**). These type of compounds also showed antioxidant/radical scavenging,[55,78–80] anti-inflammatory,[81] hepatoprotective,[79] neuroprotective,[82–84] anti-HIV,[85,86] antiviral (in particular anti-norovirus[73] and anti-rhinovirus[87–89]),[87] antitumor/anticancer,[90–93] antiallergic[94] and antimicrobial[95] activities and are also inhibitors of enzymes such as xanthine oxidase[96] and antagonists of A3 adenosine receptors.[97]

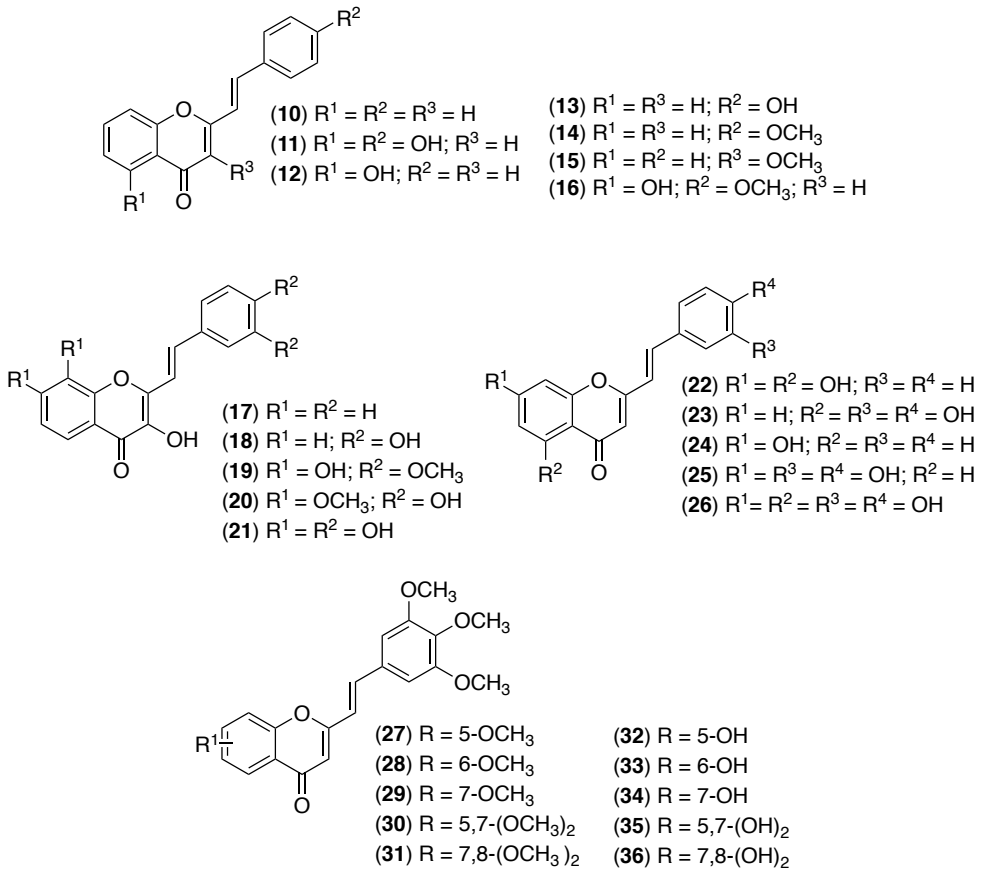

***Figure 12**. Structures of several synthetic (E)-2-styrylchromones **10**-**36** with biological interest.*

1.5 Biological activities of (*E*)-2-styrylchromones

The first-discovered (*E*)-2-styrylchromone, hormothamnione (**1**), has proved to have cytotoxic activity against P388 lymphocytic leukemia and HL-60 human promyelocytic leukemia.[98] Its natural derivative, 6-desmethoxyhormothamnione (**2**), has also shown the same type of biological activity but against nine different KERATIN-forming tumor cell lines HeLa (KB cell lines).[99] (*E*)-6-Hydroxy-2-(4-hydroxy-3-methoxystyryl)chromone (**4**) demonstrated moderate neuroprotective activity, at 10.0 μM concentration, when tested against glutamate-induced neurotoxicity in P12 pheochromocytoma cells (58.3 ± 2.8 %) when compared with the standard fluoxetine (92.5 ± 3.2 %). However, when tested against corticosterone-induced neurotoxicity in human U251 glioma cells, the

(*E*)-6-hydroxy-2-(4-hydroxy-3-methoxystyryl)chromone (**4**) showed no activity.[95] In addition, the two others, (*E*)-5-hydroxy-2-styrylchromone (**3**) and (*E*)-5,7-dihydroxy-2-(4-hydroxystyryl)chromone (**5**) are anti-inflammatory compounds that inhibit the NF-kB signaling pathway and, consequently, reduce the production of proinflammatory cytokines and chemokines, being the second the most active.[81] Also, (*E*)-5-hydroxy-2-styrylchromone (**3**) has antimicrobial activity, in particular anti-norovirus activity, with an IC_{50} value around 7.0 μM, which was more active than (*E*)-2-styrylchromone (**10**).[73] This suggests that the hydroxy group at C-5 plays an important role in anti-norovirus activity. Platachromones A-D (**6** to **9**) possess cytotoxic activity with IC_{50} values between 3.0 and 9.7 μM against two human carcinoma cell lines: HepG2 (human hepatocarcinoma cell line) and KB (human epidermoid carcinoma cell line). However, all these compounds were less active than taxol (IC_{50} = 0.04 - 0.05 μM), used as positive control. When tested in another human hepatocarcinoma cell line (SMMC-7721), the IC_{50} values were much higher (IC_{50} = 14.6 - 21.3 μM), showing that the platachromones A-D are less sensitive to this cell line, as well as MDA-MB-231 (human breast cancer cell line), with IC_{50} values of 8.7 - 22.3 μM (**Table 2**).[100]

When it comes to synthetic (*E*)-2-styrylchromones, compounds **10** and **16** have demonstrated antioxidant activity in the DPPH assay, being compound **16** the most active (71.11% of inhibition). Although having shown significant activity, it is not possible to compare the results since no value was presented for the positive control, ascorbic acid.[72] Compounds **19**-**21** were also tested for antioxidant activity in several radical scavenging assays. The positive control used was always quercetin and for the superoxide anion radical ($O_2^{\bullet -}$) assay, compound **21** showed the highest activity (IC_{50} = 30.0 ± 1.0 μM), being much more active than the control (IC_{50} = 67.0 ± 7.0 μM). For the hypochlorous acid (HOCl) assay, none of the compounds were more active than quercetin and for the singlet oxygen ($^1O_2$) the results (IC_{50} = 1.0 ± 0.1 - 1.2 ± 0.2 μM) were very similar to the control (IC_{50} = 1.3 ± 0.1 μM), although a little more active. For the hydrogen peroxide (H_2O_2) assay, none of the compounds showed activity at the highest concentration tested (1000.0 μM). In the nitric oxide radical ($NO^{\bullet}$) assay, compounds **19**-**21** showed promising radical scavenging activity since all the compounds presented IC_{50} values lower than quercetin (IC_{50} = 1.3 ± 0.1 μM), being compound **21** the most active (IC_{50} = 0.67 ± 0.08 μM).[78] Compounds **5**, **10**-**13**, **18** and **22**-**26** were tested for their ability to inhibit the NF-kB activation and to reduce the production of proinflammatory cytokines/chemokines, being the natural (*E*)-5,7-dihydroxy-2-(4-hydroxystyryl)chromone (**5**) the most active.[81] Just like (*E*)-5-hydroxy-2-styrylchromone (**3**), compounds **13**-**15** and **17** were also screened for anti-norovirus activity but none of these compounds showed better results than the unsubstituted (*E*)-2-styrylchromone [(*E*)-2-styryl-4*H*-chromen-4-one]. The growth inhibition activity of compounds **27**-**31** and **32**-**36** was tested on carcinoma cells, particularly on gastric carcinoma cells. The polymethoxy-(*E*)-2-styrylchromones **27**-**31** demonstrated to be much more active than their hydroxylated counterparts **32**-**36**. The (*E*)-5-methoxy-2-(3,4,5-trimethoxystyryl)chromone (**27**) was the most effective, with an GI_{50} value of 1.3 μM.[75] The results regarding the hydroxy-substituted

(*E*)-2-styrylchromones **32**-**36** might be due to the alteration of physical properties, particularly loss of hydrophobicity for appropriate cell membrane penetration, since these compounds are more hydrophilic and have less affinity for the membranes (**Table 3**).[75]

As demonstrated above, different substituents can lead to alterations of the pharmacological properties of the compounds and, consequently, interfere with their activity. For this reason, researchers put a lot of effort on the design and synthesis of new (*E*)-2-styrylchromones as well as on structure-activity relationship studies (SARS), in order to discover compounds with improved activity and safer, with less secondary effects.

Table 2. *Natural (E)-2-styrylchromones and their biological activities and targets.*

Biological Activity	Biological Target(s)	Compound	Ref(s)
Cytotoxic	P388 lymphocytic leukemia	Hormothamnione (**1**)	98,99
	HL-60 human promyelocytic leukemia		
	KERATIN-forming tumor cell lines HeLa	6-Desmethoxyhormothamnione (**2**)	98,99
	HepG2 (human hepatocarcinoma cell line)	Platachromone A (**6**)	81,100
		Platachromone B (**7**)	81,100
		Platachromone C (**8**)	81,100
		Platachromone D (**9**)	81,100
	KB (human epidermoid carcinoma cell line)	Platachromone A (**6**)	81,100
		Platachromone B (**7**)	81,100
		Platachromone C (**8**)	81,100
		Platachromone D (**9**)	81,100
	Human hepatocarcinoma cell line (SMMC-7721)	Platachromone A (**6**)	81,100
		Platachromone B (**7**)	81,100
		Platachromone C (**8**)	81,100
		Platachromone D (**9**)	81,100
Anti-norovirus	----------	(*E*)-5-Hydroxy-2-styrylchromone (**3**)	73
Anti-inflammatory	NF-kB signaling pathway	(*E*)-5-Hydroxy-2-styrylchromone (**3**)	81
		(*E*)-5,7-Dihydroxy-2-(4-hydroxystyryl)chromone (**5**)	95
Neuroprotective	P12 pheochromocytoma cells	(*E*)-6-Hydroxy-2-(4-hydroxy-3-methoxystyryl)chromone (**4**)	81

Table 3. *(E)-2-styrylchromones, analogues of natural derivatives, and their biological activities and targets.*

Biological Activity	Biological Target(s)	Compound(s)	Most active compound	Ref(s)
Anti-inflammatory	NF-kB signaling pathway Proinflammatory cytokines/chemokines	(**5**), (**10**), (**11**), (**12**), (**13**), (**18**), (**22**), (**23**), (**24**), (**25**) and (**26**)	(**5**)	
Antioxidant Radical Scavenging	DPPH$^{\bullet}$	(**10**) and (**16**)	(**16**)	78
	Superoxide Anion Radical ($O_2^{\bullet-}$)	(**19**), (**20**) and (**21**)	(**21**)	
	Singlet Oxygen ($^1O_2$)	(**19**), (**20**) and (**21**)	-----	
	Nitric Oxide Radical ($^{\bullet}$NO)	(**19**), (**20**) and (**21**)	(**21**)	
Antiviral	Anti-norovirus	(**13**), (**14**), (**15**) and (**17**)	-----	81
Antitumor	Gastric Carcinoma Cells	(**27**), (**28**), (**29**), (**30**), (**31**), (**32**), (**33**), (**34**), (**35**) and (**36**)	(**27**)	75

1.6 Objective of this work

The main goal of this dissertation is the synthesis of (*E*)-2-styrylchromones and evaluation of their potential inhibitory effects on the oxidative burst produced by human monocytes (**Scheme 3**).

This goal is expected to be achieved through the accomplishment of some more specific goals, which are:

1) the synthesis of a library of (*E*)-2-styrylchromones for biological studies;

2) the structural characterization of the synthesized compounds by nuclear magnetic resonance spectroscopy (NMR) and mass spectrometry techniques;

3) the biological evaluation of the obtained (*E*)-2-styrylchromones both *in chemico* and *in vitro.* These studies will involve:

a) the determination of the •NO scavenging ability of each (*E*)-2-styrylchromone;

b) the determination of the absorption and emission spectra of each (*E*)-2-styrylchromone in study;

c) the determination of the maximum non-cytotoxic concentration of each compound in human monocytes, in order to evaluate the cells' viability when exposed to the compounds;

d) the determination of the inhibitory effects of the (*E*)-2-styrylchromones in study in the oxidative burst on human monocytes;

4) the establishment of structure-activity relationships studies (SARS) to get insights for the design of novel derivatives with improved action.

It is noteworthy that these compounds were never studied on human monocytes, so these preliminary studies, on this type of cells, will be very important for further investigations in this chemical-pharmacological field.

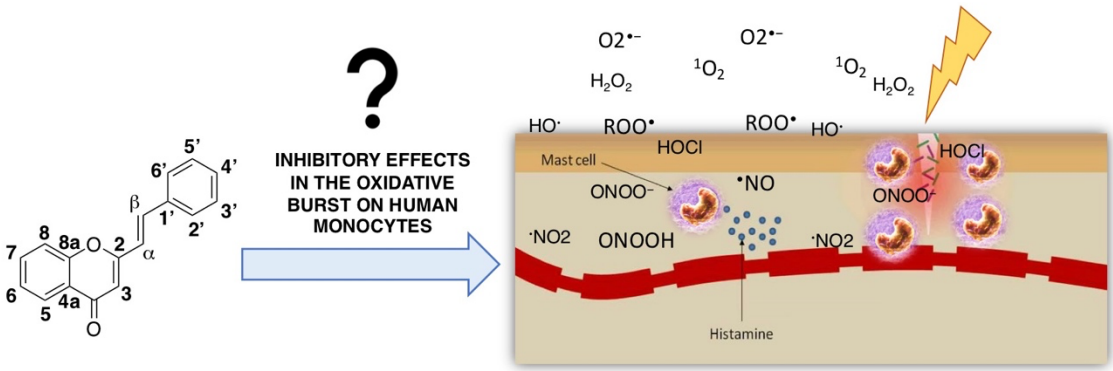

***Scheme 3**. Graphical abstract regarding the main goal of this work.*

Chapter 2 - Synthesis and Structural Characterization of (*E*)-2-Styrylchromones

2.1 Synthesis

In this section, will be presented a brief description of the methods used to prepare the target compounds of this work. The fully detailed experimental protocols as well as the NMR data of each compound may be consulted in **Chapter 5** – **Experimental Section**.

2.1.1 Methylation of the starting compounds

The synthesis of polyhydroxylated compounds, often required the protection of the hydroxy groups of the starting compounds. In this work, those protections were performed by methylation reactions.

2.1.1.1 Methylation of acetophenones

In this work, the hydroxy groups of the starting compounds 1-(2,6-dihydroxyphenyl)ethan-1-one (**1**) and 1-(2,4,6-trihydroxyphenyl)ethan-1-one (**3**), also known as 2',6'-dihydroxyacetophenone and 2',4',6'-trihydroxyacetophenone, were protected by methylation using dimethyl sulfate in the presence of potassium carbonate as base, in refluxing acetone for 1-3 h (**Scheme 4**). The protected acetophenones 1-(2-hydroxy-6-methoxyphenyl)ethan-1-one (**2**) and 1-(2-hydroxy-4,6-dimethoxyphenyl)ethan-1-one (**4**), also known as 2'-hydroxy-6'-methoxyacetophenone and 2'-hydroxy-4',6'-dimethoxyacetophenone, were obtained in good to very good yields (67-83%).

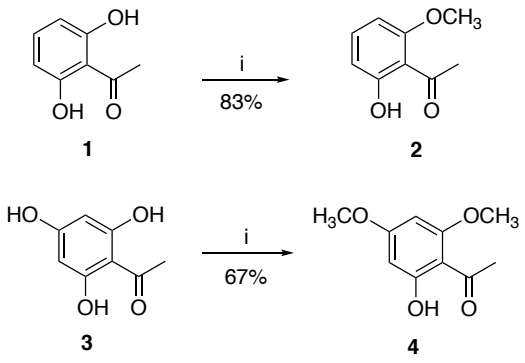

i) $(CH_3)_2SO_4$, K_2CO_3, Acetone, reflux, 1-3h

***Scheme 4**. Methylation of 1-(2,6-dihydroxy)acetophenone (**1**) and 1-(2,4,6-trihydroxy)acetophenone (**3**).*

2.1.2 Synthesis of (*E*)-2-styrylchromones

Three different methods were considered and attempted for the synthesis of (*E*)-2-styrylchromones, which will be described in detail in the following sections.

2.1.2.1 Method 1: Baker-Venkataraman rearrangement

This method involved the *O*-acylation of 2'-hydroxyacetophenones (**5**) with previously protected cinnamic acids **6a-b** in the presence of *N*,*N*′-dicyclohexylcarbodiimide (DCC) and 4-

pyrrolidinopyridine (4-PPy) in dichloromethane (DCM), at room temperature, for 7 days. The reaction afforded the expected 2-acetylphenyl acrylates **7a-b** in low yields but since the 2-acetylphenyl-(*E*)-3-(2-methoxyphenyl)acrylate (**7b**) was obtained in vestigial amounts, the next steps were only done for the 2-acetylphenyl-(*E*)-3-(3-methoxyphenyl)acrylate (**7a**). The synthesis of 1-(2-hydroxyphenyl)-5-(3-methoxyphenyl)pent-4-ene-1,3-dione (**8a**) (also referred as β-diketone **8a**), which exists in equilibrium with its enolic form **8'a**, was achieved by Baker-Venkataraman rearrangement of the corresponding 2-acetylphenyl-(*E*)-3-(3-methoxyphenyl)acrylate (**7a**), in very strong alkaline conditions [potassium hydroxide (KOH), 5 equiv], in dimethylsulfoxide (DMSO) (**Scheme 5**). Under these conditions, compound **8'a** was obtained in low yield (25%). The final step consisted in the cyclodehydration of **8'a** which was performed in DMSO with *p*-toluenesulfonic acid (*p*-TSA), at 90ºC, but no product was obtained.

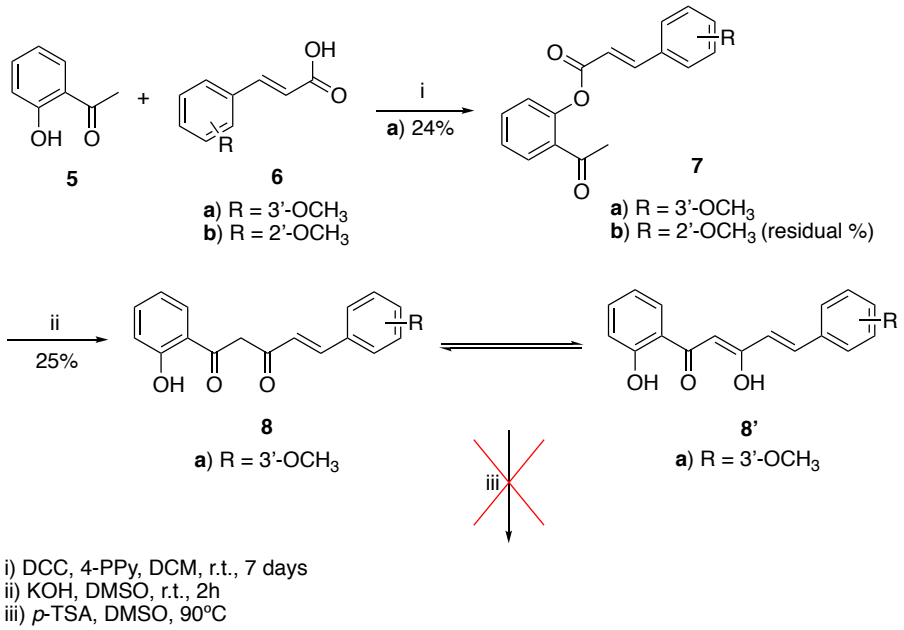

***Scheme 5**. Attempted synthesis of (E)-2-styrylchromones by Baker-Venkataraman rearrangement.*

2.1.2.2 Method 2: Aldol-type condensation of 2'-hydroxyacetophenones with cinnamaldehydes

This second strategy consisted of an Aldol-type condensation of 2'-hydroxy-4',6'-dimethoxyacetophenone (**4**) with cinnamaldehydes [(E)-3-phenylprop-2-enal according to the IUPAC nomenclature] **9a-b** in methanol (MeOH), in the presence of an aqueous sodium hydroxide (NaOH) solution (40%), at room temperature, followed by cyclodehydration of the formed 2′-hydroxycinnamylidene-acetophenones **10a-b** (31% and 50% of yield, respectively). Compound **11a** was obtained with *cis* configuration while compound **11b** was obtained with *trans* configuration. After boron tribromide (BBr_3)-promoted cleavage of the methoxy groups in dry DCM, compound **11'b** was

obtained in a moderate yield (32%). The deprotection of the methoxy groups of compound **11a** did not occur (**Scheme 6**).

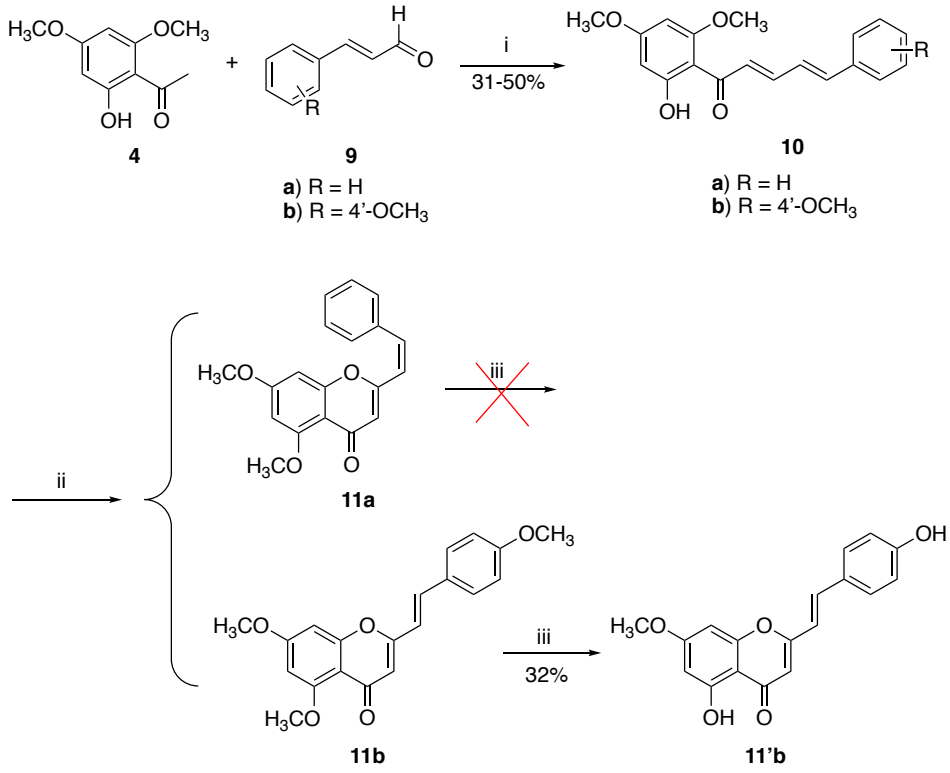

i) NaOH, MeOH, r.t., 20-22h
ii) I_2, DMSO, reflux, 50min.
iii) BBr_3, dry DCM, -70ºC to r.t., 24h

Scheme 6*. Synthesis of (Z)-5,7-dimethoxy-2-styrylchromone* ***11a,*** *(E)-5,7-dimethoxy-2-(4-methoxystyryl)chromone* ***11b*** *and (E)-5-hydroxy-7-methoxy-2-(4-hydroxystyryl)chromone* ***11'b*** *by Aldol-type condensation of 2'-hydroxyacetophenones with cinnamaldehydes.*

2.1.2.3 Method 3: Aldol condensation of 2-methylchromones with benzaldehydes

For the synthesis of (*E*)-2-styrylchromones through this method, it was necessary to synthesize the starting compounds 2-methylchromones (2-methyl-4*H*-chromen-4-ones, according to the IUPAC nomenclature). Three different methods were tested for this synthesis and when necessary, the acetophenones and phenols were previously protected by methylation.

2.2.2.3.1 Synthesis of 2-methylchromones

The first synthesis route consisted of a two-step sequence starting from 2'-hydroxy-6'-methoxyacetophenone (**2**), 2'-hydroxyacetophenone (**5**), 2'-benzyloxy-6'-hydroxyacetophenone [1-(2-(benzyloxy)-6-hydroxyphenyl)ethan-1-one] (**16**) and 2',4-dibenzyloxy-6'-hydroxyacetophenone [1-[2,4-bis(benzyloxy)-6-hydroxyphenyl]ethan-1-one] (**19**) with sodium in dry ethyl acetate at room temperature for 18 h, followed by cyclodehydrogenation in refluxing MeOH in the presence of *p*-TSA,

for 21 to 27 h. Compounds **13** and **15** containing methoxy groups are represented in **Scheme 7** while compounds **18** and **21** containing benzyloxy groups are represented in **Scheme 8**, with their respective reaction schemes.

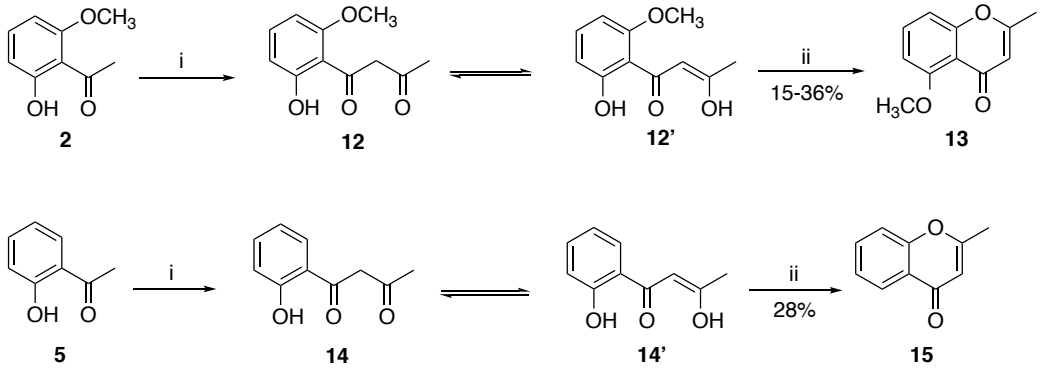

i) Na, dry AcOEt, r.t, 18-21h
ii) *p*-TSA, MeOH, reflux, N_2, 21-27h

***Scheme 7**. Synthesis of 5-methoxy-2-methylchromone (**13**) and 2-methylchromone (**15**).*

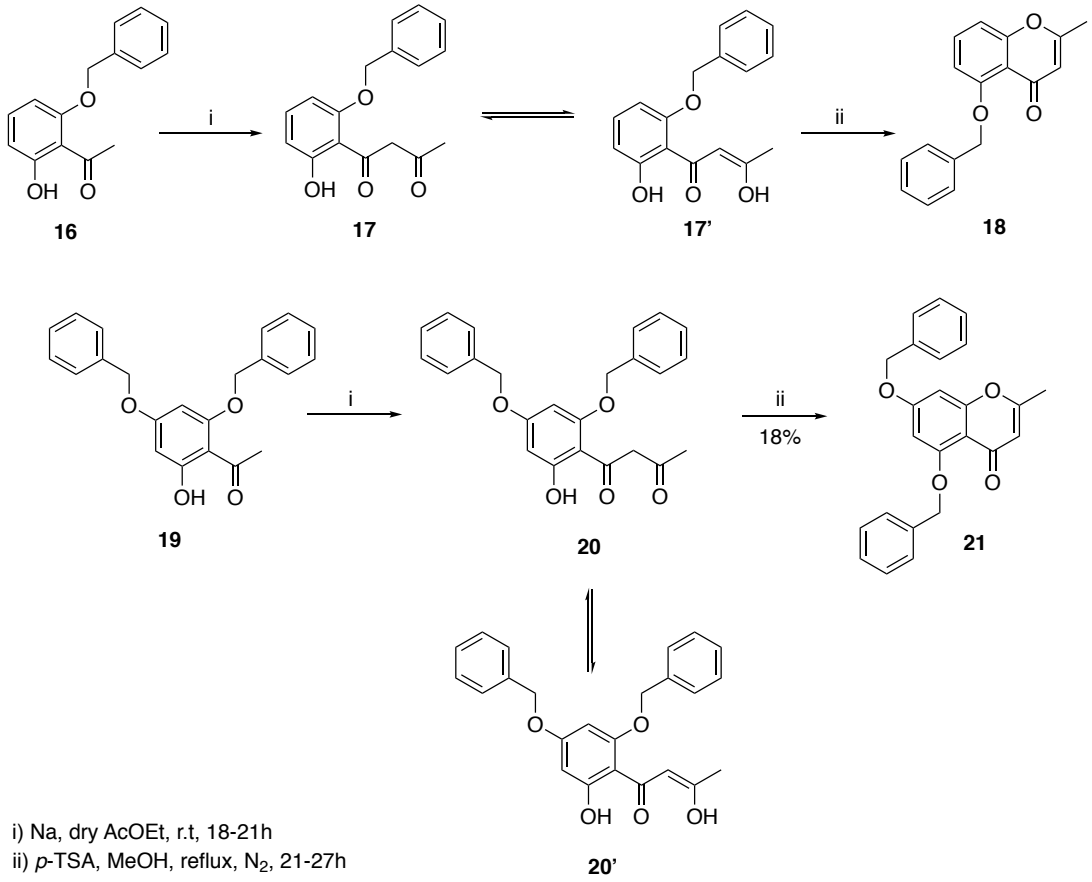

i) Na, dry AcOEt, r.t, 18-21h
ii) *p*-TSA, MeOH, reflux, N_2, 21-27h

***Scheme 8**. Synthesis of 5-benzyloxy-2-methylchromone (**18**) and 5,7-dibenzyloxy-2-methylchromone (**21**).*

The second strategy consisted of a solvent-free reaction between 3,4,5-trimethoxyphenol (**22**) and ethyl acetoacetate (**23**), with phosphorous pentoxide, at room temperature, for 20 h (**Scheme 9**), but no product was obtained.

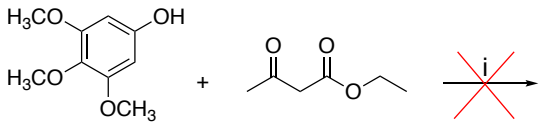

22 **23**

i) P_2O_5, r.t., 20h

***Scheme 9**. Attempted synthesis of 2-methylchromones by a solvent-free reaction.*

The third and last strategy consisted of a three-step sequence, beginning with the acylation of 3,4,5-trimethoxyphenol (**22**) with acetyl chloride in dry pyridine, at room temperature, for 27 h. The second step was the Fries rearrangement of the acyl group in aluminium(III) chloride at 150 ºC, under N_2 atmosphere, for 3 h (**Scheme 10**). The final step was not performed, but it would have consisted of the synthesis of the corresponding 2-methylchromone from 6'-hydroxy-2',3',4'-trimethoxyacetophenone (**24'**), based on the reactions of **Schemes 7** and **8**.

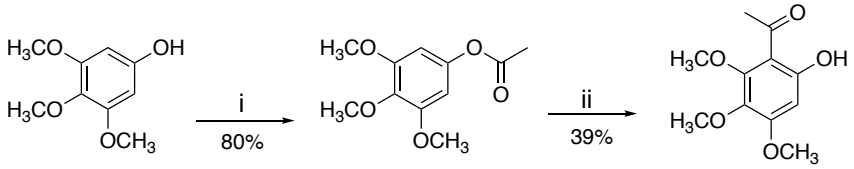

22 **24** **24'**

i) Acetyl chloride, dry pyridine, r.t, 27h
ii) Al_3Cl, 150ºC, N_2, 3h

***Scheme 10**. Synthesis of 6'-hydroxy-2',3',4'-trimethoxyacetophenone (**24'**) from 3,4,5-trimethoxyphenol (**22**).*

The synthesis of (*E*)-5-methoxy-2-styrylchromones **26a-f** and **27a** consisted of only one step: the Aldol condensation between 2-methylchromones **13**, **15**, **18** and **21,** synthesized as illustrated on **Schemes 7** and **8**, and benzaldehydes **9**, with sodium in ethanol (EtOH), at room temperature, up to 16 h. Afterward, the BBr_3-promoted cleavage of the methoxy groups in dry DCM for 24 h, gave the (*E*)-5-hydroxy-2-styrylchromones **26'a-f** and **27'a** (**Scheme 11** and **Scheme 12**).

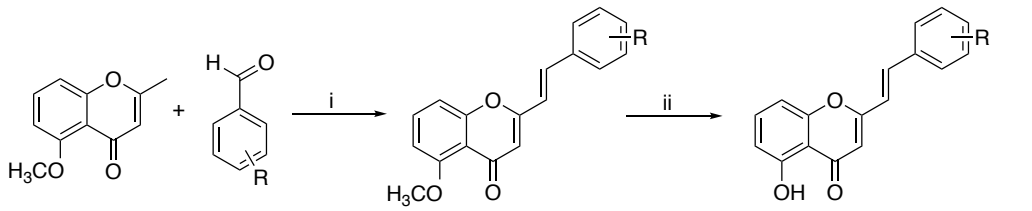

13 **25** **26** **26'**

a) R = 3'-Cl (51%)
b) R = 3',4'-$(Cl)_2$ (60%)
c) R = 2',6'-$(Cl)_2$ (48%)
d) R = 2'-OCH_3 (57%)
e) R = 3'-OCH_3 (59%)
f) R = 3',4',5'-$(OCH_3)_3$ (76%)

a) R = 3'-Cl (96%)
b) R = 3',4'-$(Cl)_2$ (80%)
c) R = 2',6'-$(Cl)_2$ (85%)
d) R = 2'-OH (83%)
e) R = 3'-OH (45%)
f) R = 3',4',5'-$(OH)_3$ (76%)

i) Na, EtOH, r.t., 16h
ii) BBr_3, dry DCM, -70ºC to r.t., 24h

***Scheme 11**. Synthesis of (E)-5-methoxy-2-styrylchromones **26a-f** and (E)-5-hydroxy-2-styrylchromones **26'a-f**.*

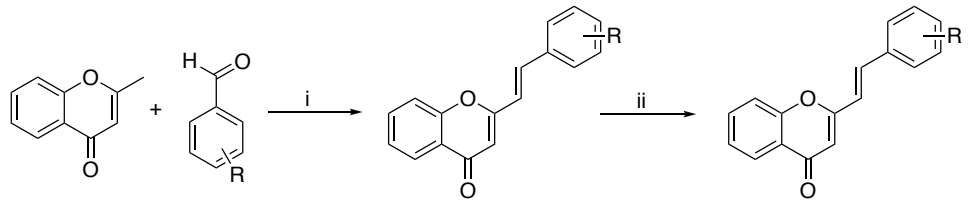

18 **25** **27** **27'**

a) R = 3'-OCH_3 (55%)

a) R = 3'-OH (16%)

i) Na, EtOH, r.t., 18h
ii) BBr_3, dry DCM, -70ºC to r.t., 24h

***Scheme 12**. Synthesis of (E)-2-(3-methoxystyryl)chromone (**27a**) and (E)-2-(3-hydroxystyryl)chromone (**27'a**).*

2.2 Structural characterization of (*E*)-2-styrylchromones

In this section will be presented and discussed the structural characterizations of the new and most relevant synthesized compounds, further used in biological assays. All these compounds were characterized by 1D (^{1}H and ^{13}C) and 2D (HSQC and HMBC) NMR techniques, and whenever possible by mass spectrometry (ESI^+) and high-resolution mass spectrometry (HRMS) techniques which together allowed an unequivocally confirmation of the compounds' structures.

The analysis of the ^{1}H NMR spectra of the synthesized (*E*)-2-styrylchromones allows the distinction between two main regions, based on their frequency values: i) the aliphatic region with lower frequency values (less than 5.00 ppm), where the chemical shifts of protons from methoxy groups ($OC\underline{H}_3$) groups appear around 3.80 - 4.00 ppm and ii) the aromatic region. The singlet due to the resonance of H-3 proton at the chemical shift values δ = 6.25 – 6.51 ppm, along with the presence of two large doublets due to the resonance of H-α and H-β protons of the exocyclic double bond with a *trans* configuration as confirmed by the coupling constant ($^3J_{H\alpha\text{-}H\beta} \cong$ 16.0 Hz), are the most characteristic signals of this family of compounds. Furthermore, the 5-O$\underline{H}$ proton appeared as a broad singlet in all compounds except for **26e**, due to the hydrogen bond with the carbonyl group

at C-4. Another major characteristic which allowed the distinction between the protected and deprotected compounds, and consequently to claim the success of the cleavage reaction, was the disappearance of the signals of the methoxy groups around δ = 3.80 – 4.00 ppm, for example from compound **26e** to compound **26'e** and, in some cases, the appearance of the OH signal around δ = 12.50 ppm.

The (*E*)-2-styrylchromones in study usually presented a doublet of doublets for H-6 and H-8 protons as well as a triplet for both H-7 and H-5' protons. In some compounds, the H-2' appeared as a small doublet or triplet when the B ring is *meta*-substituted on H-3' or both *meta*- and *para*-substituted on H-3' and H-4', respectively. The multiplicity of the protons of the B ring (H-3', H-4' and H-6' was depending on the substitution patterns. In addition, the non-substituted A ring in compound **27'a** showed a doublet of doublets for H-5 proton.

To make it easier to compare the chemical shifts of all compounds, for both ^{1}H and ^{13}C NMR, all the calculated values are presented in **Table 4** and **Table 5**, at the end of this section.

2.2.1 (*E*)-5-Hydroxy-7-methoxy-2-(4-hydroxystyryl)-4*H*-chromen-4-one (11'b)

The structure and numbering of (*E*)-5-hydroxy-7-methoxy-2-(4-hydroxystyryl)-4*H*-chromen-4-one (**11'b**) is presented on **section 5.2**. The most important signals observed in the ^{1}H NMR spectrum of (*E*)-2-styrylchromone **11'b** (**Figure 13**) are:

- a singlet (s) at δ_H = 3.96 ppm corresponding to the resonance of the protons of the OC$\underline{H}_3$ group linked to C-7;
- a singlet (s) at δ_H = 6.15 ppm corresponding to the resonance of the H-3 proton;
- two doublets (d) due to the resonance of the protons H-α and H-β of the exocyclic double bond, at δ_H = 6.77 ppm and δ_H = 7.56 ppm, respectively. The multiplicity of these signals is justified by the coupling between them, and the corresponding coupling constant (^{3}J = 16.0 Hz) highlights the *trans* configuration of these two protons in compound **11'b**;
- two small doublets (d) at δ_H = 6.36 ppm and δ_H = 6.52 ppm corresponding to the resonance of protons H-6 and H-8, whose multiplicity is due to the long-distance coupling with each other (^{4}J = 2.2 Hz);
- a large doublet (d) at δ_H = 6.88 ppm assigned to the resonance of protons H-3',5'. This multiplicity is due to the short distance coupling with the *ortho*-protons H-2',6' (^{3}J = 8.3 Hz). The signal of H-3',5' appears at lower frequency values than the signal of H-2',6' due to the shielding effect of the hydroxy group at the *ortho* positions.

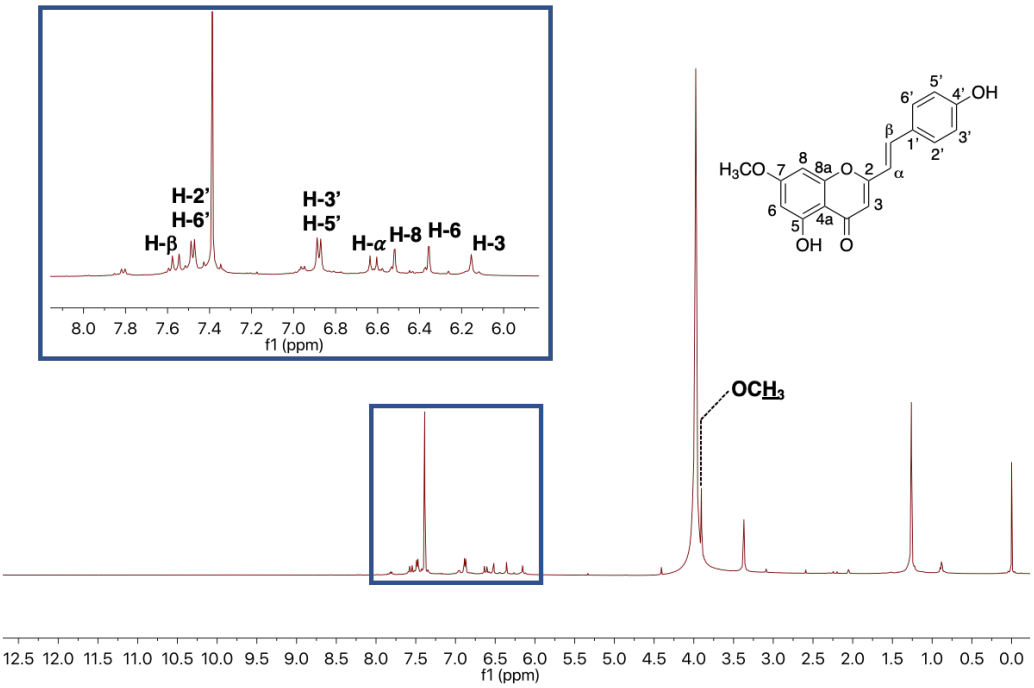

***Figure 13**. [1]H NMR spectrum of (E)-2-styrylchromone **11'b** and expansion of the corresponding aromatic region (500.16 MHz, MeOD).*

All the carbons in the [13]C NMR spectrum of (*E*)-2-styrylchromone **11'b** (**Figure 14**) were assigned based on the HSQC and HMBC spectra.

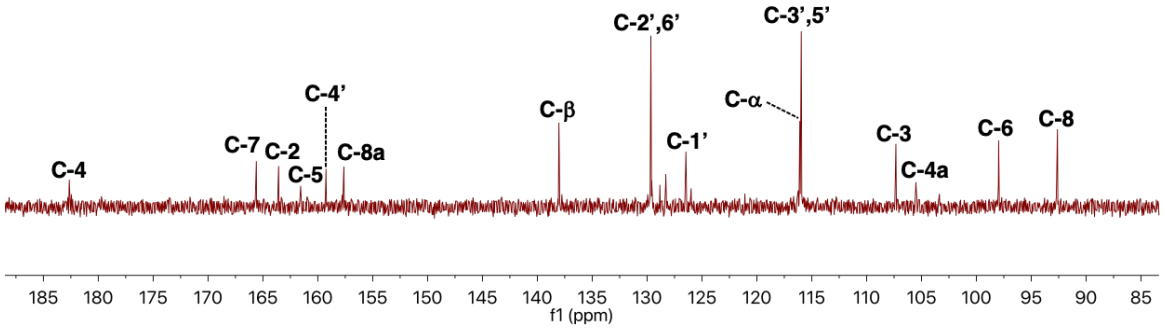

***Figure 14**. Expansion of the [13]C NMR spectrum of (E)-2-styrylchromone **11'b** (125.77 MHz, MeOD).*

The nine protonated carbons were easily assigned based on the correlations observed in the HSQC spectrum (**Figure 15**) at δ_C = 92.6 (C-8), 98.0 (C-6), 107.3 (C-3), 116.0 (C-3',5'), 116.1 (C-α), 129.7 (C-2',6') and 138.0 (C-β) ppm.

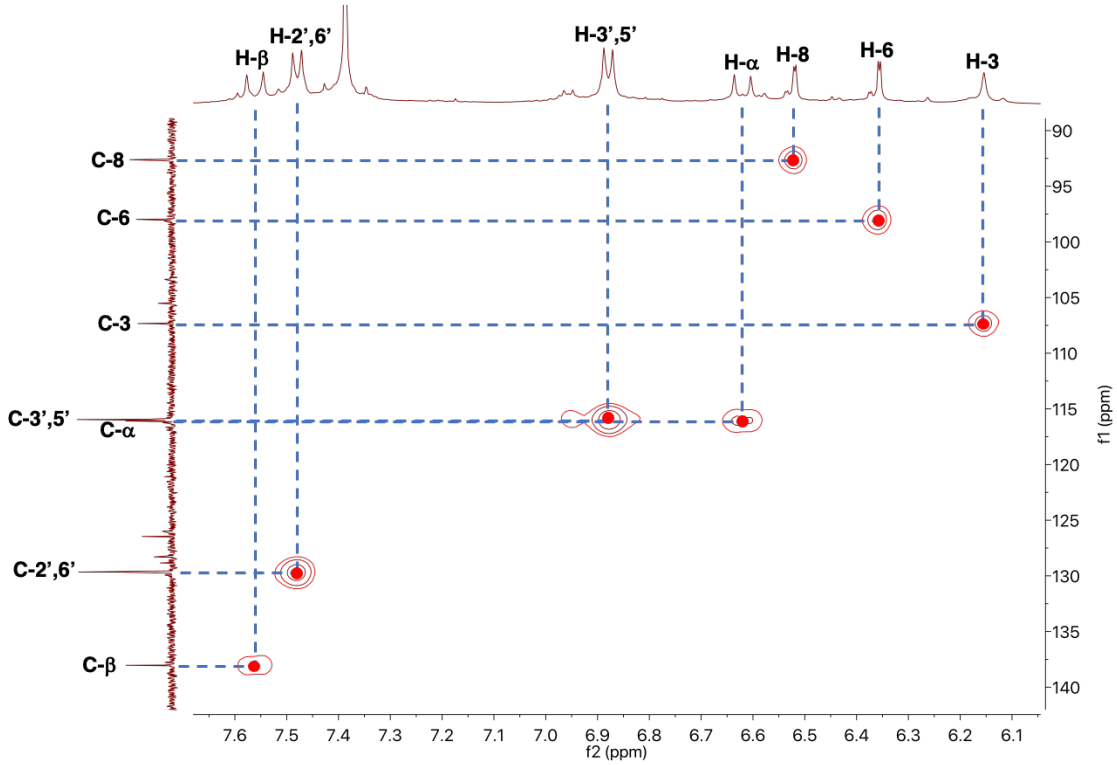

***Figure 15**. Expansion of the HSQC spectrum of (E)-2-styrylchromone **11'b**.*

The non-protonated carbons were assigned based on the correlations observed in the HMBC spectrum (**Figure 16**), namely H-6→C-4a and H-8→C-4a (δ_C = 105.5 ppm); H-α→C-1' and H-3',5'→C-1' (δ_C = 126.5 ppm); H-8→C-8a (δ_C = 157.6 ppm); H-3',5'→C-4' and H-2',6'→C-4' (δ_C = 159.2 ppm); H-3→C-2, H-α→C-2 and H-β→C-2 (δ_C = 163.6 ppm); H-8→C-7 (δ_C = 165.6 ppm). The two remaining signals correspond to C-5 at δ_C = 161.6 ppm, and to C-4 at δ_C = 182.6 ppm, which is the most deprotected carbon.

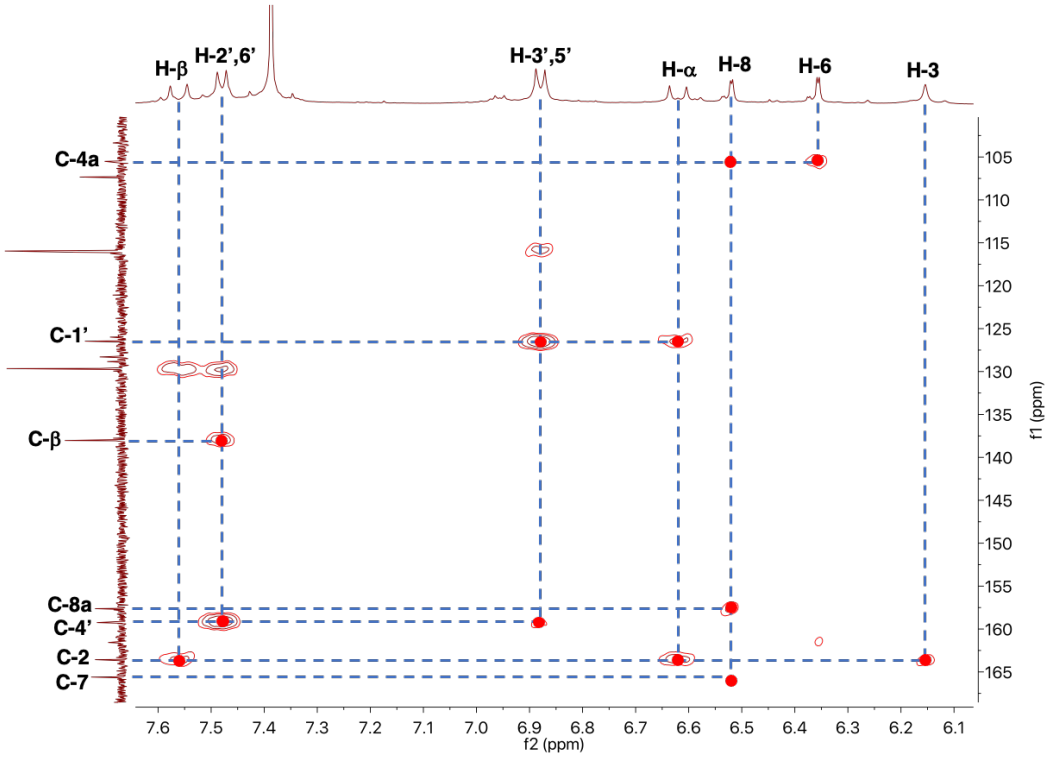

***Figure 16**. Expansion of the HMBC spectrum of (E)-2-styrylchromone **11'b**.*

2.2.2 (*E*)-5-Hydroxy-2-(3-chlorostyryl)-4*H*-chromen-4-one (26'a)

The structure and numbering of (*E*)-5-hydroxy-2-(3-chlorostyryl)-4*H*-chromen-4-one (**26'a**) is presented on **section 5.2**. The most important signals observed in the ^{1}H NMR spectrum of (*E*)-2-styrylchromone **26'a** (**Figure 17**) are:

- a singlet (s) at δ_H = 6.27 ppm corresponding to the resonance of the H-3 proton;
- two doublets (d) due to the resonance of the protons H-α and H-β of the double bond, at δ_H = 6.77 ppm and δ_H = 7.56 ppm, respectively. The multiplicity of these signals is justified by the coupling between them, and the correspondent coupling constant (^{3}J = 15.9 Hz) highlights the *trans* configuration of these two protons in compound **26'a**;
- two doublet of doublets (dd) at δ_H = 6.81 ppm and δ_H = 6.97 ppm corresponding to the resonance of protons H-6 and H-8. The multiplicity of these protons is due to the long-distance coupling between them (^{4}J = 0.9 Hz) and the coupling of each proton with H-7 (^{3}J = 8.4 Hz); these are the two most shielded aromatic protons due to their *ortho*- and *para*-positions, respectively, relatively to the 5-OH group;
- a multiplet (m) at δ_H = 7.36-7.38 ppm corresponding to the resonance of protons H-2' and H-5';
- a multiplet (m) at δ_H = 7.43-7.48 ppm corresponding to the resonance of protons H-4';
- a triplet (t) at δ_H = 7.55 ppm due to the resonance of proton H-7;
- a multiplet (m) at δ_H = 7.58-7.79 ppm assigned to the resonance of proton H-6'.

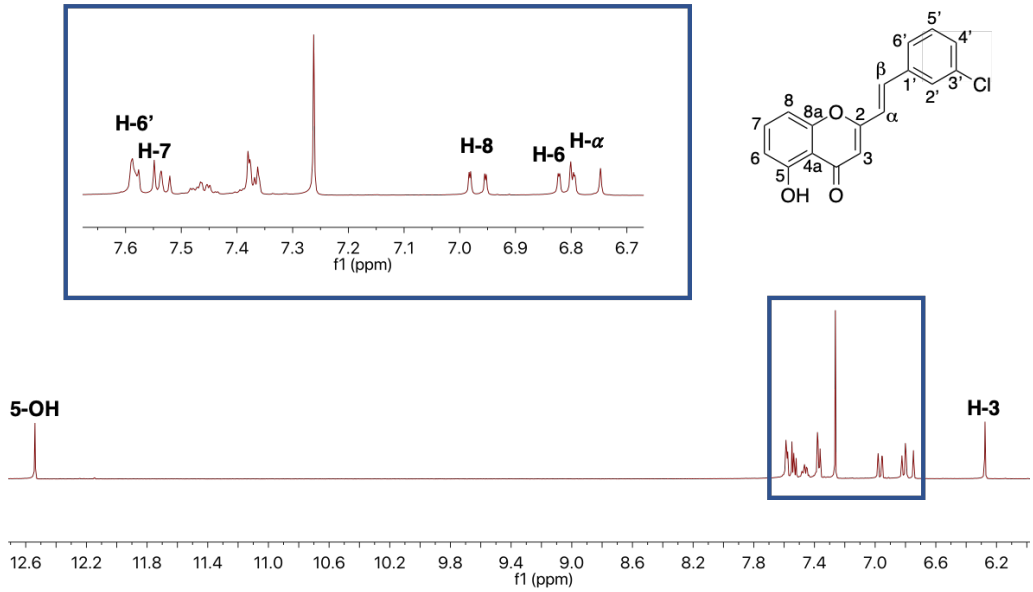

***Figure 17**. [1]H NMR spectrum of (E)-2-styrylchromone **26'a** and expansion of the corresponding aromatic region (300.13 MHz, $CDCl_3$).*

All the carbons in the ^{13}C NMR spectrum of (*E*)-2-styrylchromone **26'a** (**Figure 18**) were assigned based on the HSQC and HMBC spectra.

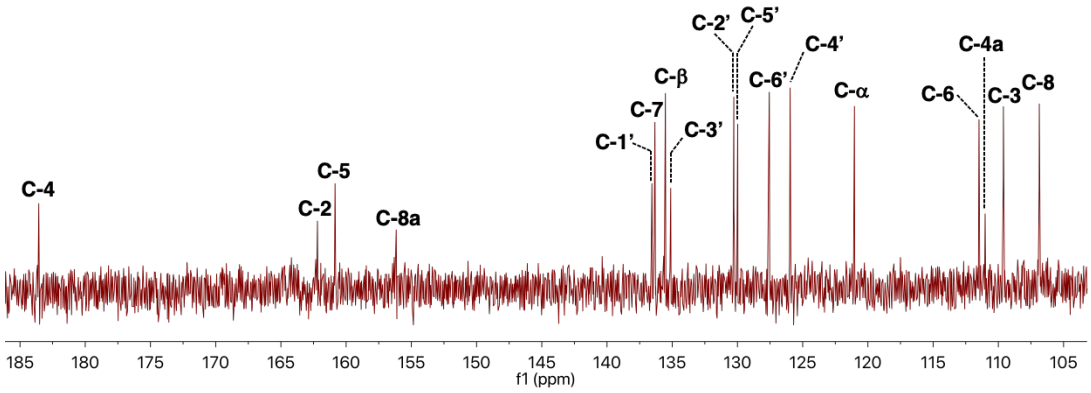

***Figure 18**. Expansion of the ^{13}C NMR spectrum of (E)-2-styryl-4H-chromen-4-one **26'a** (75.47 MHz, $CDCl_3$).*

The ten protonated carbons were easily assigned based on the correlations observed in the HSQC spectrum (**Figure 19**) at δ_C = 107.0 (C-8), 109.7 (C-3), 111.6 (C-6), 121.2 (C-α), 126.1 (C-4'), 127.7 (C-6'), 130.1 (C-5'), 130.4 (C-2'), 135.6 (C-β) and 136.4 (C-7) ppm.

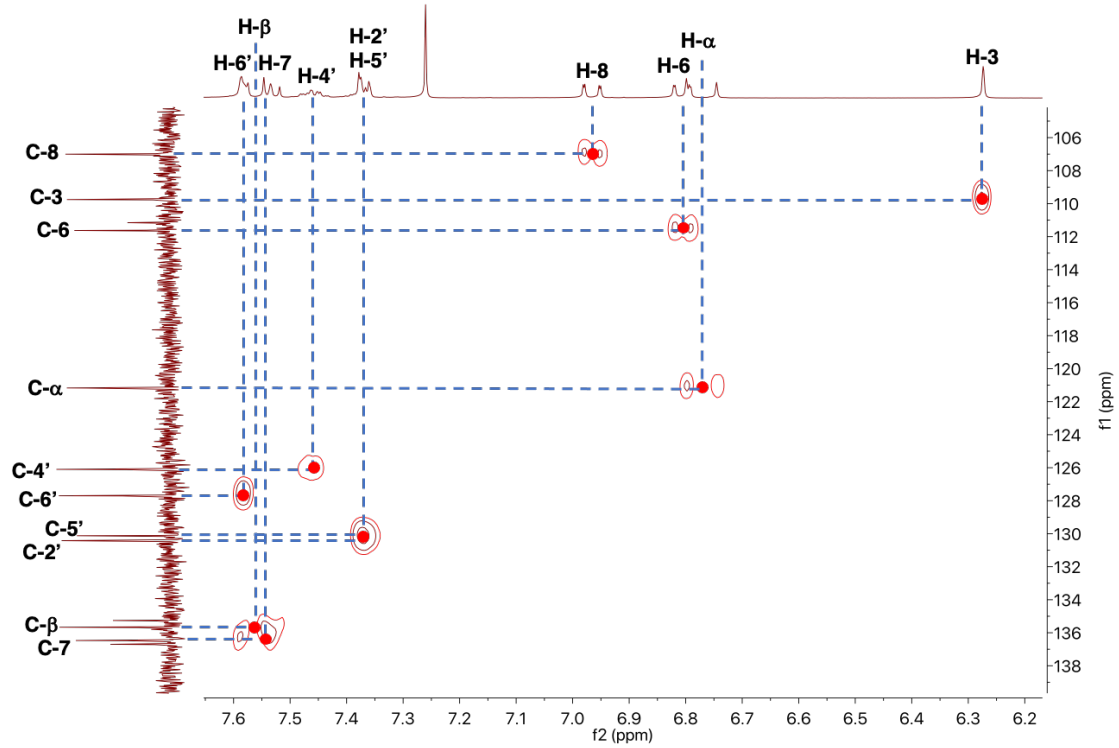

***Figure 19**. Expansion of the HSQC spectrum of (E)-2-styrylchromone **26'a**.*

The non-protonated carbons were assigned based on the correlations observed in the HMBC spectrum (**Figure 20**), namely H-3→C-4a, H-6→C-4a and H-8→C-4a (δ_C = 111.0 ppm); H-5'→C-3' and H-2'→C-3' (δ_C = 135.1 ppm); H-α→C-1' and H-2'→C-1' (δ_C = 136.6 ppm); H-8→C-8a and H-7→C-8a (δ_C = 156.2 ppm); H-7→C-5 (δ_C = 160.9 ppm); H-3→C-2 and H-α→C-2 (δ_C = 162.2 ppm); H-3→C-4 (δ_C = 183.6 ppm).

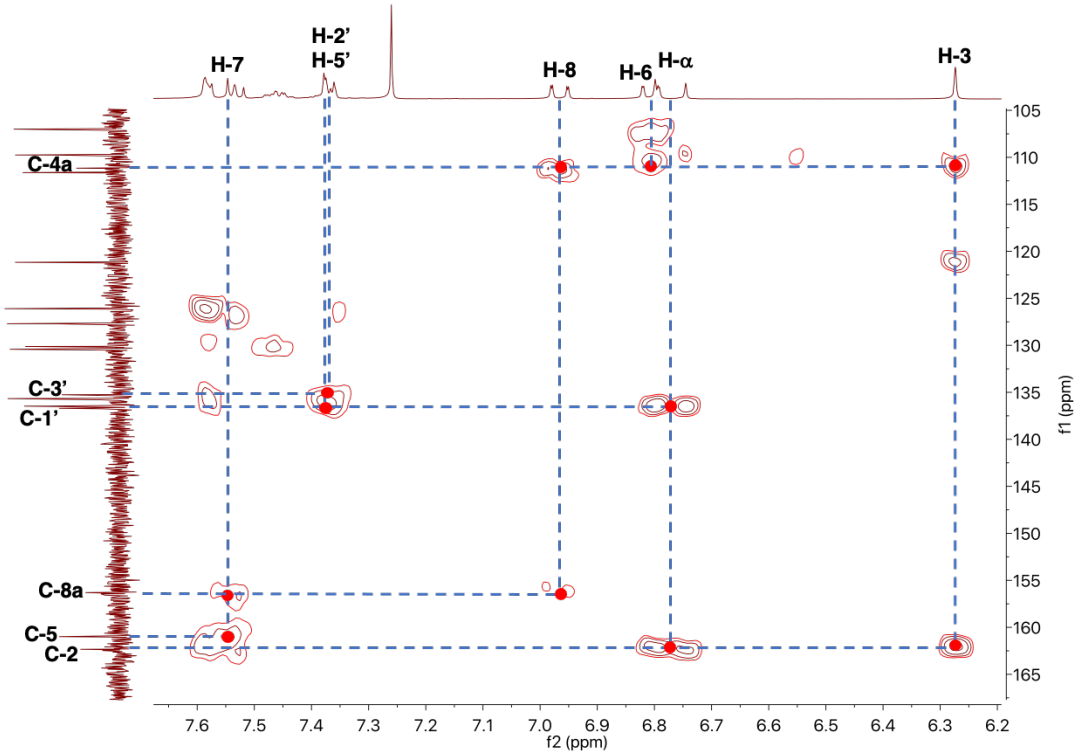

***Figure 20**. Expansion of the HMBC spectrum of (E)-2-styrylchromone **26'a**.*

2.2.3 (*E*)-5-Hydroxy-2-(3,4-dichlorostyryl)-4*H*-chromen-4-one (26'b)

The structure and numbering of (*E*)-5-hydroxy-2-(3,4-dichlorostyryl)-4*H*-chromen-4-one (**26'b**) is presented on **section 5.2**. The most important signals observed in the ^{1}H NMR spectrum of (*E*)-2-styrylchromone **26'b** (**Figure 21**) are:

- a singlet (s) at δ_H = 6.27 ppm corresponding to the resonance of the H-3 proton;
- two doublets (d) due to the resonance of the protons H-α and H-β of the double bond, at δ_H = 6.76 ppm and δ_H = 7.52 ppm, respectively. Their coupling constant (^{3}J = 16.0 Hz) confirms the *trans* configuration of these two protons in compound **26'b**;
- two doublet of doublets (dd) at δ_H = 6.81 ppm and δ_H = 6.96 ppm corresponding to the resonance of protons H-6 and H-8, respectively. This multiplicity is due to the long-distance coupling between them (^{4}J = 0.9 Hz) and the coupling of each proton with H-7 (^{3}J = 8.3 Hz); these are the two most shielded aromatic protons due to their *ortho*- and *para*-positions, respectively, relatively to the 5-OH group;
- a doublet of doublets (dd) at δ_H = 7.42 ppm assigned to the resonance of proton H-6'. The multiplicity of this proton is due to the coupling with H-5' (^{3}J = 8.3 Hz) and the long-distance coupling with H-2' (^{4}J = 2.1 Hz);
- two doublets (d) at δ_H = 7.51 ppm and δ_H = 7.68 ppm corresponding to the resonance of protons H-5' and H-2', respectively. The multiplicity of proton H-5' is due to the coupling with H-6' (^{3}J = 8.3 Hz) and of proton H-2' is due to the long-distance coupling with H-6' (^{4}J = 2.1 Hz);

- a triplet (t) at δ_H = 7.55 ppm due to the resonance of proton H-7 (^3J = 8.3 Hz);
- a singlet (s) at δ_H = 12.51 ppm due to the resonance of the proton of the 5-OH group.

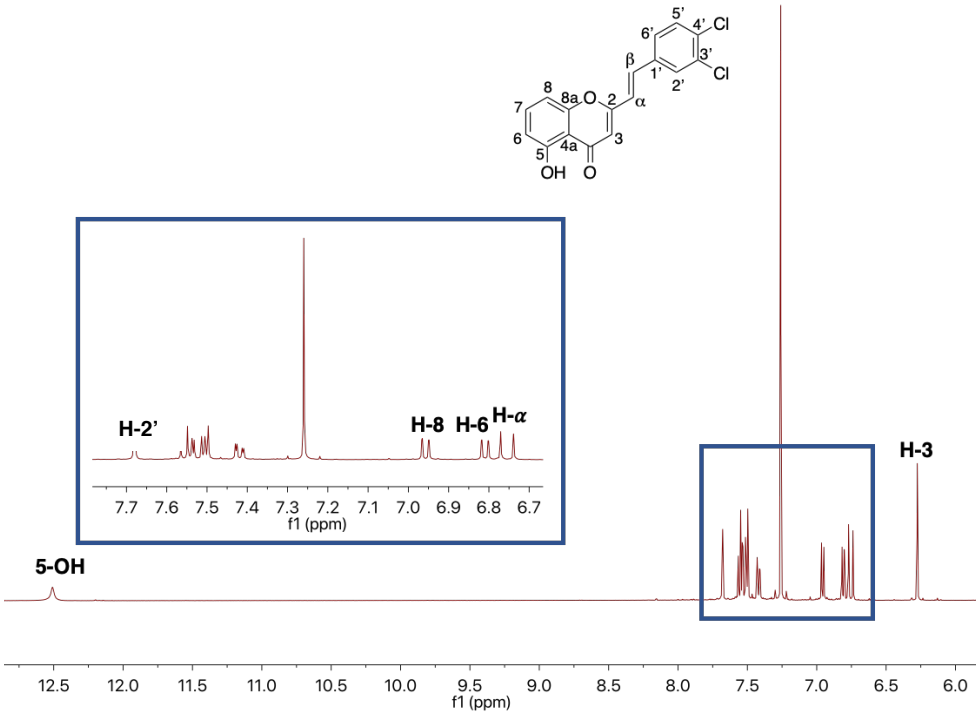

***Figure 21**. [1]H NMR spectrum of (E)-2-styrylchromone **26'b** and expansion of the corresponding aromatic region (500.16 MHz, $CDCl_3$).*

All the carbons in the ^{13}C NMR spectrum of (*E*)-2-styrylchromone **26'b** (**Figure 22**) were assigned based on the HSQC and HMBC spectra.

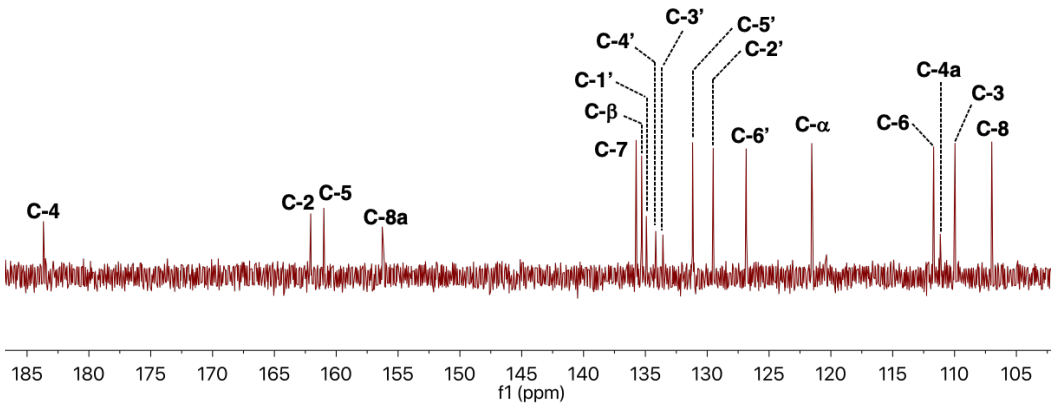

***Figure 22**. Expansion of the ^{13}C NMR spectrum of (E)-2-styrylchromone **26'b** (125.77 MHz, $CDCl_3$).*

The nine protonated carbons were easily assigned based on the correlations observed in the HSQC spectrum (**Figure 23**) at δ_C = 106.9 (C-8), 109.8 (C-3), 111.6 (C-6), 121.4 (C-α), 126.7 (C-6'), 129.4 (C-2'), 131.1 (C-5'), 135.2 (C-β) and 135.6 (C-7) ppm.

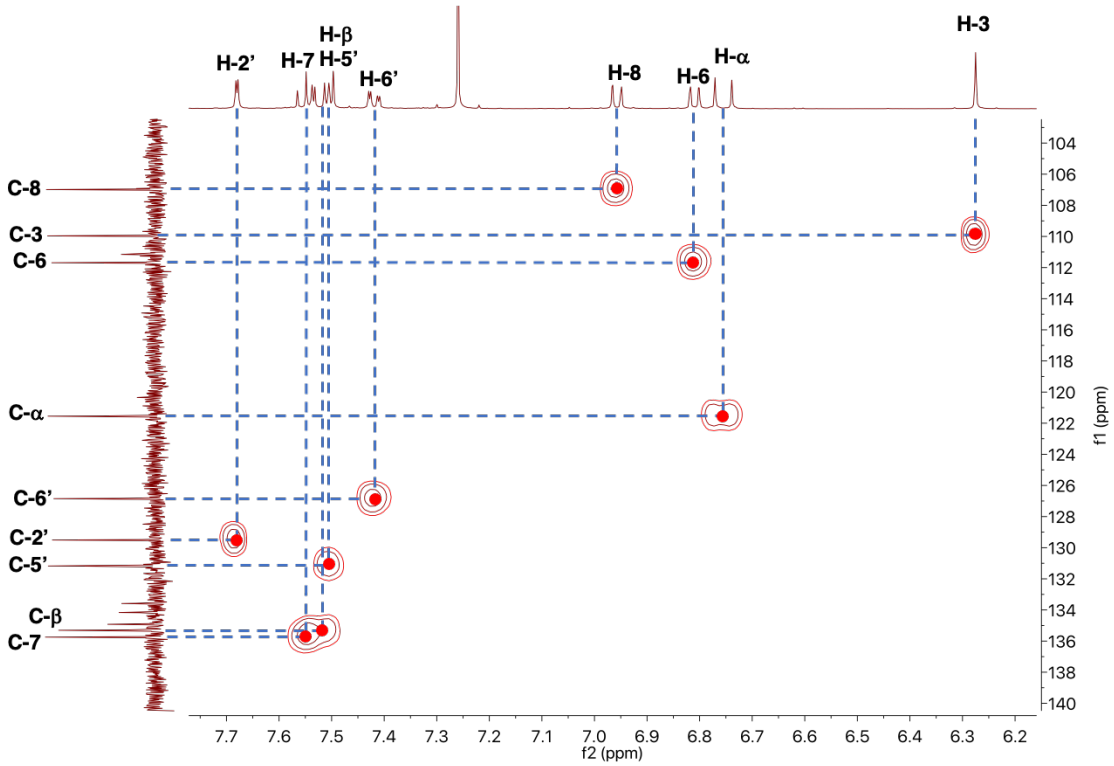

***Figure 23**. Expansion of the HSQC spectrum of (E)-2-styrylchromone **26'b**.*

The seven non-protonated carbons were assigned based on the correlations observed in the HMBC spectrum (**Figure 24**), namely H-3→C-4a and H-6→C-4a (δ_C = 111.0 ppm); H-5'→C-3' and H-6'→C-3' (δ_C = 133.5 ppm), H-6'→C-4', H-5'→C-4' and H-2'→C-4' (δ_C = 134.0 ppm), H-α→C-1' and H-2'→C-1' (δ_C = 134.8 ppm); H-7→C-8a (δ_C = 156.1 ppm), H-7→C-5 (δ_C = 160.9 ppm); H-3→C-2 and H-α→C-2 (δ_C = 161.9 ppm); H-3→C-4 (δ_C = 183.6 ppm).

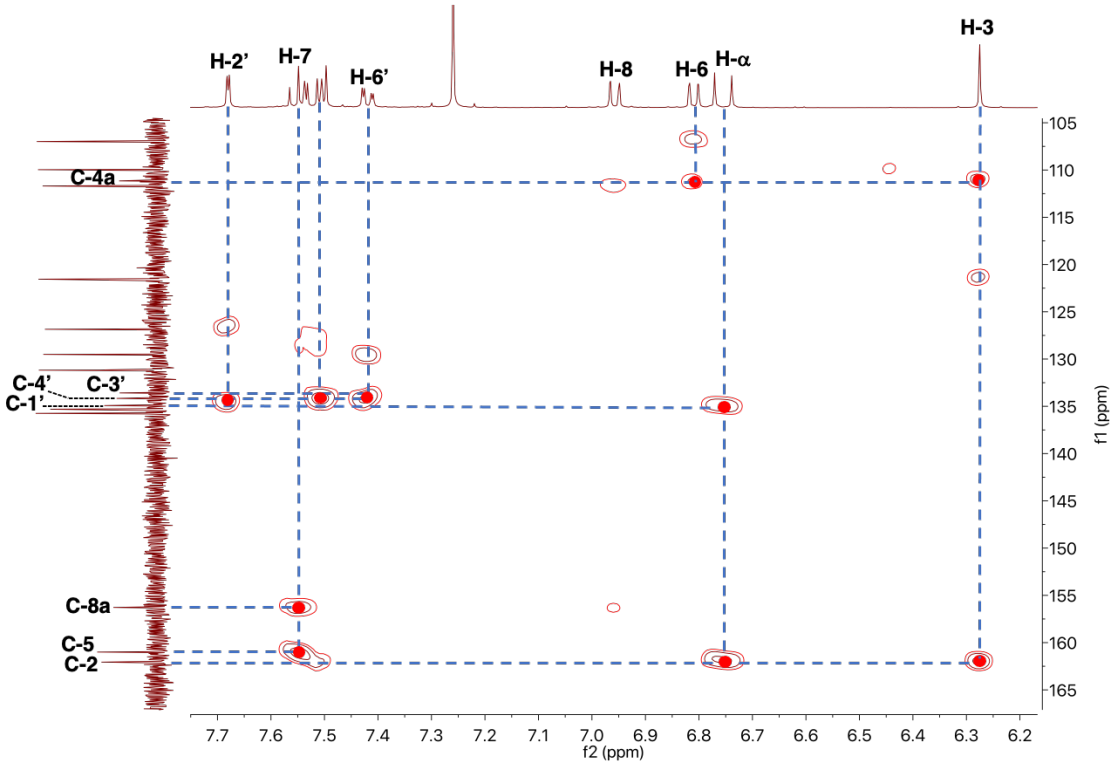

***Figure 24**. Expansion of the HMBC spectrum of (E)-2-styrylchromone **26'b**.*

2.2.4 (*E*)-5-Hydroxy-2-(2,6-dichlorostyryl)-4*H*-chromen-4-one (26'c)

The structure and numbering of (E)-5-hydroxy-2-(2,6-dichlorostyryl)-4*H*-chromen-4-one (**26'c**) is presented on **section 5.2**. The most important signals observed in the ^{1}H NMR spectrum of (*E*)-2-styrylchromone **26'c** (**Figure 25**) are:

- a singlet (s) at δ_H = 6.30 ppm corresponding to the resonance of the H-3 proton;
- two doublet of doublets (dd) at δ_H = 6.81 ppm and δ_H = 7.00 ppm corresponding to the resonance of protons H-6 and H-8, respectively, whose multiplicity is due to the long-distance coupling between them (^{4}J = 0.9 Hz) and the coupling of each proton with H-7 (^{3}J = 8.4 Hz); these are the two most shielded aromatic protons due to their *ortho*- and *para*-positions, respectively, relatively to the 5-OH group;
- two doublets (d) due to the resonance of the protons H-α and H-β of the double bond, at δ_H = 6.95 ppm and δ_H = 7.72 ppm, respectively, with a coupling constant (^{3}J = 16.4 Hz) that highlights the *trans* configuration of these two protons in compound **26'c**;
- a triplet (t) at δ_H = 7.22 ppm due to the resonance of proton H-4' (^{3}J = 8.1 Hz);
- a doublet (d) at δ_H = 7.40 ppm assigned to the resonance of both protons H-3' and H-5' due to the coupling with H-4' (^{3}J = 8.1 Hz);
- a triplet (t) at δ_H = 7.56 ppm due to the resonance of proton H-7 (^{3}J = 8.4 Hz);
- a singlet (s) at δ_H = 12.51 ppm due to the resonance of the proton of the 5-OH group.

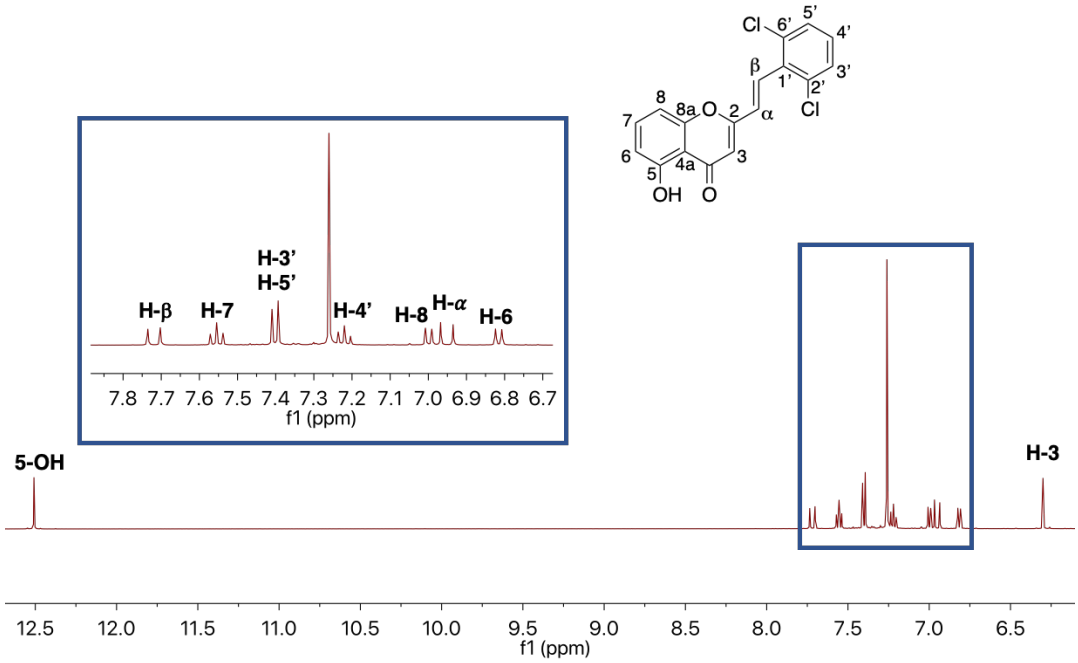

***Figure 25**. [1]H NMR spectrum of (E)-2-styrylchromone **26'c** and expansion of the corresponding aromatic region (500.16 MHz, $CDCl_3$).*

All the carbons in the ^{13}C NMR spectrum of (*E*)-2-styrylchromone **26'c** (**Figure 26**) were assigned based on the HSQC and HMBC spectra.

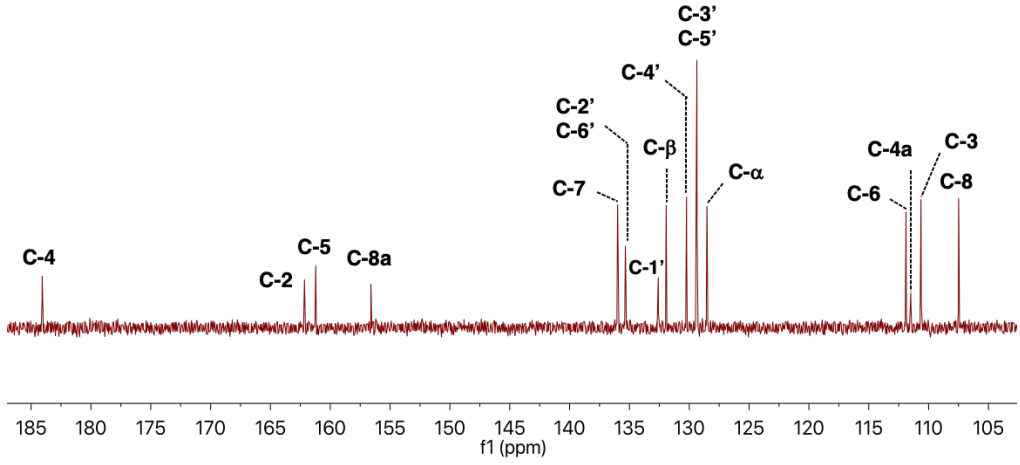

***Figure 26**. Expansion of the ^{13}C NMR spectrum of (E)-2-styrylchromone **26'c** (125.77 MHz, $CDCl_3$).*

The nine protonated carbons were easily assigned based on the correlations observed in the HSQC spectrum (**Figure 27**) at δ_C = 107.1 (C-8), 110.3 (C-3), 111.5 (C-6), 128.1 (C-α), 129.0 (C-3',5'), 129.8 (C-4'), 131.5 (C-β) and 135.6 (C-7) ppm.

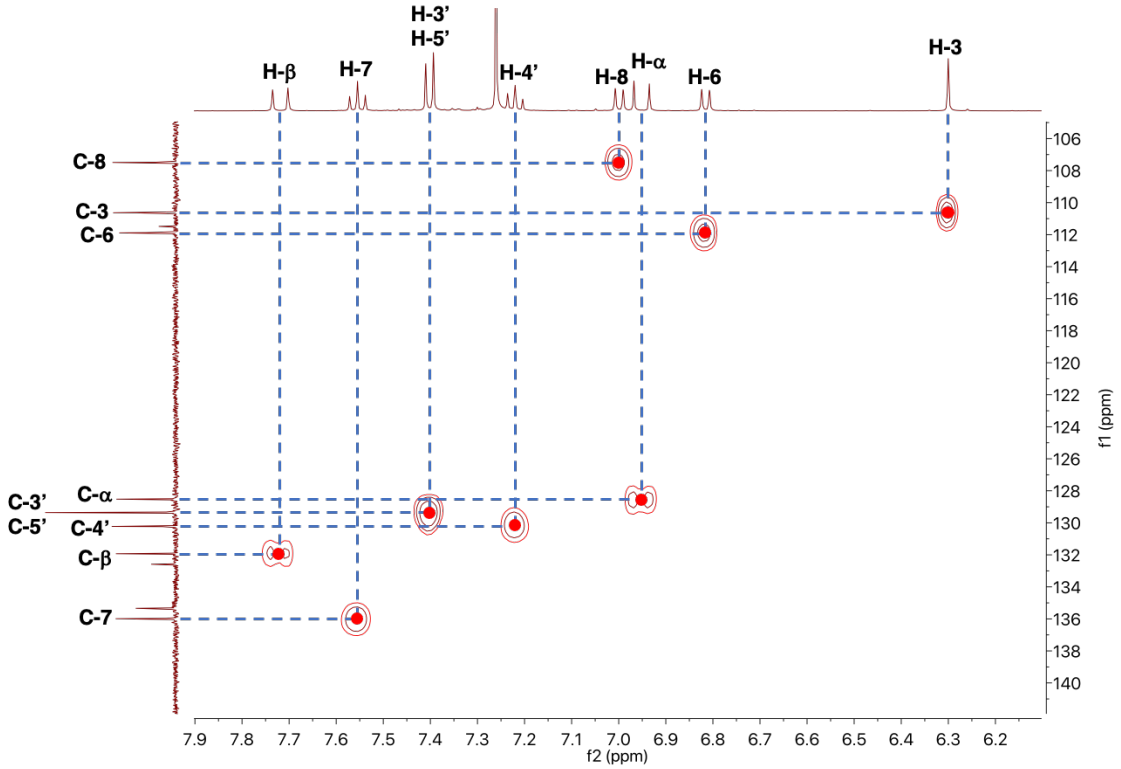

***Figure 27**. Expansion of the HSQC spectrum of (E)-2-styrylchromone **26'c**.*

The non-protonated carbons were assigned based on the correlations observed in the HMBC spectrum (**Figure 28**), namely H-3→C-4a, H-6→C-4a and H-8→C-4a (δ_C = 111.1 ppm); H-3',5'→C-1' (δ_C = 132.2 ppm); H-4'→C-2',6' and H-β→C-2',6' (δ_C = 135.0 ppm); H-7→C-8a (δ_C = 156.2 ppm); H-7→C-5 (δ_C = 160.8 ppm); H-3→C-2, H-α→C-2 and H-β→C-2 (δ_C = 161.8 ppm); H-3→C-4 (δ_C = 183.7 ppm).

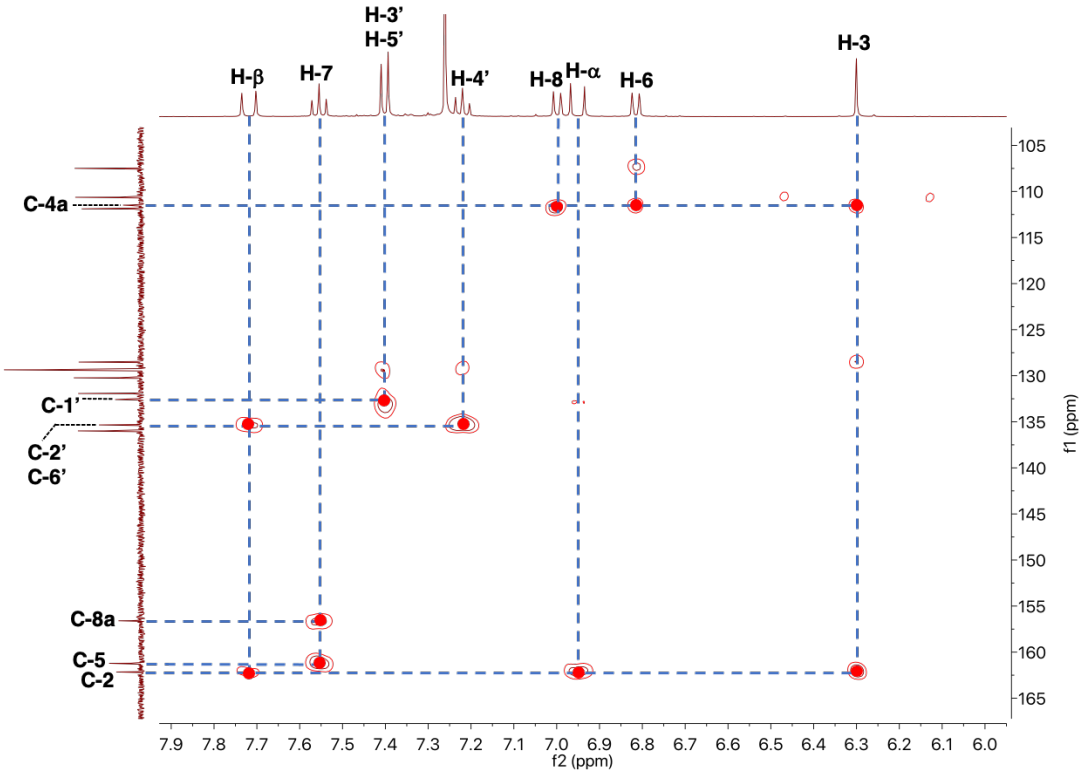

***Figure 28**. Expansion of the HMBC spectrum of (E)-2-styrylchromone **26'c**.*

2.2.5 (*E*)-5-Hydroxy-2-(2-hydroxystyryl)-4*H*-chromen-4-one (26'd)

The structure and numbering of (*E*)-5-hydroxy-2-(2-hydroxystyryl)-4*H*-chromen-4-one (**26'd**) is presented on **section 5.2**. The most important signals observed in the ^{1}H NMR spectrum of (*E*)-2-styrylchromone **26'd** (**Figure 29**) are:

- a singlet (s) at δ_H = 6.33 ppm corresponding to the resonance of the H-3 proton;
- two doublet of doublets (dd) at δ_H = 6.77 ppm and δ_H = 7.09 ppm corresponding to the resonance of protons H-6 and H-8, respectively. This multiplicity is due to the long-distance coupling between them (^{4}J = 1.0 Hz) and the coupling of each proton with H-7 (^{3}J = 8.4 Hz); these are the two most shielded aromatic protons due to their *ortho*- and *para*-positions, respectively, relatively to the 5-OH group;
- a doublet of doublets (dd) at δ_H = 6.87 ppm corresponding to the resonance of the H-3' proton, that couples with H-4' (^{3}J = 7.9 Hz), and at long-distance with H-5' (^{4}J = 1.1 Hz);
- a doublet of doublets of doublets (ddd) at δ_H = 6.88 ppm corresponding to the resonance of the H-5' proton, which is coupling with H-4' (^{3}J = 7.4 Hz) and H-6' (^{3}J = 8.1 Hz), and at long-distance with H-3' (^{4}J = 1.1 Hz);
- two doublets (d) due to the resonance of the protons H-α and H-β of the double bond, at δ_H = 7.12 ppm and δ_H = 8.01 ppm, respectively, with a coupling constant (^{3}J = 16.2 Hz) that highlights the *trans* configuration of these two protons in compound **26'd**;

- a doublet of doublets of doublets (ddd) at δ_H = 7.22 ppm corresponding to the resonance of the H-4' proton, whose multiplicity is due to the long-distance coupling with H-6' (^4J = 1.6 Hz) and the coupling at a shorter distance with H-5' (^3J = 7.4 Hz) and H-3' (^3J = 7.9 Hz);
- a doublet of doublets (dd) at δ_H = 7.61 ppm corresponding to the resonance of the H-6' proton, whose multiplicity is due to the long-distance coupling with H-4' (^4J = 1.6 Hz) and the short distance coupling with H-5' (^3J = 8.1 Hz);
- a triplet (t) at δ_H = 7.62 ppm due to the resonance of proton H-7 (^3J = 8.4 Hz).

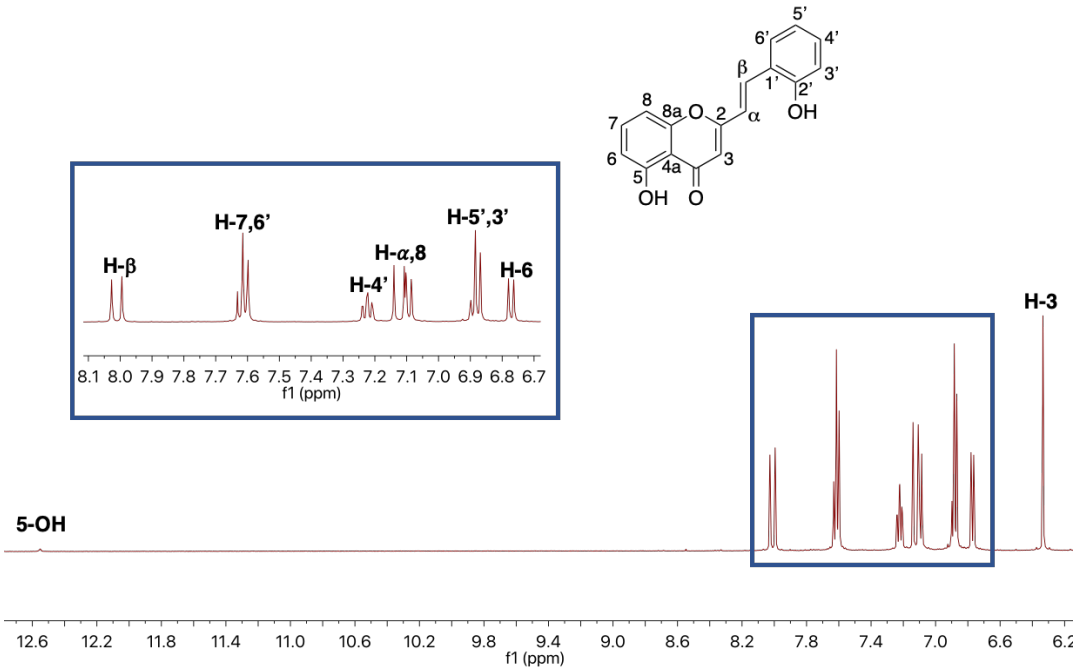

***Figure 29**. [1]H NMR spectrum of (E)-2-styrylchromone **26'd** and expansion of the corresponding aromatic region (500.16 MHz, MeOD).*

All the carbons in the [13]C NMR spectrum of (*E*)-2-styrylchromone **26'd** (**Figure 30**) were assigned based on the HSQC and HMBC spectra.

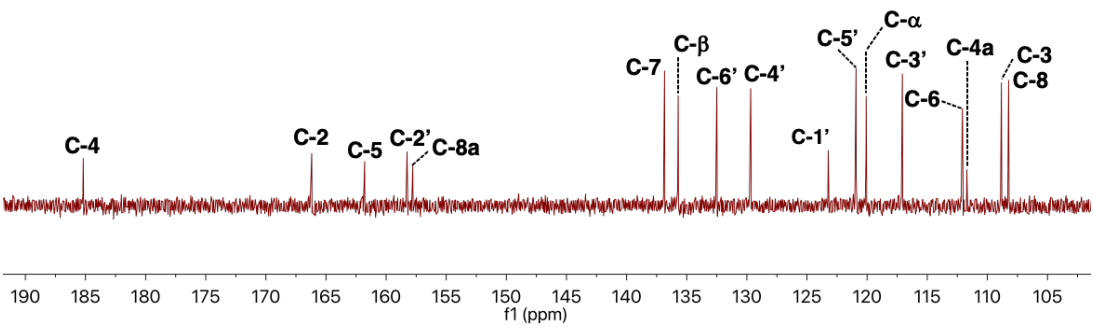

***Figure 30**. Expansion of the [13]C NMR spectrum of (E)-2-styrylchromone **26'd** (125.77 MHz, MeOD).*

The ten protonated carbons were easily assigned based on the correlations observed in the HSQC spectrum (**Figure 31**) at δ_C = 106.8 (C-8), 107.4 (C-3), 110.7 (C-6), 115.7 (C-3'), 118.7 (C-α), 119.5 (C-5'), 128.3 (C-6'), 131.1 (C-4'), 134.3 (C-β) and 135.4 (C-7) ppm.

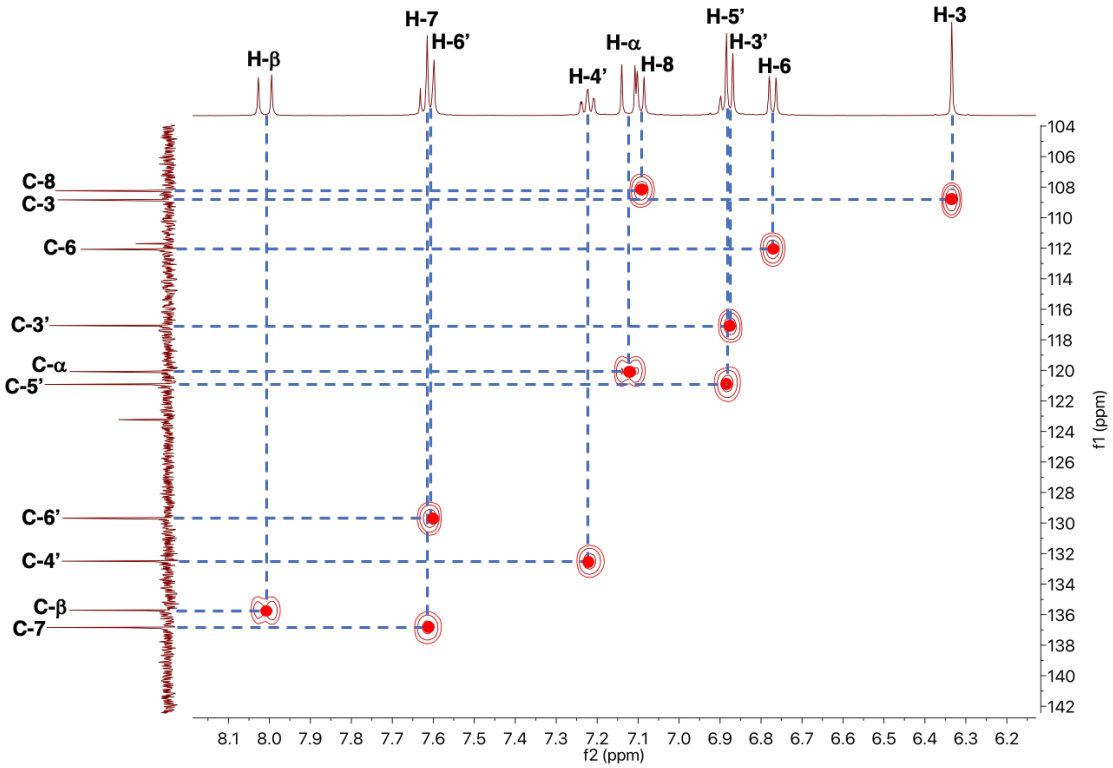

***Figure 31**. Expansion of the HSQC spectrum of (E)-2-styrylchromone **26'd**.*

The non-protonated carbons were assigned based on the correlations observed in the HMBC spectrum (**Figure 32**), namely H-3→C-4a, H-6→C-4a and H-8→C-4a (δ_C = 110.3 ppm), H-α→C-1' (δ_C = 121.8 ppm), H-7→C-8a (δ_C = 156.4 ppm), H-4'→C-2' (δ_C = 156.9 ppm) H-7→C-5 (δ_C = 160.4 ppm), H-3→C-2 and H-α→C-2 (δ_C = 164.8 ppm), H-3→C-4 (δ_C = 183.8 ppm).

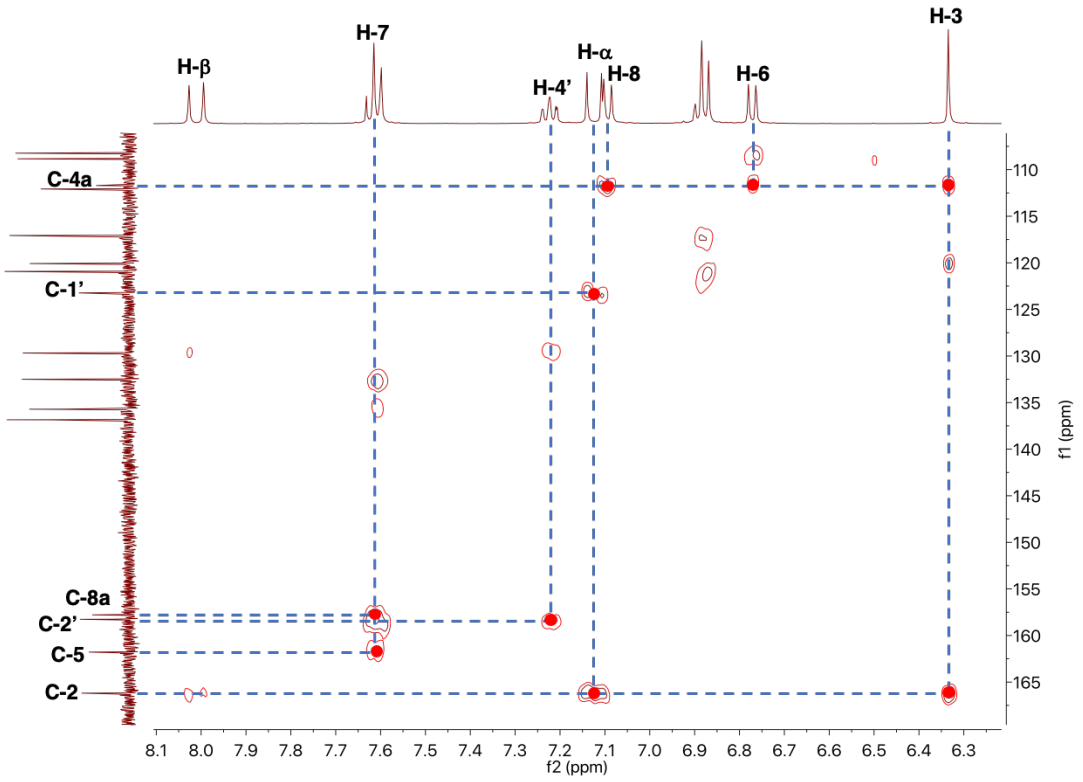

***Figure 32**. Expansion of the HMBC spectrum of (E)-2-styrylchromone **26'd**.*

2.2.6 (*E*)-5-Methoxy-2-(3-methoxystyryl)-4*H*-chromen-4-one (26e)

The structure and numbering of (*E*)-5-methoxy-2-(3-methoxystyryl)-4*H*-chromen-4-one (**26e**) is presented on **section 5.2**. The most important signals observed in the ^{1}H NMR spectrum of (*E*)-2-styrylchromone **26e** (**Figure 33**) are:

- two singlets (s) at δ_H = 3.87 ppm and δ_H = 4.00 ppm corresponding to the resonance of the six protons of the 5-OC$\underline{H}_3$ and 3'-OC$\underline{H}_3$ groups;
- a singlet (s) at δ_H = 6.25 ppm corresponding to the resonance of the H-3 proton;
- two doublets (d) due to the resonance of the protons H-α and H-β of the double bond, at δ_H = 6.71 ppm and δ_H = 7.51 ppm, respectively. The multiplicity of these signals is justified by the coupling between them, and the coupling constant (^{3}J = 16.1 Hz) highlights the *trans* configuration of these two protons in compound **26e**;
- two doublet of doublets (dd) at δ_H = 6.81 ppm and δ_H = 7.11 ppm corresponding to the resonance of protons H-6 and H-8, respectively, whose multiplicity is due to the long-distance coupling between them (^{4}J = 1.0 Hz) and the coupling of each proton with H-7 (^{3}J = 8.4 Hz);
- a doublet of doublets of triplets (ddt) at δ_H = 6.93 ppm corresponding to the resonance of the H-4' proton, whose multiplicity is due to the short-distance coupling with H-5' (^{4}J = 8.1 Hz) and the long-distance coupling with H-2' (^{4}J = 2.2 Hz) and H-6' (^{4}J = 0.9 Hz);

- a small triplet (t) at δ_H = 7.08 ppm due to the resonance of proton H-2', whose multiplicity is due to the long-distance coupling with H-4' and H-6' (^4J = 2.2 Hz);
- a doublet of doublets of triplets (ddt) at δ_H = 7.17 ppm corresponding to the resonance of the H-6' proton, whose multiplicity is due to the short-distance coupling with H-5' (^4J = 8.1 Hz) and the long-distance coupling with H-2' (^4J = 2.2 Hz) and H-4' (^4J = 0.9 Hz);
- two triplets (t) at δ_H = 7.33 ppm and δ_H = 7.57 ppm corresponding to the resonance of protons H-5' (^3J = 8.1 Hz) and H-7 (^3J = 8.4 Hz), respectively.

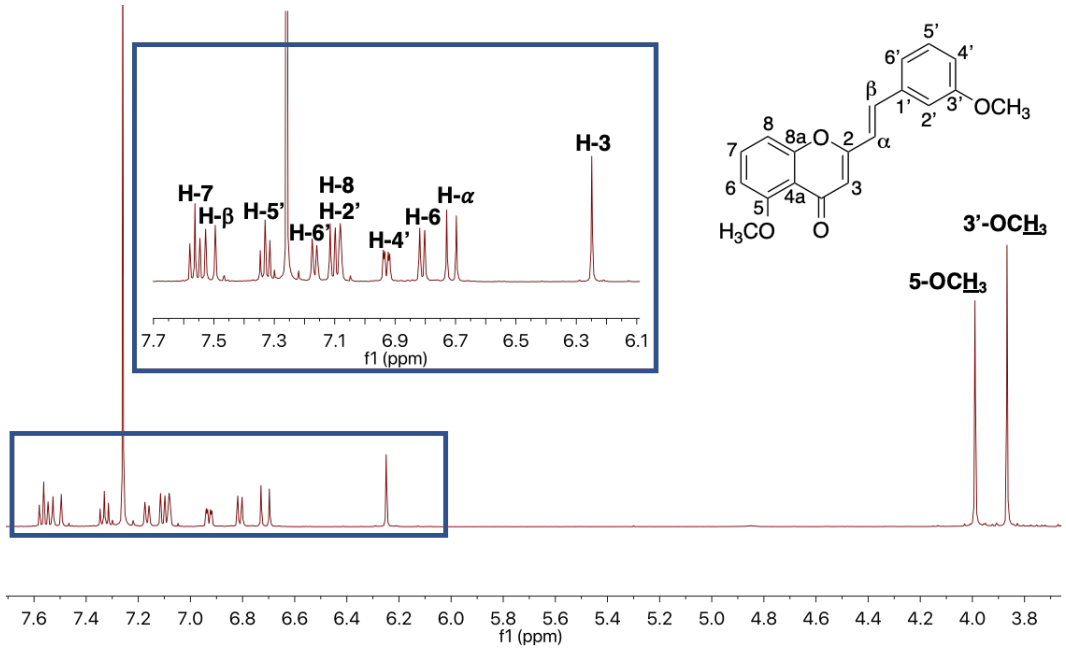

***Figure 33**. [1]H NMR spectrum of (E)-2-styrylchromone **26e** and expansion of the corresponding aromatic region (500.16 MHz, $CDCl_3$).*

All the carbons in the ^{13}C NMR spectrum of (*E*)-2-styrylchromone **26e** (**Figure 34**) were assigned based on the HSQC and HMBC spectra.

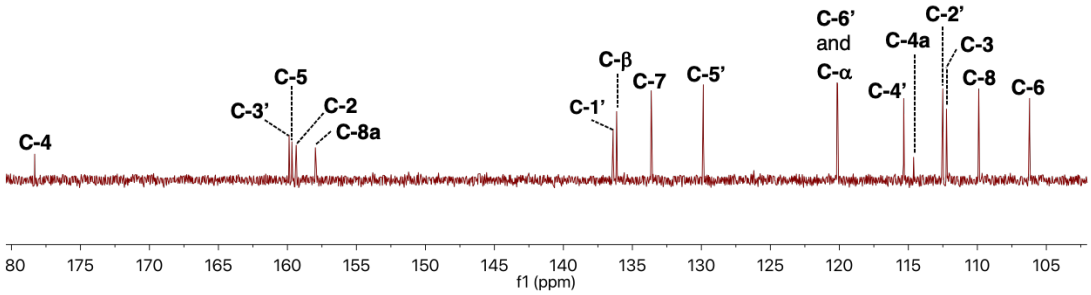

***Figure 34**. Expansion of the ^{13}C NMR spectrum of (E)-2-styrylchromone **26e** (125.77 MHz, $CDCl_3$).*

The ten protonated carbons were easily assigned based on the correlations observed in the HSQC spectrum (**Figure 35**) at δ_C = 106.3 (C-6), 110.0 (C-8), 112.4 (C-3), 112.6 (C-2'), 115.5 (C-4'), 120.2 (C-α), 120.3 (C-6'), 130.0 (C-5'), 133.7 (C-7) and 136.3 (C-β) ppm.

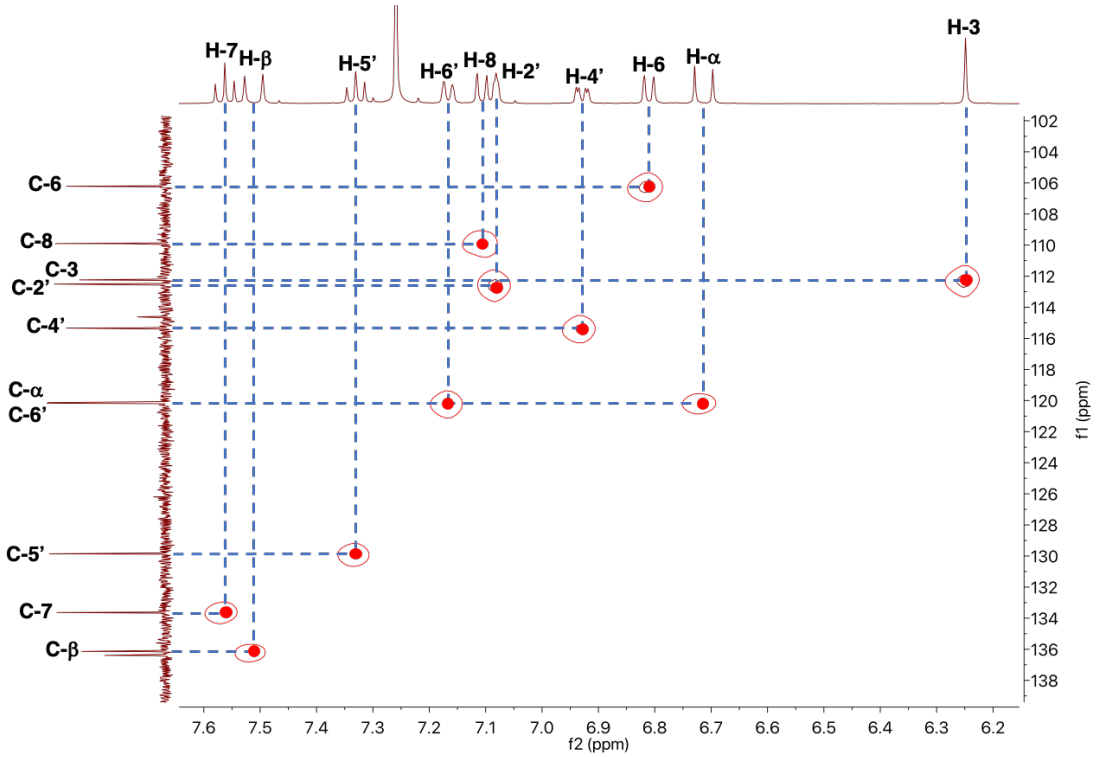

***Figure 35**. Expansion of the HSQC spectrum of (E)-2-styrylchromone **26e**.*

The non-protonated carbons were assigned based on the correlations observed in the HMBC spectrum (**Figure 36a-b**), namely H-3→C-4a and H-6→C-4a (δ_C = 110.3 ppm); H-α→C-1' (δ_C = 136.5 ppm); H-8→C-8a and H-7→C-8a (δ_C = 158.1 ppm); H-3→C-2 and H-α→C-2 (δ_C = 159.5 ppm); H-7→C-5 (δ_C = 159.8 ppm); H-5'→C-3' (δ_C = 160.0 ppm); H-3→C-4 (δ_C = 183.8 ppm).

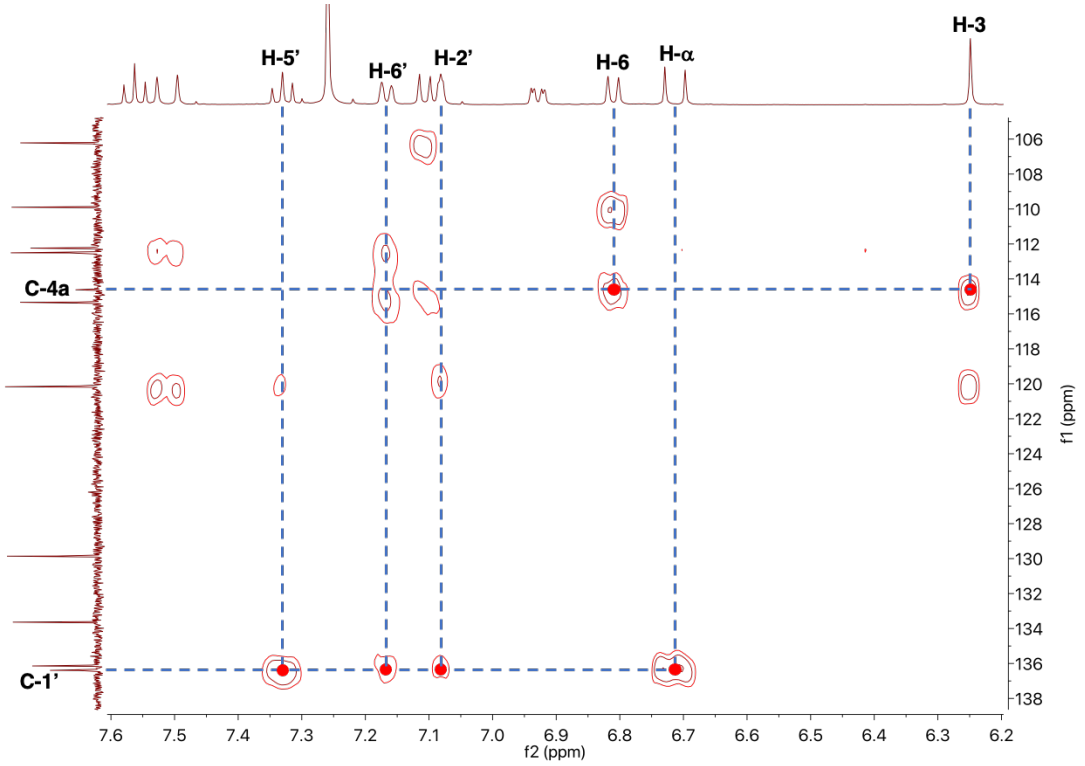

***Figure 36a**. Expansion of the HMBC spectrum of (E)-2-styrylchromone **26e**.*

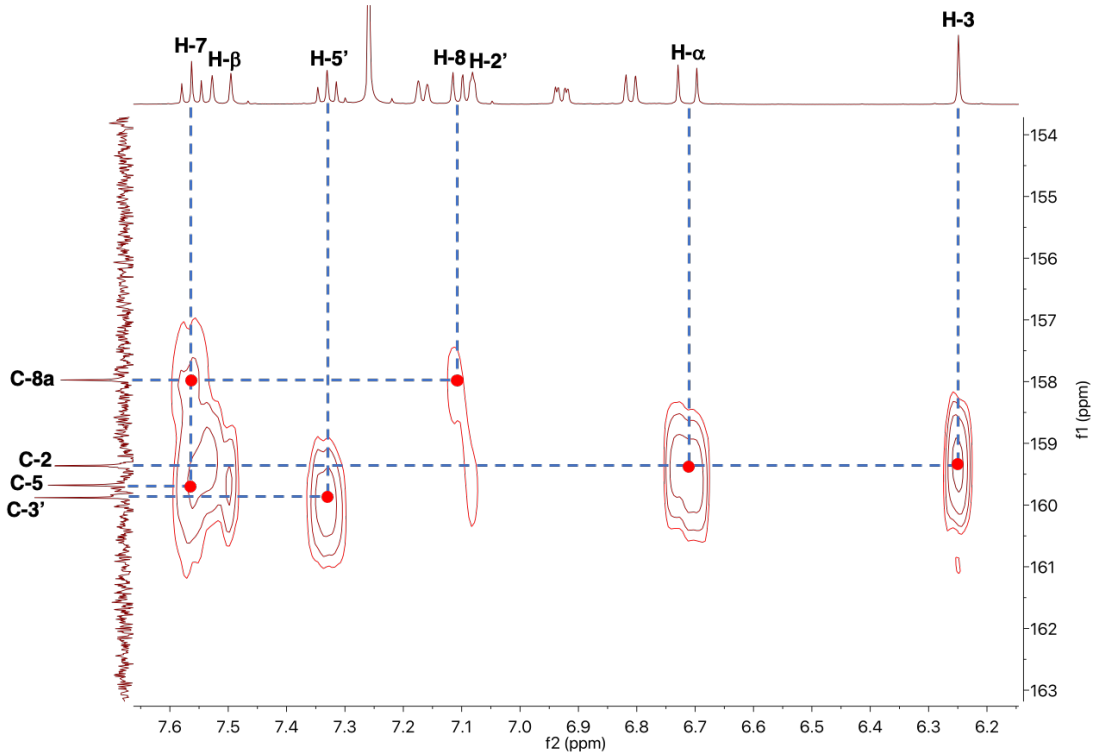

***Figure 36b**. Expansion of the HMBC spectrum of (E)-2-styrylchromone **26e**.*

2.2.7 (*E*)-5-Hydroxy-2-(3-hydroxystyryl)-4*H*-chromen-4-one (26'e)

The structure and numbering of (*E*)-5-hydroxy-2-(3-hydroxystyryl)-4*H*-chromen-4-one (**26'e**) is presented on **section 5.2**. The most important signals observed in the ^{1}H NMR spectrum of (*E*)-2-styrylchromone **26'e** (**Figure 37**) are:

- a singlet (s) at δ_H = 6.40 ppm corresponding to the resonance of the H-3 proton;
- two doublet of doublets (dd) at δ_H = 6.80 ppm and δ_H = 7.11 ppm corresponding to the resonance of protons H-6 and H-8, respectively, whose multiplicity is due to the long-distance coupling between them (^{4}J = 0.9 Hz) and the coupling of each proton with H-7 (^{3}J = 8.3 Hz);
- a doublet of doublets of triplets (ddt) at δ_H = 6.86 ppm corresponding to the resonance of the H-4' proton, whose multiplicity is due to the short distance coupling with H-5' (^{4}J = 7.8 Hz) and the long-distance coupling with H-2' (^{4}J = 2.3 Hz) and H-6' (^{4}J = 1.1 Hz);
- two doublets (d) due to the resonance of the protons H-α and H-β of the exocyclic double bond, at δ_H = 7.00 ppm and δ_H = 7.67 ppm, respectively. The multiplicity of these signals is justified by the coupling between them, and the correspondent coupling constant (^{3}J = 16.1 Hz) highlights the *trans* configuration of these two protons in compound **26'e**;
- a triplet (t) at δ_H = 7.08 ppm due to the resonance of proton H-2', whose multiplicity is due to the long-distance coupling with H-4' and H-6' (^{4}J = 2.3 Hz);
- a doublet of doublets (dd) at δ_H = 7.17 ppm corresponding to the resonance of the H-6' proton, whose multiplicity is due to the short distance coupling with H-5' (^{4}J = 7.8 Hz) and the long-distance coupling with H-4' (^{4}J = 1.1 Hz);
- two triplets (t) at δ_H = 7.27 ppm and δ_H = 7.64 ppm corresponding to the resonance of protons H-5' (^{3}J = 7.8 Hz) and H-7 (^{3}J = 8.4 Hz), respectively.

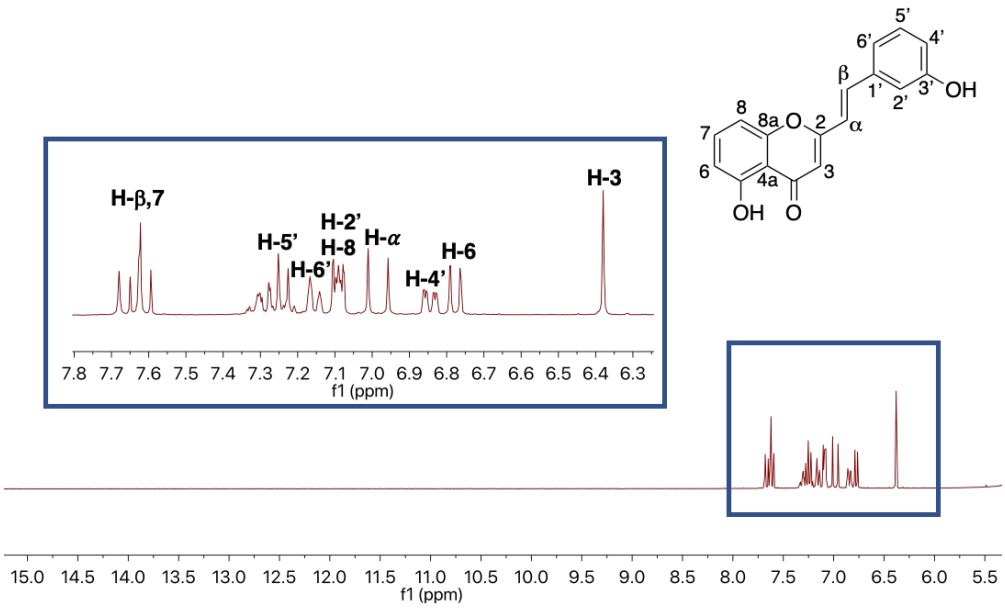

***Figure 37**. ^{1}H NMR spectrum of (E)-2-styrylchromone **26'e** and expansion of the corresponding aromatic region (300.13 MHz, MeOD).*

All the carbons in the ^{13}C NMR spectrum of (*E*)-2-styrylchromone **26'e** (**Figure 38**) were assigned based on the HSQC and HMBC spectra.

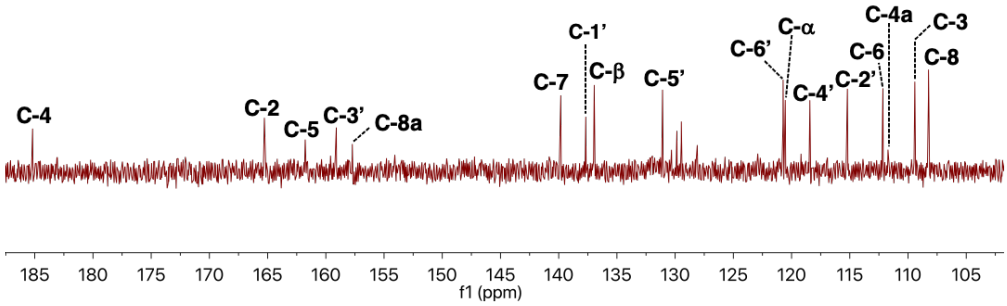

***Figure 38**. Expansion of the ^{13}C NMR spectrum of (E)-2-styrylchromone **26'e** (75.47 MHz, MeOD).*

The ten protonated carbons were easily assigned based on the correlations observed in the HSQC spectrum (**Figure 39**) at δ_C = 106.8 (C-8), 108.0 (C-3), 110.8 (C-6), 113.8 (C-2'), 117.0 (C-4'), 119.1 (C-α), 119.3 (C-6'), 129.7 (C-5'), 135.6 (C-7) and 138.4 (C-β) ppm.

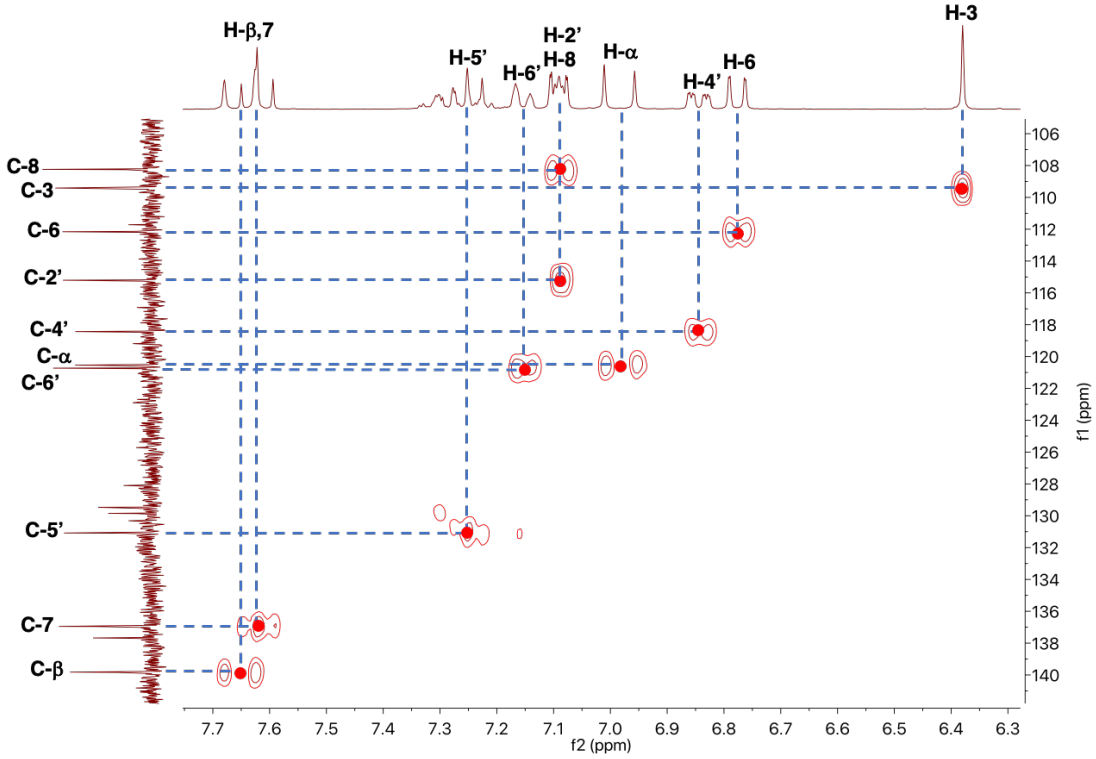

***Figure 39**. Expansion of the HSQC spectrum of (E)-2-styrylchromone **26'e**.*

The non-protonated carbons were assigned based on the correlations observed in the HMBC spectrum (**Figure 40**), namely H-3→C-4a and H-8→C-4a (δ_C = 110.3 ppm); H-α→C-1' (δ_C = 136.3 ppm); H-5'→C-3' (δ_C = 157.7 ppm); H-7→C-5 (δ_C = 160.4 ppm); H-3→C-2 and H-α→C-2 (δ_C = 163.9 ppm); H-3→C-4 (δ_C = 183.8 ppm). The remaining carbon which was not possible to identify through

the correlations observed in the 2D spectra is C-8a, since all the other non-protonated carbons were already identified.

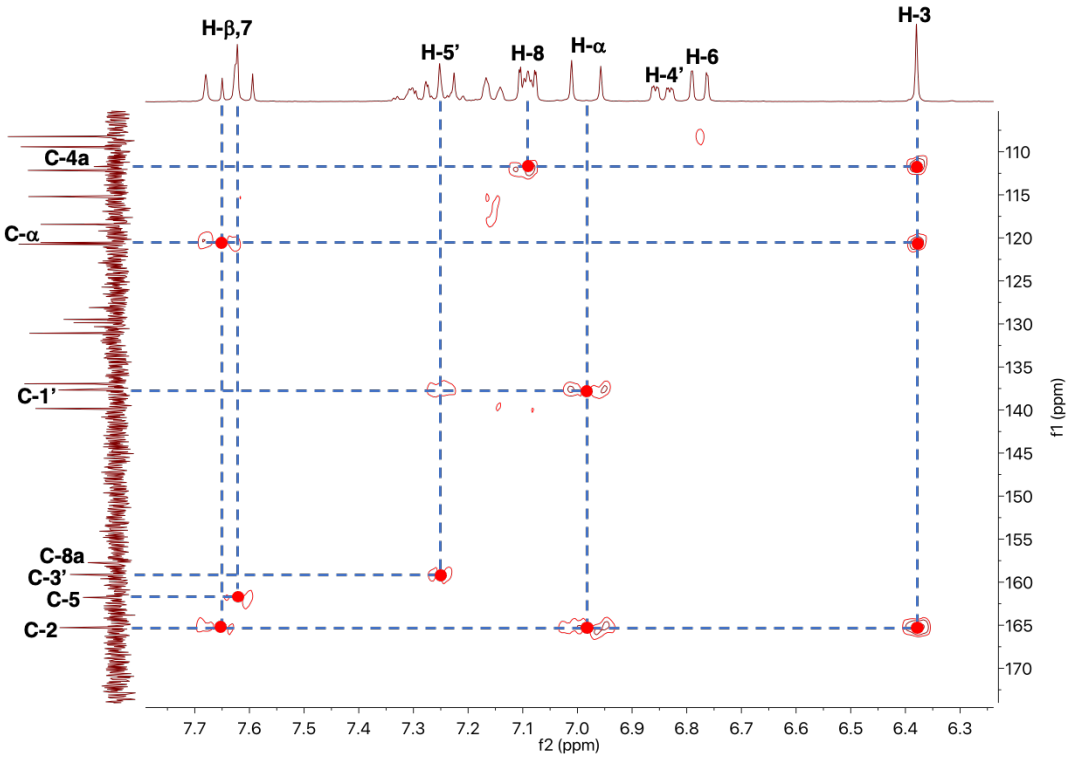

***Figure 40**. Expansion of the HMBC spectrum of (E)-2-styrylchromone **26'e**.*

2.2.8 (*E*)-5-Hydroxy-2-(3,4,5-trihydroxystyryl)-4*H*-chromen-4-one (26'f)

The structure and numbering of (*E*)-5-hydroxy-2-(3,4,5-trihydroxystyryl)-4*H*-chromen-4-one **(26'f)** is presented on **section 5.2**. The most important signals observed in the ^{1}H NMR spectrum of (*E*)-2-styrylchromone **26'f** (**Figure 41**) are:

- a singlet (s) at δ_H = 6.51 ppm corresponding to the resonance of the H-3 proton;
- a singlet (s) at δ_H = 6.67 ppm corresponding to the resonance of protons H-2',6';
- two doublets (d) at δ_H = 6.78 ppm and δ_H = 7.14 ppm corresponding to the resonance of protons H-6 and H-8, respectively, whose multiplicity is due to the coupling of each proton with H-7 (^{3}J = 8.2 Hz);
- two doublets (d) due to the resonance of the protons H-α and H-β of the double bond, at δ_H = 6.81 ppm and δ_H = 7.51 ppm, respectively. The coupling constant (^{3}J = 16.1 Hz) confirms the *trans* configuration of these two protons in compound **26'f**;
- a triplet (t) at δ_H = 7.65 ppm due to the resonance of proton H-7, whose multiplicity is due to the coupling with both protons H-6 and H-8 (^{3}J = 8.2 Hz).

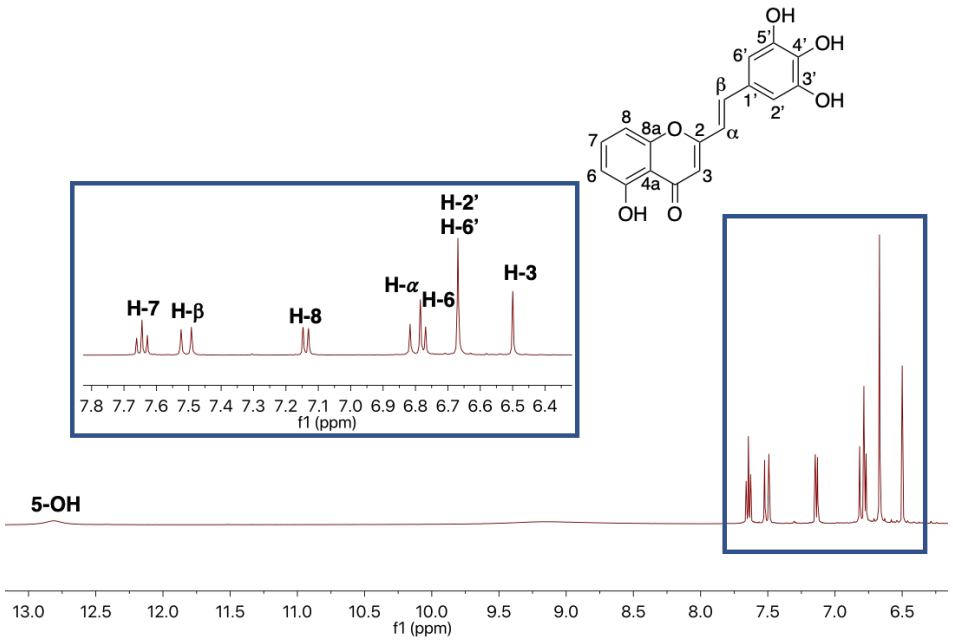

Figure 41. *^{1}H NMR spectrum of (E)-2-styrylchromone **26'f** and expansion of the corresponding aromatic region (500.16 MHz, DMSO-d_6).*

All the carbons in the ^{13}C NMR spectrum of (*E*)-2-styrylchromone **26'f** (**Figure 42**) were assigned based on the HSQC and HMBC spectra.

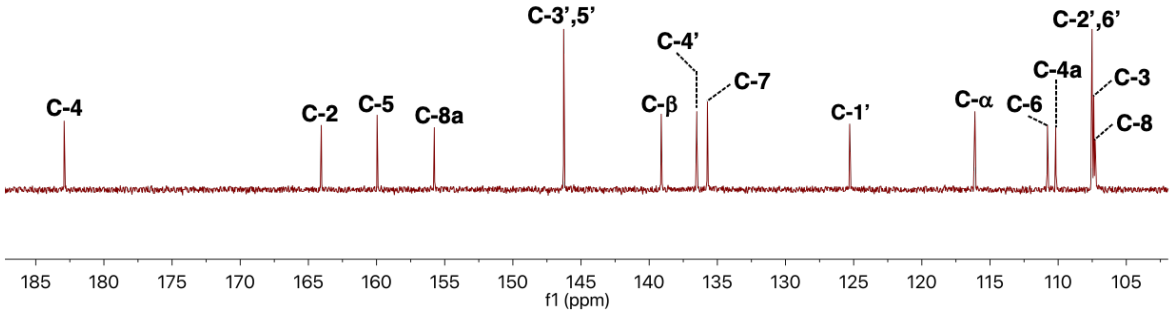

Figure 42. *Expansion of the ^{13}C NMR spectrum of (E)-2-styrylchromone **26'f** (125.77 MHz, DMSO-d_6).*

The eight protonated carbons were easily assigned based on the correlations observed in the HSQC spectrum (**Figure 43a-b**) at δ_C = 107.3 (C-8), 107.4 (C-3), 117.5 (C-2',6'), 110.8 (C-6), 125.3 (C-α), 135.7 (C-7) and 139.1 (C-β) ppm.

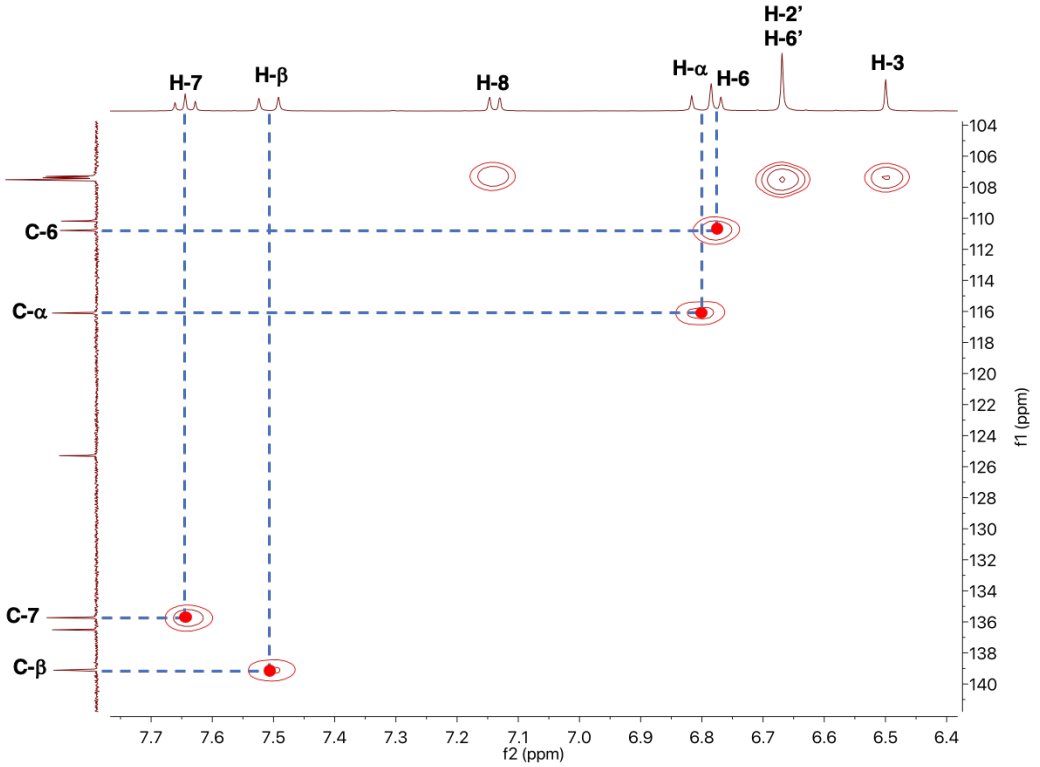

***Figure 43a**. Expansion of the HSQC spectrum of (E)-2-styrylchromone **26'f**.*

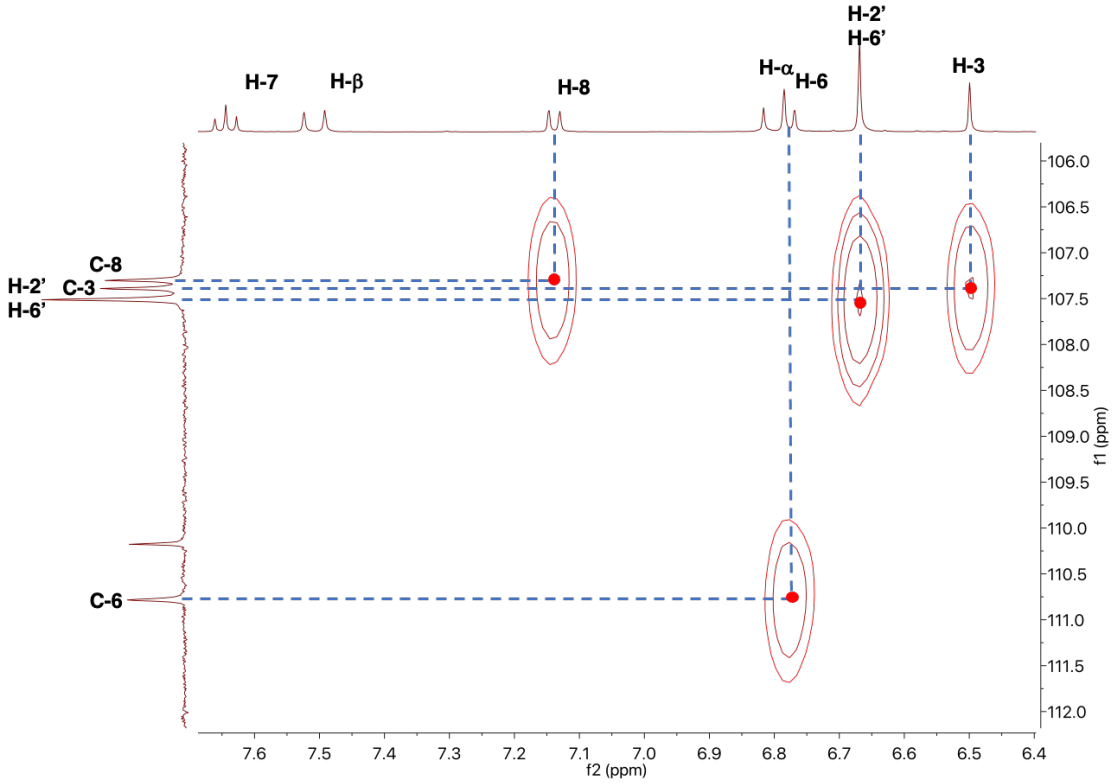

***Figure 43b**. Expansion of the HSQC spectrum of (E)-2-styrylchromone **26'f**.*

The non-protonated carbons were assigned based on the correlations observed in the HMBC spectrum (**Figure 44**), namely H-3→C-4a and H-8→C-4a (δ_C = 110.2 ppm); H-α→C-1' (δ_C = 125.9 ppm); H-2',6'→C-4' (δ_C = 136.5 ppm); H-2',6'→C-3',5' (δ_C = 146.3 ppm); H-8→C-8a and H-7→C-8a (δ_C = 155.8 ppm); H-7→C-5 (δ_C = 160.0 ppm); H-3→C-2, H-α→C-2 and H-β→C-2 (δ_C = 164.1 ppm); H-3→C-4 (δ_C = 182.9 ppm).

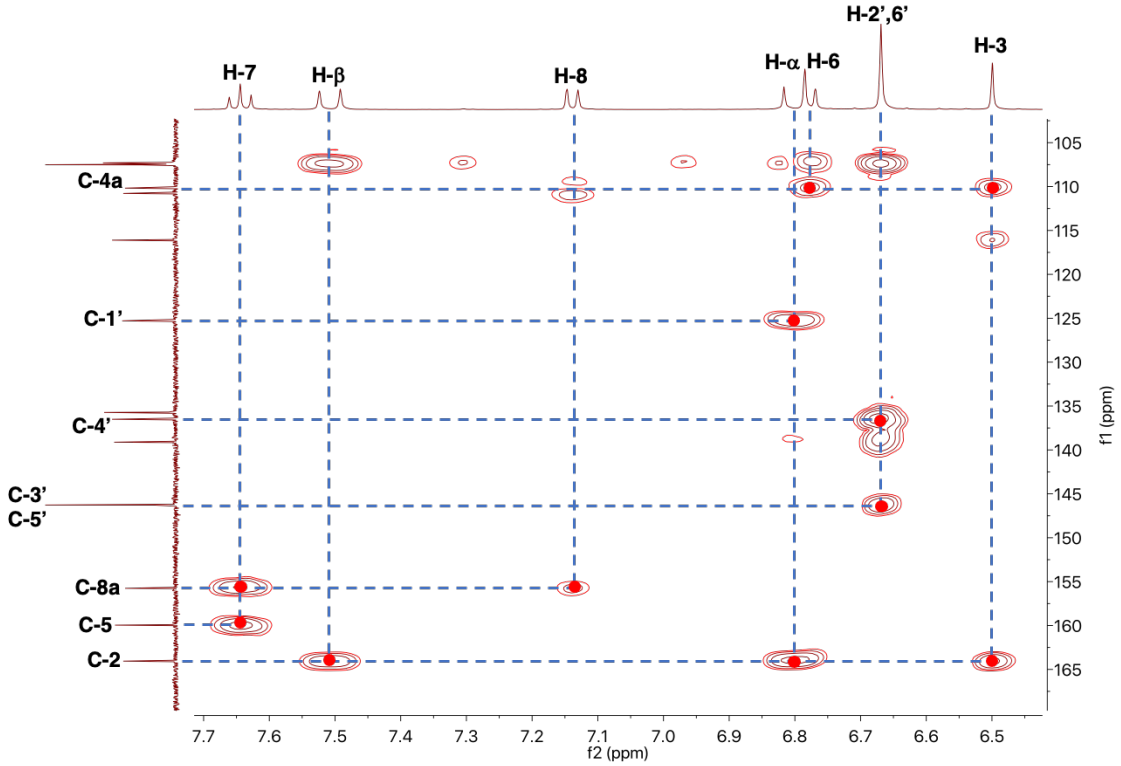

***Figure 44**. Expansion of the HMBC spectrum of (E)-2-styrylchromone **26'f**.*

2.2.9 (*E*)-2-(3-Hydroxystyryl)-4*H*-chromen-4-one (27'a)

The structure and numbering of (*E*)-2-(3-hydroxystyryl)-4*H*-chromen-4-one **(27'a)** is presented on **section 5.2**. The most important signals observed in the ^{1}H NMR spectrum of (*E*)-2-styrylchromone **27'a** (**Figure 45**) are:

- a singlet (s) at δ_H = 6.42 ppm corresponding to the resonance of the H-3 proton;
- two doublets (d) due to the resonance of the protons H-α and H-β of the double bond, at δ_H = 6.83 ppm and δ_H = 7.58 ppm, respectively. The coupling constant (^3J = 16.2 Hz) confirms the *trans* configuration of these two protons in compound **27'a**;
- two doublets (d) at δ_H = 6.86 ppm and δ_H = 7.06 ppm corresponding to the resonance of protons H-4' and H-6', respectively, whose multiplicity is due to the coupling of each proton with H-5' (^3J = 7.5 Hz);
- a singlet (s) at δ_H = 7.09 ppm corresponding to the resonance of proton H-2';

- a triplet (t) at δ_H = 7.41 ppm due to the resonance of proton H-6, whose multiplicity is due to the coupling with both protons H-5 and H-7 (^3J = 7.7 Hz);
- a doublet of doublets of doublets (ddd) at δ_H = 7.70 ppm corresponding to the resonance of the H-7 proton, whose multiplicity is due to the short distance coupling with H-6 (^3J = 7.7 Hz) and H-8 (^3J = 8.2 Hz) and the long-distance coupling with H-5;

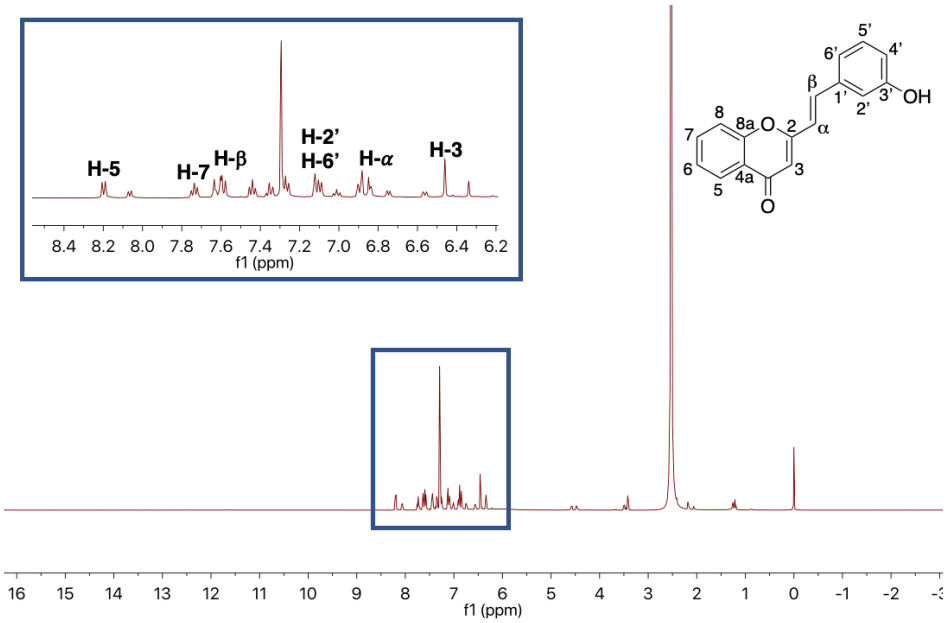

***Figure 45**. [1]H NMR spectrum of (E)-2-styrylchromone **27'a** and expansion of the corresponding aromatic region (500.16 MHz, $CDCl_3$).*

All the carbons in the ^{13}C NMR spectrum of (*E*)-2-styrylchromone **27'a** (**Figure 46**) were assigned based on the HSQC and HMBC spectra.

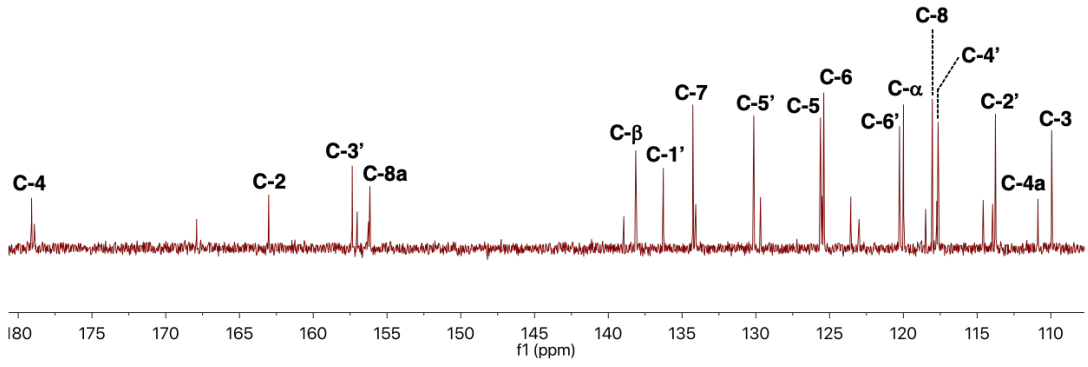

***Figure 46**. Expansion of the ^{13}C NMR spectrum of (E)-2-styrylchromone **27'a** (125.77 MHz, $CDCl_3$).*

The eleven protonated carbons were easily assigned based on the correlations observed in the HSQC spectrum (**Figure 47**) at δ_C = 109.9 (C-3), 113.8 (C-2'), 117.6 (C-4'), 118.0 (C-8), 120.0 (C-α), 120.3 (C-6'), 125.4 (C-6), 125.6 (C-5), 130.1 (C-5'), 134.3 (C-7) and 138.1 (C-β) ppm.

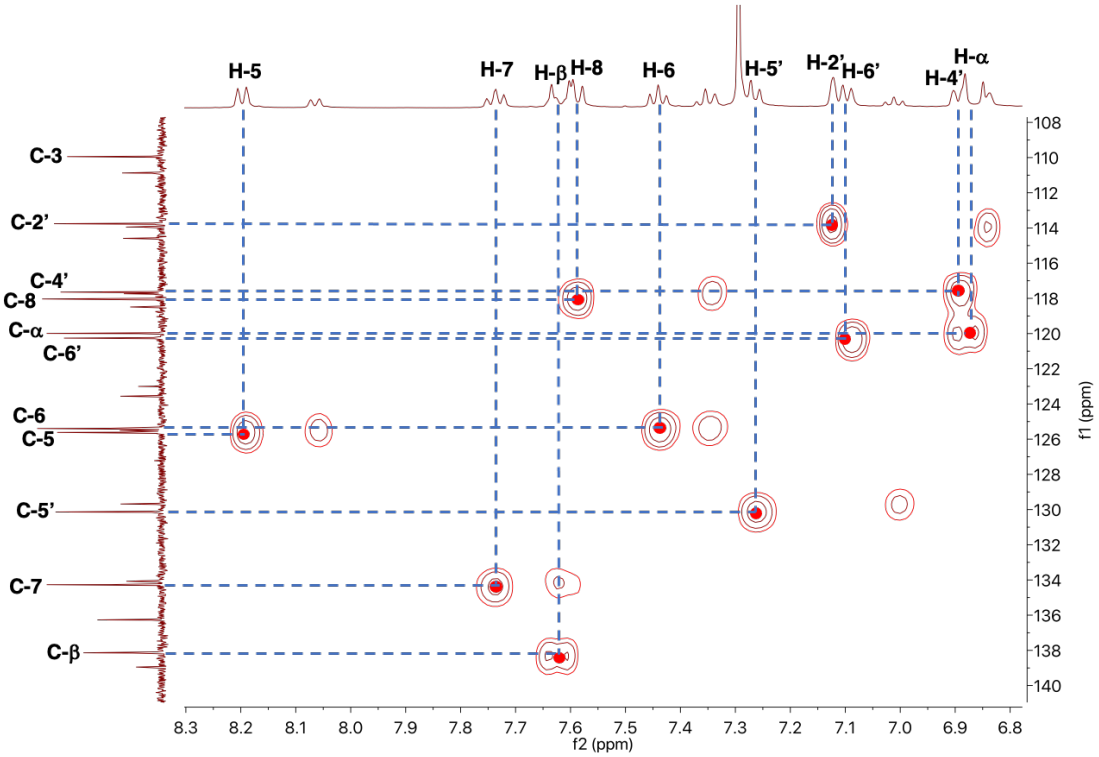

***Figure 47**. Expansion of the HSQC spectrum of (E)-2-styrylchromone **27'a**.*

The non-protonated carbons were assigned based on the correlations observed in the HMBC spectrum (**Figure 48**), namely H-5'→C-1' (δ_C = 136.3 ppm); H-7→C-8a and H-5→C-8a (δ_C = 156.2 ppm); H-5'→C-3' (δ_C = 157.4 ppm); H-α→C-2 and H-β→C-2 (δ_C = 163.0 ppm). The two remaining signals correspond to C-4a at δ_C = 110.9 ppm, and to C-4 at δ_C = 179.1 ppm, which is the most deprotected carbon.

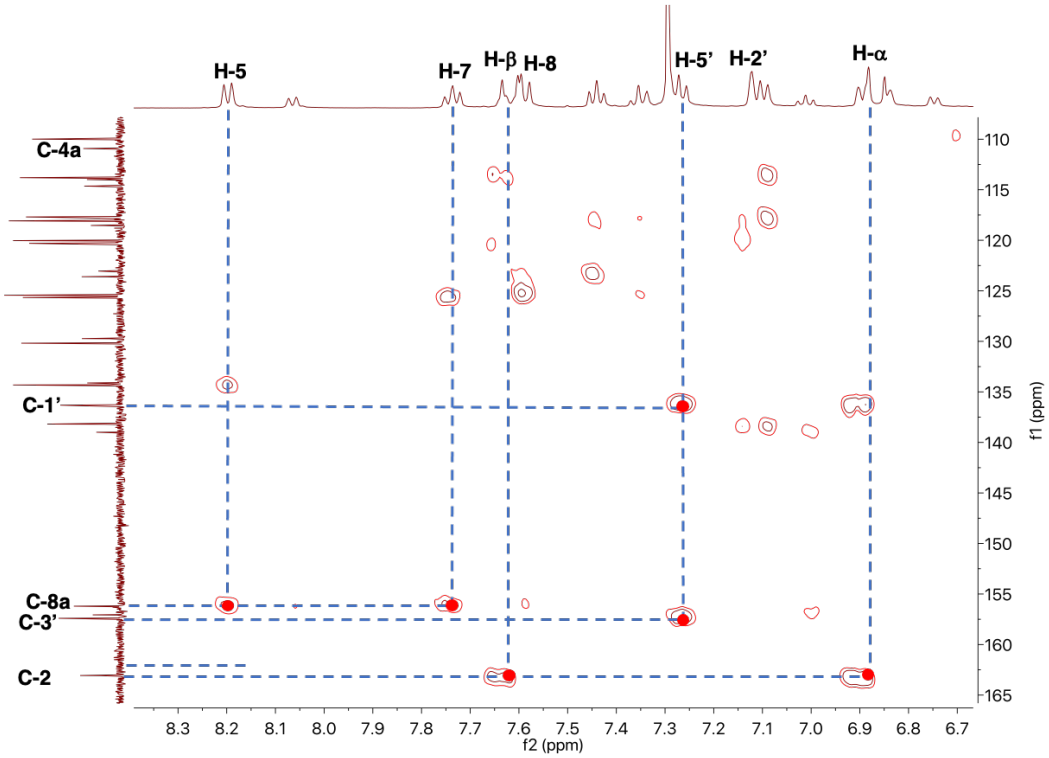

***Figure 48**. Expansion of the HMBC spectrum of (E)-2-styrylchromone **27'a**.*

Table 4. *Chemical shifts (δ in ppm, from TMS) of ^{1}H NMR of the synthesized (E)-2-styrylchromones for biological assays.*

	11'b	**26'a**	**26'b**	**26'c**	**26'd**	**26e**	**26'e**	**26'f**	**27'a**
H-3	6.15	6.28	6.27	6.30	6.35	6.25	6.40	6.51	6.42
H-5	7.39[a]	12.54[a]	12.55[a]	12.51[a]	-----[d]	4.00[b]	-----[d]	12.82[a]	8.16
H-6	6.36	6.80	6.81	6.81	6.79	6.81	6.80	6.78	7.41
H-7	3.96[b]	7.55	7.55	7.56	7.63	7.57	7.64	7.65	7.70
H-8	6.52	6.97	6.96	7.00	7.11	7.11	7.11	7.14	7.55
H-α	6.62	6.77	6.76	6.95	7.14	6.71	7.00	6.81	6.83
H-β	7.56	7.56	7.52	7.72	8.03	7.51	7.67	7.51	7.58
H-2'	7.48	7.36-7.38	7.68	-----	-----[d]	7.08	7.10	6.57	7.09
H-3'	6.88	-----	-----	7.40	6.90	3.87[b]	-----[d]	-----[d]	-----[d]
H-4'	7.39[c]	7.43-7.48	-----	7.22	7.24	6.93	6.86	-----[d]	6.86
H-5'	6.88	7.36-7.38	7.51	7.40	6.91	7.33	7.27	-----[d]	7.24
H-6'	7.48	7.58-7.59	7.42	-----	7.62	7.17	7.17	6.57	7.06

[a] The chemical shift belongs to the proton of the 5-OH group.

[b] The chemical shift of the O$C\underline{H}_3$ protons linked to C-5, C-7 and C-3'.

[c] The chemical shift belongs to the proton of the 4'-OH group.

[d] The chemical shifts and signals for the OH groups were not found on the ^{1}H NMR spectra.

Table 5. *Chemical shifts (δ in ppm, from TMS) of ^{13}C NMR of the synthesized (E)-2-styrylchromones for biological assays.*

	11'b	**26'a**	**26'b**	**26'c**	**26'd**	**26e**	**26'e**	**26'f**	**27'a**
C-2	163.3	162.2	161.9	161.8	164.8	159.5	163.9	164.1	163.0
C-3	107.3	109.6	109.8	110.3	107.4	112.4	108.0	107.4	109.9
C=O	182.6	183.6	183.6	183.7	183.8	178.4	183.8	182.9	179.1
C-4a	105.5	111.0	111.0	111.1	110.3	114.7	110.3	110.2	110.9
C-5	161.6	160.9	160.9	160.8	160.4	159.8[a]	160.4	160.0	125.6
C-6	98.0	111.5	111.6	111.5	110.7	106.3	110.8	110.8	125.4
C-7	165.6[b]	135.5	135.6	135.6	135.4	133.7	135.6	135.7	134.3
C-8	92.6	106.9	106.9	107.1	106.8	110.0	106.8	107.3	118.0
C-8a	157.6	156.2	156.1	156.2	156.4	158.1	156.3	155.8	156.2
C-α	116.1	121.1	121.4	128.1	118.7	120.2	119.1	125.3	120.0
C-β	138.0	136.3	135.2	131.5	134.3	136.3	138.4	139.1	138.1
C-1'	126.5	136.6	134.8	132.2	121.8	136.5	136.3	125.9	136.3
C-2'	129.7	130.3	129.4	135.0	156.9	112.6	113.8	117.5	113.8
C-3'	116.0	135.1	133.5	129.0	115.7	160.0[c]	157.7	146.3	157.4
C-4'	159.2	126.0	134.0	129.8	131.1	115.5	117.0	136.5	117.6
C-5'	116.0	130.0	131.1	129.0	119.5	130.0	129.7	146.3	130.1
C-6'	129.7	127.6	126.7	135.0	128.3	120.3	119.3	117.5	120.3

[a] The chemical shift of the carbon atom of the 5-O<u>C</u>H3 group appears at 56.5 ppm.
[b] The chemical shift of the carbon atom of the 7-O<u>C</u>H3 group appears at 55.8 ppm.
[c] The chemical shift of the carbon atom of the 3'-O<u>C</u>H3 group appears at 55.4 ppm.

Chapter 3 - Biological Effects of (*E*)-2-Styrylchromones in the Oxidative Burst of Human Monocytes

3.1 General considerations

A library of nine synthesized (*E*)-2-styrylchromones (**Figure 49**) was submitted to several studies, aiming to evaluate these compounds' inhibitory effects against the production of reactive species by human monocytes. Considering that the main goal stands on *in vitro* biological assays, a previous *in chemico* assay was performed, regarding the antioxidant activity and radical scavenging capacity of the compounds of interest, as an indicator of these (*E*)-2-styrylchromones' antioxidant potential, before testing them on human cells.

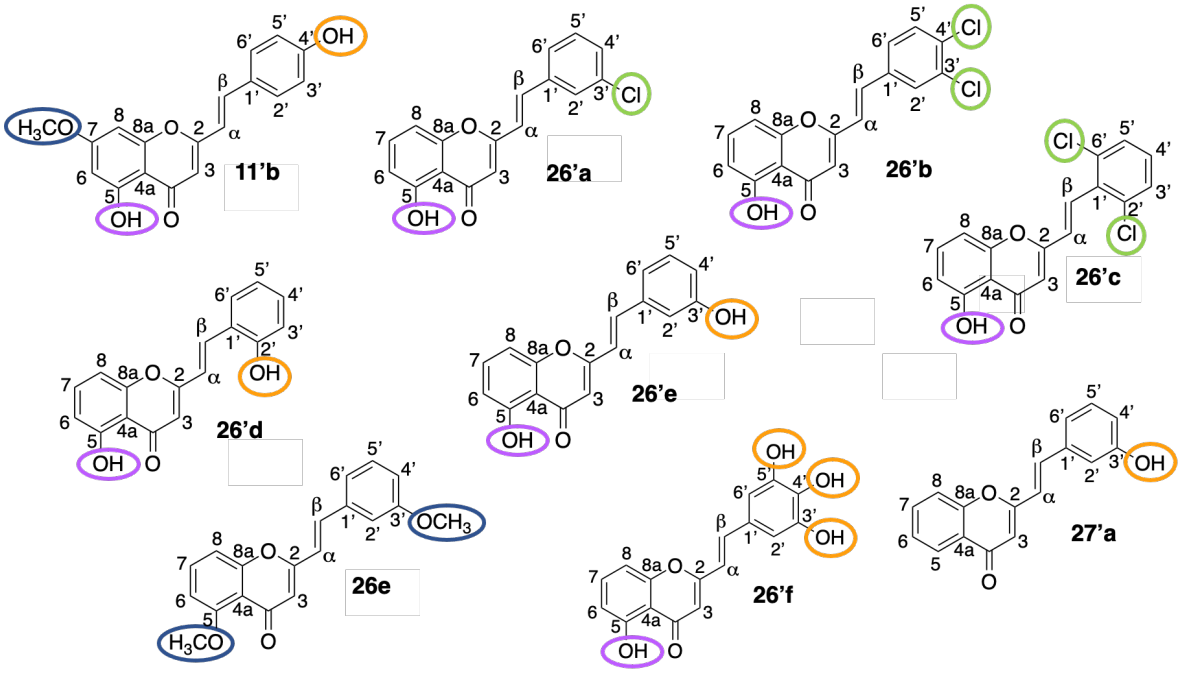

***Figure 49**. Structures of the nine synthesized (E)-2-styrylchromones in study.*

3.2 *In chemico* assays

In order to have more concise studies, the first biological assay was based on the •NO radical scavenging, since this is one of the most RS associated with the inflammatory process. Moreover, •NO is produced in monocytes in a reaction catalyzed by iNOS (inducible nitric oxide synthase), as demonstrated in **Chapter 1**, and is an important precursor of other RNS, in particular of $NOOH^-$, which is formed in a reaction with $O_2^{\bullet -}$. As such, the chosen assay is not only important to understand the compounds effects regarding •NO, but also all the other RS involved. In this section, will be presented the principle of the method use, as well as the results obtained, whereas the detailed procedures are described in **Chapter 5** - **Experimental Section**.

3.2.1 •NO scavenging assay

According to the Griess Illosvoy reaction, nitric oxide generated from aqueous sodium nitroprusside (SNP) solution interacts with oxygen to produce nitrite ions which may be measured spectrophotometrically, at 540 nm, against a blank sample. The absorbance values are then graphically represented, and the IC_{50} value of each compound is obtained from a logarithmic tendency curve.[101,102]

This assay was performed with gallic acid as standard (reference compound) due to the optimization of the method and also because this compound is a well-known •NO inhibitor. The tested concentrations for both control and compounds in study were optimized during the assay. As such, the final tested concentrations for gallic acid were between 0.006 μM and 0.39 μM, while for the compounds were between 3.125 μM and 400 μM.

Only four of the tested compounds, including the reference sample, were active, so it was only possible to determine the IC_{50} values for three compounds. Each graphic was adjusted according to the results since some concentrations were similar to the previous or next ones. The detailed results are represented in **Figures 50-53** and in **Table 6**.

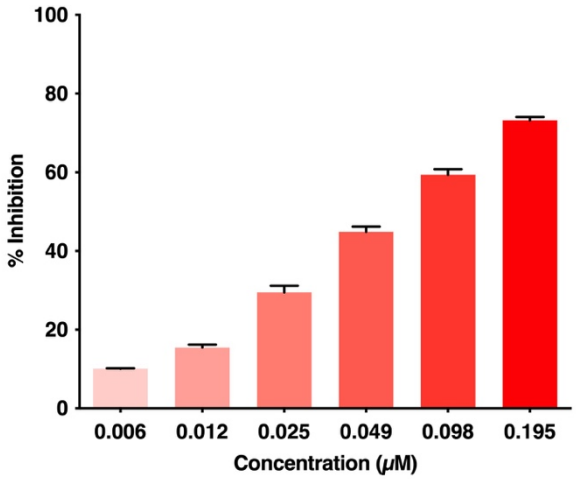

***Figure 50**. Graphical representation of the percentage (%) of scavenging of •NO versus concentration, for gallic acid (standard).*

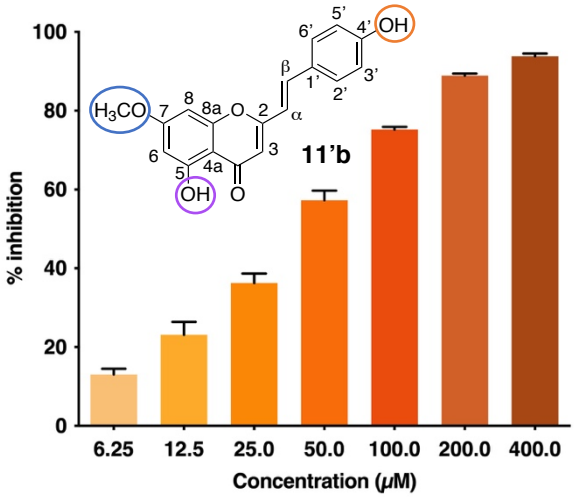

Figure 51. *Graphical representation of the percentage (%) of scavenging of •NO versus concentration, for compound* ***11'b***.

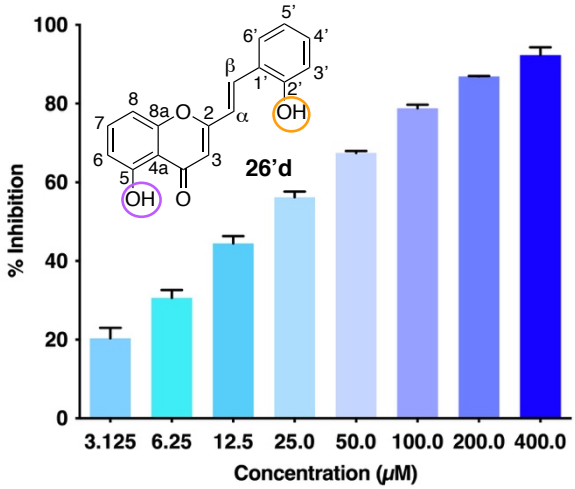

Figure 52. *Graphical representation of the percentage (%) of scavenging of •NO versus concentration, for compound* ***26'd***.

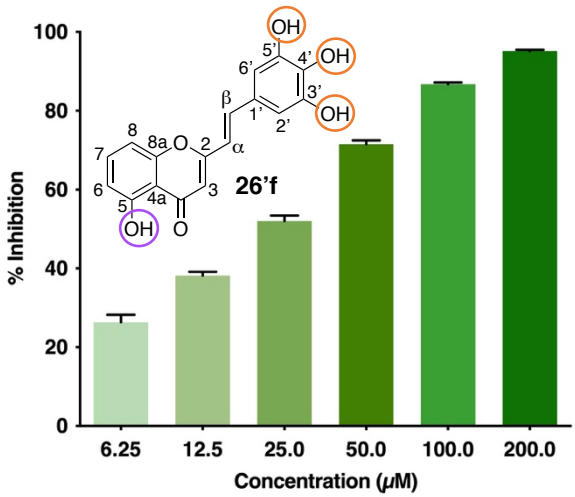

Figure 53. *Graphical representation of the percentage (%) of scavenging of •NO versus concentration, for compound* ***26'f***.

***Table 6**. Percentage (%) of inhibition for the maximum tested concentration for each compound and IC_{50} values in μM. The results are given as mean ± SEM (μM). *No activity (NA).*

Compound	Maximum tested concentration (μM)	Percentage (%) of inhibition	IC_{50} values as mean ± SEM (μM)
Gallic Acid	**0.195**	**76.7**	**0.06927 ± 0.003940**
11'b	**400.0**	**94.3**	**37.72 ± 3.360**
26'a	400.0	NA*	-------
26'b	400.0	NA*	-------
26'c	400.0	NA*	-------
26'd	**400.0**	**95.8**	**17.95 ± 1.109**
26e	400.0	NA*	-------
26'e	400.0	NA*	-------
26'f	**400.0**	**98.5**	**18.79 ± 0.08452**
27'a	400.0	NA*	-------

The IC_{50} value obtained for the standard compound (0.06927 ± 0.003940 μM) was very low when compared to those of the compounds. For this reason, the IC_{50} value for gallic acid is not represented in **Figure 54**.

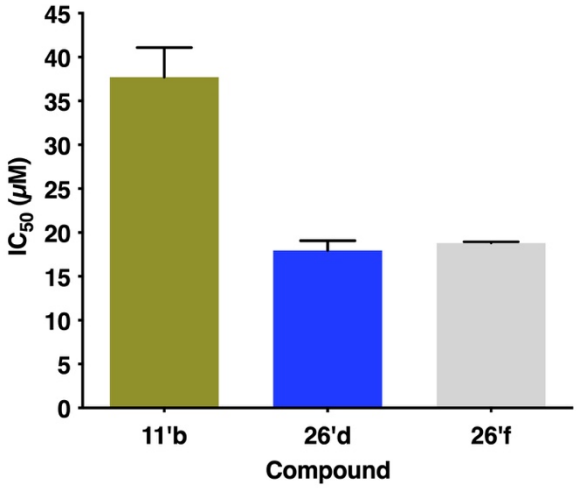

***Figure 54**. Graphical representation of the IC_{50} values in μM for the active compounds on the •NO scavenging assay. The results are given as the mean ± SEM (μM).*

3.3 *In vitro* biological assays

Regarding the *in vitro* biological assays, several studies and detailed procedures had to be previously undertook for the evaluation of the inhibitory effect of (*E*)-2-styrylchromones against PMA-induced RS production by human monocytes itself. In this section, will be presented the principles of all the methods used, as well as the results obtained, and the detailed procedures are described in **Chapter 5 – Experimental Section**.

3.3.1 UV/Vis absorption and emission spectra of (*E*)-2-styrylchromones

All chemical compounds absorb light, and some can also emit light. For this reason, it is crucial to know the absorption and emission spectra of each compound to avoid any type of interference in further spectrophotometric determinations.[103] Therefore, absorption and emission spectra were obtained for 25.0 μM, 12.5 μM and 6.25 μM concentrations of each (*E*)-2-styrylchromone.

The concentrations of (*E*)-2-styrylchromones that not only presented absorbances below 0.1 in the range of wavelengths between 431-500 nm but also very low values of emission, were chosen for the following *in vitro* studies (**Figures 55-56** and **Table 7**). Each study corresponded to, at least, two independent assays.

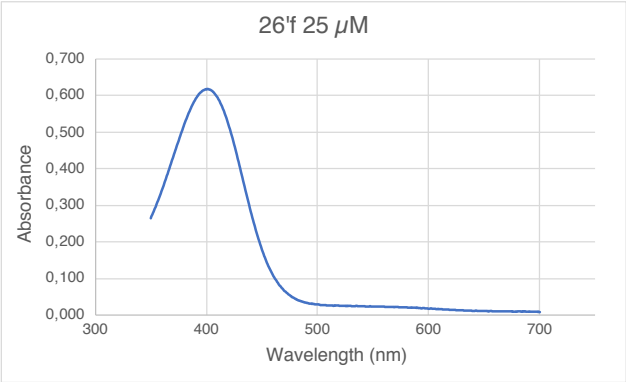

***Figure 55**. Graphical representation of a UV-Vis absorption spectrum with interference between 431-500 nm.*

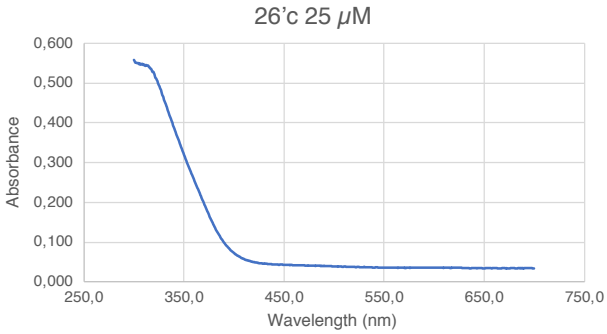

***Figure 56**. Graphical representation of a UV-Vis absorption spectrum with no interference between 431-500 nm.*

Regarding the emission spectra, these were not presented since they were dependent on the maximum absorbance value. Below, in **section 3.3.4.1** is described a more accurate method for the interference of the compounds, when it comes to emission.

***Table 7**. Maximum concentration for the following studies, selected according to UV-Visible absorption and emission spectra of (E)-2-styrylchromones.*

Compound	11'b	26'a	26'b	26'c	26'd	26e	26'e	26'f	27'a
Maximum tested concentration (μM)	≤ 25.0	≤ 25.0	≤ 25.0	≤ 25.0	≤ 25.0	≤ 25.0	≤ 25.0	≤ 25.0	≤ 25.0
Maximum concentration without interference (μM)	≤ 25.0	≤ 25.0	≤ 12.5	≤ 12.5	≤ 25.0	≤ 25.0	≤ 12.5	≤ 12.5	≤ 25.0

3.3.2 Isolation of monocytes from human blood

The monocytes, the cells required for these *in vitro* biological studies, were isolated from all the other human blood components, based on the density gradient centrifugation method described by Bland *et al.*, bearing in mind that some modifications were made.[104,105] This method relies on the principle of separation of blood components according to their different densities, when a centrifugal force is applied. Therefore, the erythrocytes are disposed at the bottom of the tube, followed by the granulocytes, and the agranulocytes and platelets above all (**Figure 57**).

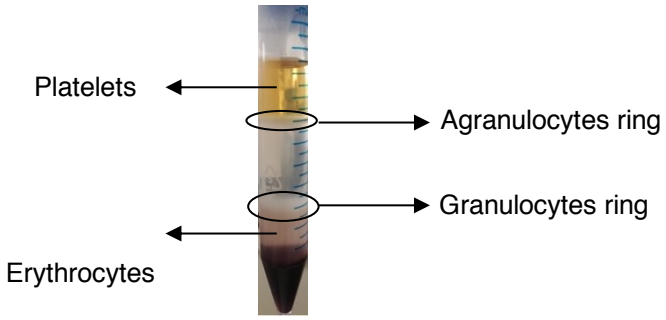

***Figure 57**. Separation of blood components based on the density gradient centrifugation method.*

3.3.3 Cell count and viability assessment

The trypan blue dye exclusion method is one of the most common methods used to determine the number of viable cells present in a cell suspension. This particular reagent is an organic azo dye, hydrophilic and negatively charged, used to identify only non-viable cells.[106] It is based on the principle that viable cells possess intact cell membranes which precludes the penetration of the trypan blue dye. The opposite occurs with non-viable cells, since their membranes are damaged, allowing the entrance of trypan blue dye, which binds to the intracellular proteins and grants them a bluish color.[107]

Once the suspension of cells mixed with trypan blue dye is observed at the microscope, a viable cell will have a clear cytoplasm whereas a non-viable cell will have a bluish cytoplasm (**Figure 58**).[107] Each study corresponded to, at least, two independent assays.

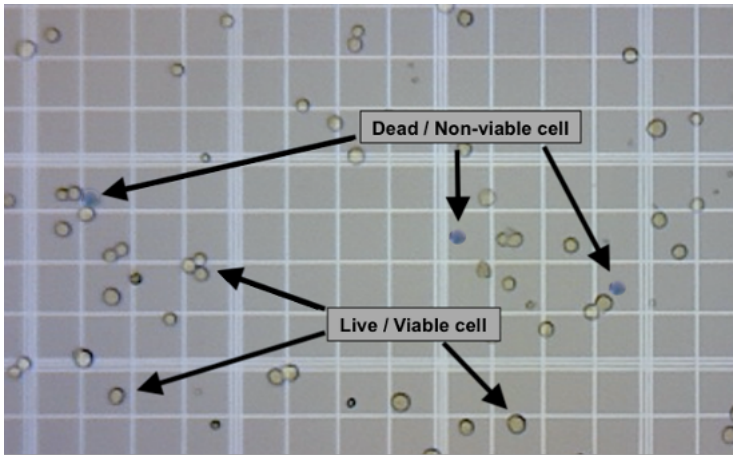

***Figure 58**. Microscopic observation of monocytes after the trypan blue dye exclusion method (400x).*

3.3.4. Cell death assessment by flow cytometry

In the early stages of apoptosis, changes occur at the cell surface (**Figure 59A**), being the translocation of phosphatidylserine (PS) from the inner side of the plasma membrane to the outer layer, by which PS becomes exposed at the external surface of the cell, one of those major changes. This translocation is also a characteristic of the necrotic process, although a loss of integrity of the membrane in this stage marks the difference between cell apoptosis and necrosis.[108–111]

Annexin V is a phospholipid binding-protein with high affinity for negatively charged phospholipids, in the presence of Ca^{2+}, in particular for PS. Therefore, this protein can be labeled with fluorescein isothiocyanate (FITC) and used as a sensitive probe for PS exposure upon the cell membrane, and consequently for apoptosis detection, considering the emission of fluorescence when Annexin V binds to PS (**Figure 59B**). On the other hand, the nuclear fluorescent marker propidium iodine (PI) is used to detect necrotic cells. Due to its high molecular weight, PI is only able to penetrate the cells if the cell membrane is damaged, which occurs during necrosis. Once the cell membrane begins to disintegrate, PI binds to DNA strands, intercalating between the bases, emitting fluorescence (**Figure 59C**).[110,111]

The fluorescence emitted by both probes during these two different stages of cell death can be detected by flow cytometry, making them good indicators of cell viability.[110]

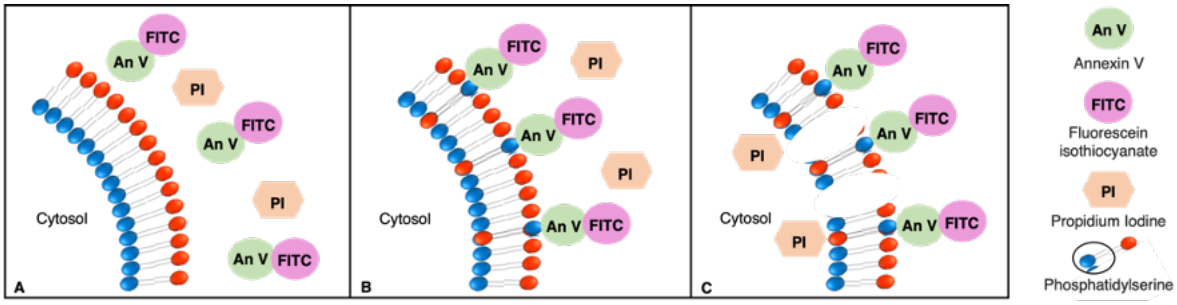

***Figure 59**. Illustration of Live Cell (A) and phosphatidylserine, Apoptotic Cell (B) detected by Annexin V FITC binding and Necrotic Cell (C) detected by PI uptake.*

3.3.4.1 Effects of (*E*)-2-styrylchromones on human monocytes cell death

The knowledge of possible effects of the selected (*E*)-2-styrylchromones on human monocyte cell death is of extreme importance and required for the *in vitro* studies, considering that the maximum concentrations tested must not interfere with the probes nor promote cytotoxic effects.

In this line of thought, the nine (*E*)-2-styrylchromones in study were submitted to a flow cytometry assay to reject concentrations that would interfere with the fluorescence emission of the probes. Furthermore, **Figure 60** shows a representative flow cytometry plot for cell population (**A**) and the forward scatter (FSC-A) and side scatter (SSC-A) parameters used to measure the relative size of cells (through the measurement of the amount of the laser beam that passes around the cell) and the granularity of the cells (by measuring the amount of the laser beam that bounces off particles inside of the cell), respectively. The plot on the right side (**B**) of **Figure 60** is an example of how a flow cytometry plot must be when the concentrations of the compounds have no interference with the fluorescence emission of the probes. This assay is a more precise study of the compounds' fluorescence emission, providing a more precise result when compared to the spectrophotometry method. The results obtained for the interference assay and other crucial information are further presented in **Table 8,** in **section 3.3.4.2**. Each study corresponded to, at least, two independent assays.

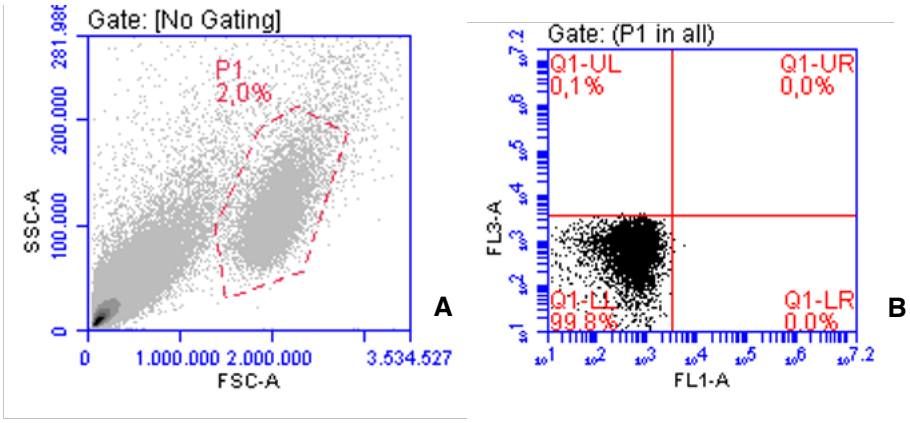

***Figure 60**. Representative flow cytometry plots for cell population (**A**) and control of fluorescence emission interference (**B**).*

3.3.4.2 Measurement of cell death by Annexin V binding and PI uptake

According to the results obtained in **section 3.3.4.1**, a cytotoxic assay by flow cytometry was performed based on the principles aforementioned in **section 3.3.4**., aiming to select the maximum concentration of each compound that would not affect the monocytes' viability. The specific fluorescence intensity of Annexin V FITC positive cells, measured in channel 1 (FL1-A), provided information about the percentage of apoptotic cells while the specific fluorescence intensity of PI positive cells, measured in channel 3 (FL3-A), provided information about the percentage of necrotic cells in the monocytes' population (**Figure 61**). Each study corresponded to, at least, two independent assays.

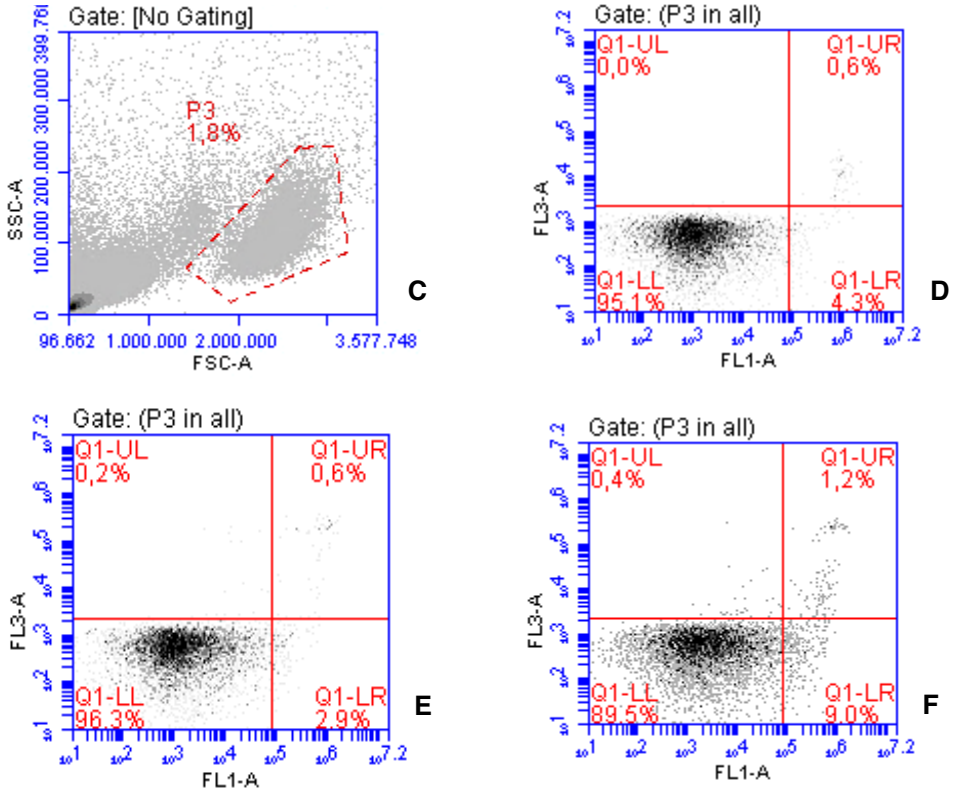

***Figure 61**. Representative flow cytometry plots of controls for cell population (**C**) and monocytes' viability (**D**) and the effects of different studied compounds' concentrations on cell viability: plot (**E**) shows a proper concentration while plot (**F**) demonstrates a cytotoxic concentration, with higher cell death percentage.*

In addition, the percentage of live cells obtained by flow cytometry for each one of the tested (*E*)-2-styrylchromones, is graphically represented in **Figure 62**, and the results given the as mean plus standard error of the mean (SEM).

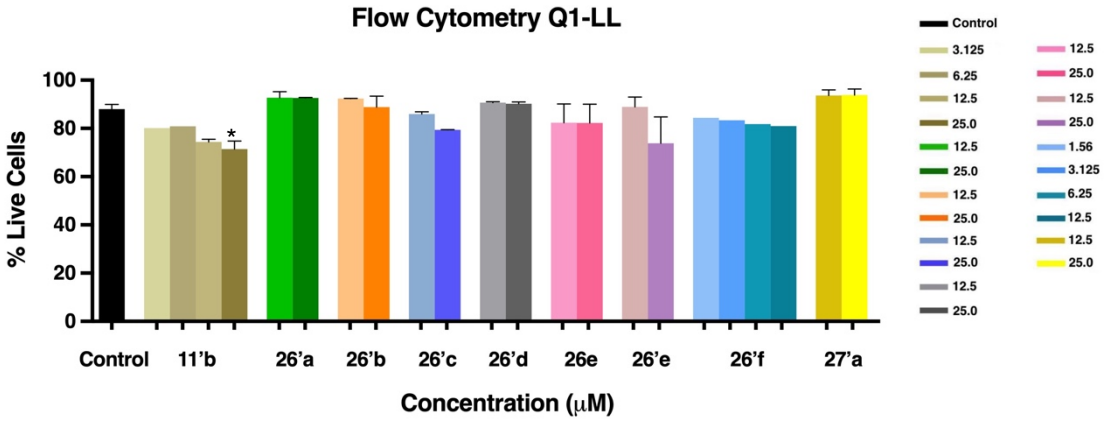

***Figure 62**. Graphical representation of the percentage of live cells, an indicator of monocytes' viability for each (E)-2-styrylchromone. *p < 0.05 when compared with the control assay (without compound). The results are given as the mean ± SEM (μM) (n ≥ 2).*

The results obtained for both the interference and viability assays, regarding the tested concentrations, as well as the maximum concentrations further chosen for the oxidative burst assay are presented in **Table 8**.

***Table 8**. Compilation of the results obtained for the interference and viability assays in human monocytes, regarding the tested compounds and respective concentrations. Maximum concentration of each compound chosen for the oxidative burst assay.*

Compound	Tested concentration (μM)	Tested concentration with no fluorescence interference (μM)	Tested concentration with no effects on cell viability (μM)	Tested concentration for the oxidative burst assay (μM)
11'b	≤ 25.0	≤ 25.0	≤ 25.0	≤ 25.0
26'a	≤ 25.0	≤ 25.0	≤ 25.0	≤ 25.0
26'b	≤ 25.0	≤ 12.5	≤ 12.5	≤ 12.5
26'c	≤ 25.0	≤ 12.5	≤ 12.5	≤ 12.5
26'd	≤ 25.0	≤ 25.0	≤ 25.0	≤ 25.0
26e	≤ 25.0	≤ 25.0	≤ 25.0	≤ 25.0
26'e	≤ 25.0	≤ 12.5	≤ 12.5	≤ 12.5
26'f	≤ 25.0	≤ 12.5	≤ 12.5	≤ 12.5
27'a	≤ 25.0	≤ 25.0	≤ 25.0	≤ 25.0

3.3.5 Evaluation of the inhibitory effect of (*E*)-2-styrylchromones against PMA-induced RS production by human monocytes

After all the preliminary studies to determine the maximum concentration of each (*E*)-2-styrylchromone that could be tested without promoting any cytotoxic effects on the cells, the last and most promising study was performed.

The isolated human monocytes were activated by phorbol 12-myristate 13-acetate (PMA), a chemical compound that acts by mimicking the action of diacylglycerol (DAG), which consequently activates protein kinase C (PKC) and promotes its translocation from the cytosol to the membrane. This translocation is then responsible for triggering the key step of NADPH oxidase activation, the phosphorylation of the $p47^{phox}$ subunit. Once activated, NADPH oxidase generates a large number of RS. The detection of the RS generated during the activation of the isolated human monocytes was performed using a fluorescence method with dihydrorhodamine (DHR). DHR is a non-fluorescent compound which becomes fluorescent when oxidized to rhodamine by several RS and chlorine species produced intra and/or extracellularly by monocytes, namely $O_2^{\bullet -}$, H_2O_2, HO•, HOCl, •NO and $ONOO^-$ (**Scheme 13**). The aim of this assay was to determine the percentage of inhibition of each compound and their respective IC_{50} values.

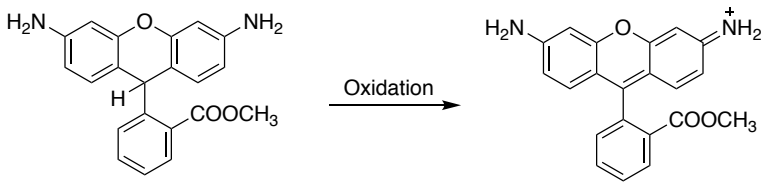

Dihydrorhodamine 123 Rhodamine 123

***Scheme 13**. Oxidation reaction from dihydrorhodamine 123 to rhodamine, which occurs in the presence of RS, culminating in the emission of fluorescence (λ = 528 nm).*

Afterwards, considering the absorbance values obtained it was possible to determine the percentage of inhibition of each compound for at least five concentrations. The results are presented in (**Table 9**) as the percentage of inhibition obtained for the maximum concentration of each compound. There were three active compounds, but only two of them presented a range of inhibition values that allowed to calculate the respective IC_{50} values. This assay was performed with diphenyleneiodonium chloride (DPI), a known PKC inhibitor and, consequently, a NADPH oxidase inhibitor, as a control (**Figure 63**). Each study corresponded to, at least, two independent assays.

***Table 9**. Percentage (%) of inhibition for the maximum tested concentration for each compound and IC_{50} values in μM. The results are given as mean ± SEM (μM). *No activity (NA).*

Compound	Maximum tested concentration (μM)	Percentage (%) of inhibition	IC_{50} values as mean ± SEM (μM)
DPI	12.5	90.7	0.8535 ± 0.1254
11'b	25.0	80.5	9.953 ± 1.6680
26'a	25.0	NA*	-------
26'b	12.5	NA*	-------
26'c	12.5	NA*	-------
26'd	25.0	NA*	-------
26e	25.0	NA*	-------
26'e	12.5	44.4	-------
26'f	12.5	78.6	10.24 ± 1.121
27'a	25.0	NA*	-------

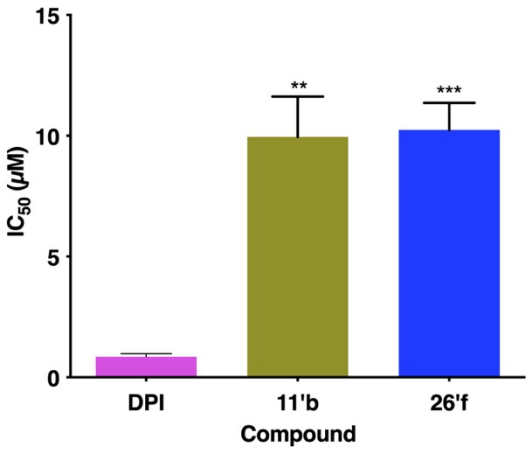

***Figure 63**. Graphical representation of the IC_{50} values in μM for the control and active compounds on the oxidative burst assay in human monocytes. *p < 0.05 compared between assays. The results are given as the mean ± SEM (μM) (n ≥ 5).*

3.3.6. Structure-activity relationship studies (SARS)

The establishment of SARS is a major contribution for future studies and should be done and analyzed at the end of every research work.

In this work, the newly synthesized and tested (*E*)-2-styrylchromone **26'f** was, in general, the most active compound. This compound has four hydroxy-substituent groups at C-5 of the A ring and at C-3', C-4' and C-5' of the B ring, respectively, highlighting the importance of hydroxy groups for the increase of the inhibitory effects regarding the scavenging of •NO and the oxidative burst in human monocytes. In addition, (*E*)-2-styrylchromone **11'b** has also demonstrated similar inhibitory effects in the oxidative burst in human monocytes, however the presence of the methoxy-substituent group at C-7 of the A ring, seems to be relevant in the •NO scavenging assay, since it decreases the compound's scavenging potential. Also, (*E*)-2-styrylchromone **26'd**, which possess two hydroxy groups at C-5 and C-2' of the A and B rings, respectively, was a potent scavenger of the •NO.

Considering that (*E*)-2-styrylchromone **26'e** was analogous to **26'd**, but *meta*-substituted on the B ring, and did not demonstrate any activity in comparison to the other non-active compounds, the (*E*)-2-styrylchromones must be hydroxy-substituted at C-5 and hydroxy-substituted at *ortho*- or *para*-positions of the B ring, for the •NO scavenging. This conclusion is also supported by non-active (*E*)-2-styrylchromones **26'a**, **26'b** and **26'c** since these three compounds are hydroxy-substituted at C-5 of the A ring but have chlorine substituent groups on the B ring and by (*E*)-2-styrylchromone **27'a**, which is not substituted at the A ring.

Despite the previous studies found on the literature about the polyhydroxylated compounds, the number of hydroxy groups does not seem to make any difference in the •NO scavenging assay, contrariwise to the substitution position.

Regarding the preliminary studies in the oxidative burst in human monocytes, (*E*)-2-styrylchromones **11'b** and **26'f** were the most active, with similar IC_{50} values (IC_{50} = 9.953 ± 1.6680 μM and 10.24 ± 1.121 μM, respectively). Considering the IC_{50} value for the standard DPI (IC50 = 0.8535 ± 0.1254 μM), the tested (*E*)-2-styrylchromones may be considered less active. However, DPI is a well-known inhibitor of the PKC, which is crucial for the activation and assembling of the NADPH complex and consequently the inflammatory process, a knowledge that is not yet established for the tested compounds. Nevertheless, these promising results may indicate the possibility of (*E*)-2-styrylchromones' potential as scavengers of the •NO radicals produced, *in vitro*, in human monocytes during the inflammatory process, but without further studies, it is not possible to affirm this hypothesis (**Figure 64**).

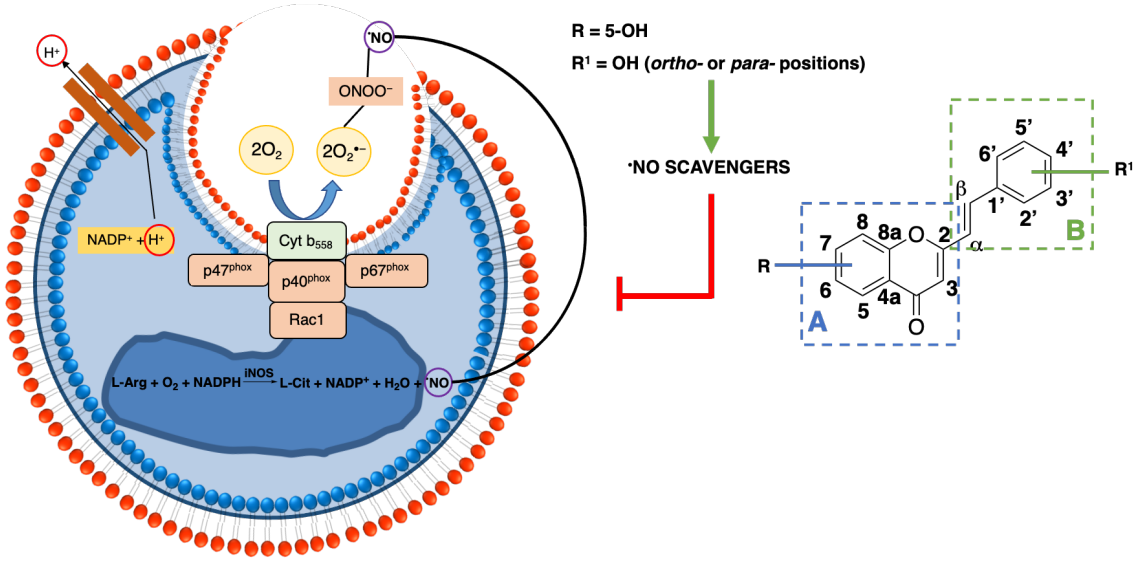

***Figure 64**. Illustration of the conclusions of this work, regarding the most important features in the (E)-2-styrylchromones in study.*

Chapter 4 - Discussion and Future Perspectives

Over the past few years, several studies were undertaken regarding the effects of oxidative stress and reactive species in inflammation, mainly chronic inflammation, and consequently in chronic diseases which are considered the main cause of death or loss of quality of life. Alongside with each study comes a promising result which leads to the development of even more research in this field. (*E*)-2-styrylchromones, polyphenolic compounds, have demonstrated to be biologically active when it comes to anti-inflammatory and antioxidant activities, mainly through studies of their ability to scavenge reactive species. For these reasons polyphenolic compounds play a huge role on pharmacological targets and, nowadays, it is well-known that several of these compounds are the active principles of commercially available drugs, namely anti-inflammatory and antioxidant drugs. Despite the major interest on this family of compounds, (*E*)-2-styrylchromones have not yet been as studied as other related compounds, such as chalcones and flavones, concerning their biological potential for being applied for the well-being of individuals with chronic inflammatory diseases.

This work is a contribution to increase knowledge about the potential of a library of synthesized (*E*)-2-styrylchromones as anti-inflammatory agents by studying their possible inhibitory effects on the oxidative burst in human monocytes and consequently their antioxidant and anti-inflammatory benefits in human cells. It also allowed the establishment of important structure-activity relationships (SARS) studies that will guide the design of new (*E*)-2-styrylchromones towards the improvement of their activity. Furthermore, this study contributed to advance the state-of-the-art since most of the studies found in the literature rely on human neutrophilic cells and their role in inflammatory pathways while herein attention was given to the role of human monocytes. The selection of the nine compounds in study was carefully done based on their different substitution patterns, to allow SARS and, on the literature, regarding the already known effects of the hydroxy groups.

To achieve the most promising results, this work was divided into two main goals: the synthesis of (*E*)-2-styrylchromones and their inhibitory effects on the oxidative burst produced by monocytes.

The synthesis of the compounds was performed through several methods and the most effective was the condensation of 2-methylchromones with benzaldehydes, followed by cleavage of the protected groups, with BBr_3. Nevertheless, different methods were attempted and/or optimized for the synthesis of 2-methylchromones and the most used consisted of a two-step sequence, starting from different acetophenones with sodium in dry ethyl acetate at room temperature, followed by cyclodehydrogenation in refluxing MeOH, in the presence of *p*-TSA. Since this route of synthesis showed low yields (18-36%), two other methods were attempted: a solvent-free reaction, known as the Pechmann rection, between phenols and ethyl acetoacetate, with phosphorous pentoxide (**Scheme 9**) and a two-step synthesis involving the acylation of phenols followed by a Fries rearrangement to achieve non-commercial acetophenones and, consequently, 2-methylchromones. However, no products were obtained which is why 2-methylchromones were always achieved by the

first mentioned method, keeping in mind that the other two must be further optimized. In fact, eight of the nine studied compounds, were achieved from 2-methylchromones and benzaldehydes, while compound **11'b** was obtained through an aldol condensation of 2′-hydroxyacetophenones with cinnamaldehydes followed by cyclodehydration. (*E*)-2-styrylchromone **10'a**, with a *cis* configuration, was synthesized through the same method but the final step involving the deprotection of the methoxy groups did not give any products.

The second main goal of this work consisted in different steps, beginning with the plot of absorption and emission spectra of every compound, to avoid any kind of interference during the next steps. In the same line of thought, all compounds were tested regarding the cytotoxic effects against human monocytes, with the aim of choosing the maximum concentrations that would be used later, on the following methodologies. For the cytotoxic interference assay, were used two different probes, Annexin V and Propidium Iodine, to determine the percentage of apoptotic and necrotic cells, respectively. Once these results were treated, the maximum non-toxic concentrations of each compound were established, considering that only compound **26'f** affected the cells' viability at 25.0 μM. Subsequently, each (*E*)-2-styrylchromone was tested for their inhibitory effects on the oxidative burst in human monocytes, stimulated by PMA, a known promotor of the oxidation of dihydrorhodamine 123 to rhodamine, a reaction that consequently promotes the production of reactive species. The control sample DPI is known for its ability to inactivate protein kinase C, a crucial precursor for the assembling of the NADPH complex during inflammation and consequently for the overproduction of reactive species. Thus, when compared to the control, none of the compounds was closely as active as DPI (IC_{50} = 0.8535 ± 0.1254 μM). In fact, only (*E)*-2-styrylchromones **11'b** and **26'f** have demonstrated to be active (IC_{50} = 9.9530 ± 1.6680 μM and IC_{50} = 10.2400 ± 1.1210 μM, respectively), but with higher IC_{50} values regarding the one for DPI (IC_{50} = 0.8535 ± 0.1254 μM).

These preliminary studies on human monocytes demonstrated to be promising, since two compounds were active as inhibitors of the inflammatory process. However, many more studies must be done in this field, to understand the mechanisms behind these benefic effects of (*E*)-2-styrylchromones. Nevertheless, based on the SARS and looking at the structures of compounds **11'b** and **26'f**, it can be highlighted that the presence of the hydroxy groups at both C-5 and C-4' may be crucial to the activity thus justifying the promising results obtained for these two compounds.

As future perspectives, it would be crucial to optimize the Pechmann reaction, mainly due to the environmental benefits of a solvent-free reaction and, regarding the biological activities, to evaluate their antioxidant activity against other ROS and RNS present in the inflammatory process, as well as the design of new and more active (*E*)-2-styrylchromones, bearing in mind the results obtained in this work and the importance of the substituent groups and substitution pattern. Further studies should be performed in human monocytes, using different methods, in order to understand

exactly how this type of compounds interacts with the inflammatory pathways and, consequently, improve the knowledge of their respective mechanisms of action.

Chapter 5 - Experimental Section

5.1 Materials and chemicals

Reagents and solvents were purchased as reagent-grade and used without further purification unless otherwise stated. Solvents were dried with molecular sieves, under N_2 atmosphere. Column chromatography was carried out with silica gel Aldrich 63-200 μm. Preparative thin-layer chromatography (TLC) was carried out with silica gel (60 DGF_{254}) plates with a thickness of 0.5 mm. After elution of the compounds, the plates were observed under ultraviolet (UV) light at λ 254 and / or 366 nm. The progress of chemical reactions performed was monitored by (TLC) using silica gel 60 F_{254} Merck or Macherey Nigel 60 NHR / UV_{254} silica gel coated plasticized sheets which after elution were observed under UV light at λ 254 and / or 366 nm.

NMR spectra were recorded with 300 or 500 MHz [300.13 MHz (^{1}H), 75.47 MHz (^{13}C), or 500.16 MHz (^{1}H), 125.77 MHz (^{13}C)] Bruker Avance III NMR spectrometers with tetramethylsilane as the internal reference. Deuterated solvent used was specified for each compound. Chemical shifts (δ) are reported in ppm and coupling constants (*J*) in Hz. The internal standard was TMS. Unequivocal ^{13}C assignments were made based on 2D *g*HSQC (^{1}H/^{13}C) and *g*HMBC (delays for one-bond and long-range *J*C/H couplings were optimized for 145 and 7 Hz, respectively) experiments.

Regarding the *in vitro* biological assays, the following reagents were purchased from Sigma Chemical Co. (St. Louis, MO, USA): histopaque 1077, histopaque 1119, trypan blue 0.4%, Dulbecco's phosphate buffer saline without calcium and magnesium ions (PBS), phorbol 12-myristate 13-acetate (PMA) and dimethyl sulfoxide (DMSO). The FITC Annexin V Apoptosis Detection Kit was purchased from BD Biosciences and the dihydrorhodamine (DHR) from Enzo Life Sciences. The ethylenediamine tetraacetic acid K3 (EDTA) tubes to collect the blood were purchased from Vacuette S.A. (Porto, Portugal).

5.2 Synthesis

5.2.1 Methylation of the starting compounds

The synthesis of polyhydroxylated compounds, often required the protection of the hydroxy groups of the starting compounds. In this work that protection was performed by methylation reactions.

5.2.1.1 Methylation of acetophenones

To a round-bottomed flask containing 2',6'-dihydroxyacetophenone (**1**) (6.0 g, 39.0 mmol) or 2',4',6'-trihydroxyacetophenone (**3**) (6.0 g, 35.7 mmol) in 100.0 mL of acetone were added potassium carbonate (3.0 equiv, 16.3 g, 118.2 mmol and 6.0 equiv, 29.6 g, 214.2 mmol, respectively) and dimethyl sulfate (1.0 equiv, 3.7 mL, 39.0 mmol and 2.0 equiv, 6.8 mL, 71.4 mmol, respectively). The reaction was left stirring for 1 to 3 h, at reflux. After that period the reaction mixture was poured into

iced water and acidified with hydrochloric acid. The resulting precipitate was washed with DCM and then evaporated to dryness, thus obtaining compounds **2, 4** and **23'**.

1-(2-Hydroxy-6-methoxyphenyl)ethan-1-one (2)

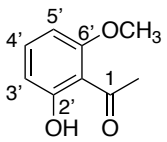

Compound **2** was obtained as a yellow solid after being washed with DCM (5.37 g, 83%).

^{1}H NMR (300.13 MHz, $CDCl_3$): δ = 2.68 (s, 3H, C<u>H</u>$_3$), 3.90 (s, 3H, 6'-OC<u>H</u>$_3$), 6.40 (dd, 1H, *J* = 8.4, 1.1 Hz, H-3'), 6.57 (dd, 1H, *J* = 8.4, 1.1 Hz, H-5'), 7.35 (t, 1H, *J* = 8.4 Hz, H-4'), 13.26 (s, 1H, 2'-O<u>H</u>) ppm.

1-(2-Hydroxy-4,6-dimethoxyphenyl)ethan-1-one (4)

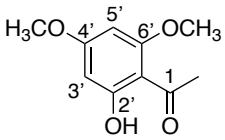

Compound **4** was obtained as a white solid after crystallization with ethanol (4.0 g, 67%).

^{1}H NMR (300.13 MHz; $CDCl_3$): δ = 2.61 (s, 3H, C<u>H</u>$_3$), 3.82 (s, 3H, 4'-OC<u>H</u>$_3$), 3.86 (s, 3H, 6'-OC<u>H</u>$_3$), 5.92 (d, 1H, *J* = 2.4 Hz, H-3'), 6.06 (d, 1H, *J* = 2.4 Hz, H-5'), 14.04 (s, 1H, 2'-O<u>H</u>) ppm.

1-(6-Hydroxy-2,3,4-trimethoxyphenyl)ethan-1-one (23')

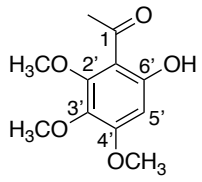

Compound **23'** was obtained as a white solid after thin layer chromatography with DCM. The overall yield of the synthesis was 25% (0.0156 g).

^{1}H NMR (300.13 MHz; $CDCl_3$): δ = 2.66 (s, 3H, C<u>H</u>$_3$), 3.78 (s, 3H, -OC<u>H</u>$_3$), 3.89 (s, 3H, -OC<u>H</u>$_3$), 3.99 (s, 3H, -OC<u>H</u>$_3$), 6.24 (s, 1H, H-3'), 13.44 (s, 1H, 2'-O<u>H</u>) ppm.

5.2.2 Synthesis of (2*E*,4*E*)-1,5-diphenylpenta-2,4-dien-1-ones

For the synthesis of (2*E*,4*E*)-1,5-diphenylpenta-2,4-dien-1-ones**,** commonly known as cinnamylidene-acetophenones, was added 2'-hydroxy-4',6'-dimethoxyacetophenone (**4**) (1.0 equiv, 1.00 g, 5.0 mmol) dissolved in 24.0 mL of methanol to a round-bottomed flask, capped with aluminium, followed by 18.0 mL of an aqueous sodium hydroxide solution (40%). After cooling down to room temperature, was added cinnamaldehyde [(*E*)-3-phenylprop-2-enal according to the IUPAC nomenclature] (**9a**) (1.2 equiv, 0.830 mL, 6.6 mmol). After 22 h, the reaction was poured into iced water and then acidified, resulting in a precipitate. The precipitate was dissolved in ethyl acetate (AcOEt), washed with water and the organic layer was dried with anhydrous sodium sulfate and, at last, the solvent was evaporated to afford compound **10a**.

(2*Z*,4*Z*)-1-(2-Hydroxy-4,6-dimethoxyphenyl)-5-phenylpenta-2,4-dien-1-one (10a)

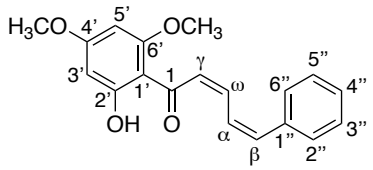

Compound **10a** was obtained as a solid after thin layer chromatography with DCM/Hexane (1:1) as eluent, and crystallization with ethanol (0.480 g, 31%).*

^{1}H NMR (300.13 MHz, $CDCl_3$): δ = 3.82 (s, 3H, OC<u>H</u>$_3$), 3.85 (s, 3H, OC<u>H</u>$_3$), 5.92 (d, 1H, *J* = 2.4 Hz, H-3'), 6.06 (d, 1H, *J* = 2.4 Hz, H-5'), 7.31-7-43 (m, 4H, H-γ, δ, 3", 5"), 7.43-7.52 (m, 4H, H-α, β, 2", 6"), 7.59-7.64 (m, 1H, H-4"), 14.04 (s, 1H, 2'-O<u>H</u>) ppm.*

To a round-bottomed flask, capped with aluminium, with 2'-hydroxy-4',6'-dimethoxyacetophenone (**4**) (1.0 equiv, 0.550 g, 2.8 mmol) dissolved in 14.0 mL of methanol, were added 10.0 mL of an aqueous sodium hydroxide solution (40%). After cooling down to room temperature, was added (*E*)-3-(4-methoxy)cinnamaldehyde (**9b**) (1.2 equiv, 0.535 g, 3.4 mmol). After 20 h, the reaction was poured into iced water and then acidified, resulting in a precipitate. The precipitate was dissolved in ethyl acetate, washed with water and the organic layer was dried with anhydrous sodium sulfate and, at last, the solvent was evaporated to afford compound **10b**.

(2*E*,4*E*)-1-(2-Hydroxy-4,6-dimethoxyphenyl)-5-(4-methoxyphenyl)penta-2,4-dien-1-one (10b)

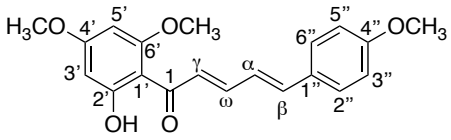

Compound **10b** was obtained as a solid after thin layer chromatography with DCM and crystallization with ethanol, in *trans* configuration (0.425 g, 50%).*

^{1}H NMR (300.13 MHz; $CDCl_3$): δ = 3.83 (s, 3H, OC<u>H</u>$_3$), 3.84 (s, 3H, OC<u>H</u>$_3$), 3.85 (s, 3H, OC<u>H</u>$_3$), 5.96 (d, 1H, *J* = 2.4 Hz, H-3'), 6.11 (d, 1H, *J* = 2.4 Hz, H-5'), 6.86-6.92 (m, 4H, H-γ, δ, 3", 5"), 7.37-7-47 (m, 4H, H-α, β, 2", 6"), 14.42 (s, 1H, 2'-O<u>H</u>) ppm.*

5.2.3 Synthesis of (*E*)-2-styrylchromones from cinnamylidene-acetophenones

The obtained compound (2*Z*,4*Z*)-1-(2-hydroxy-4,6-dimethoxy)cinnamylidene-acetophenone **(10a**) was dissolved in 3.0 mL of DMSO and a catalytic amount of iodine (0.039 equiv, 0.015 g, 0.06 mmol) was added. The reaction was heated at reflux for 50 min. and after the mixture was poured into an iced sodium thiosulfate solution. The resulting precipitate was dissolved in chloroform, washed with water and the organic layer was dried over anhydrous sodium sulfate. At last, the solvent was evaporated to afford compound **11a.**

(*Z*)-5,7-Dimethoxy-2-styryl-4*H*-chromen-4-one (11a)

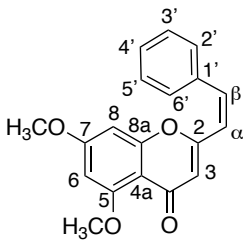

Compound **11a** was obtained as a brown solid after evaporation of the solvent to dryness, in *cis* configuration (0.415 g, 87%).*

^{1}H NMR (300.13 MHz, $CDCl_3$): δ = 3.93 (m, 6H, 5-OC<u>H</u>$_3$, 7-OC<u>H</u>$_3$), 6.20 (s, 1H, H-3), 6.35 (d, 1H, *J* = 2.4 Hz, H-6), 6.55 (d, 1H, *J* = 2.4 Hz, H-8), 6.69 (d, 1H, *J* = 10.0 Hz, H-α), 7.39 (dd, 2H, *J* = 9.0 Hz, H-3',5'), 7.47-7.56 (m, 3H, H-β, 2', 6'), 7.85-7.88 (m, 1H, H-4') ppm.

The obtained compound (2*E*,4*E*)-1-(2-hydroxy-4,6-dimethoxy)-5-(4-methoxy)cinnnamylidene-acetophenone **(10b)** was dissolved in 2.0 mL of DMSO and a catalytic amount of iodine (0.039 equiv, 0.012 g, 0.05 mmol) was added. The reaction was heated at reflux for 55 min. and after the mixture was poured into an iced sodium thiosulfate solution. The resulting precipitate was dissolved in chloroform, washed with water and the organic layer was dried over anhydrous sodium sulfate. At last, the solvent was evaporated, affording compound **11b**.

(*E*)-5,7-Dimethoxy-2-(4-methoxystyryl)-4*H*-chromen-4-one (11b)

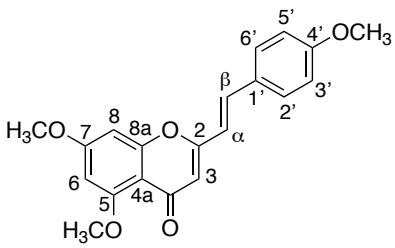

Compound **11b** was obtained as a brown solid after evaporation of the solvent to dryness (0.415 g, 87%).

^{1}H NMR (300.13 MHz, $CDCl_3$): δ = 3.92 (s, 3H, OC<u>H</u>$_3$), 3.95 (s, 3H, OC<u>H</u>$_3$), 3.96 (s, 3H, OC<u>H</u>$_3$), 6.20 (s, 1H, H-3), 6.38 (d, 1H, *J* = 2.3 Hz, H-6), 6.57 (d, 1H, *J* = 2.3 Hz, H-8), 6.62 (d, 1H, *J* = 16.1 Hz, H-α), 7.00 (d, 2H, *J* = 7.8 Hz, H-2',6'), 7.51 (d, 1H, *J* = 16.1 Hz, H-β), 7.83 (d, 2H, *J* = 7.8 Hz, H-3',5') ppm.

The protected compound (*E*)-5,7-dimethoxy-2-(4-methoxystyryl)-4*H*-chromen-4-one (**11b**) (1.0 equiv, 0.279 g, 0.80 mmol) was dissolved in 6.0 mL of dry DCM, in a round-bottomed flask, and 2.5 equiv of BBr_3 per methoxy group to be cleaved were added to the mixture (5.0 equiv, 4.15 mL, 4.15 mmol), at ~-70ºC. After the addition of BBr_3, the reaction was left stirring at room temperature, for 2 h. The reaction mixture was then poured into iced water, resulting in a precipitate which was filtered and recrystallized, affording compound **11'b**.

(*E*)-5-Hydroxy-7-methoxy-2-(4-hydroxystyryl)-4*H*-chromen-4-one (11'b)

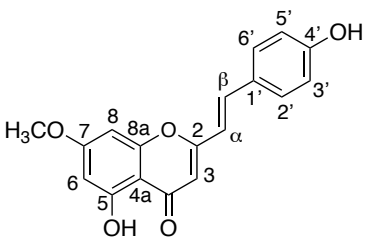

Compound **11'b** was obtained as a brown solid after crystallization with DCM and hexane (0.083 g, 32%).

^{1}H NMR (500.16 MHz, MeOD): δ = 3.86 (s, 3H, 7-OC<u>H</u>$_3$), 6.15 (s, 1H, H-3), 6.36 (d, 1H, *J* = 2.2 Hz, H-6), 6.52 (d, 1H, *J* = 2.2 Hz, H-

8), 6.62 (d, 1H, *J* = 16.0 Hz, H-α), 6.88 (d, 2H, *J* = 8.3 Hz, H-3',5'), 7.39 (s, 2H, 5-O<u>H</u>, 4'-O<u>H</u>), 7.48 (d, 2H, *J* = 8.3 Hz, H-2',6'), 7.56 (d, 1H, *J* = 16.0 Hz, H-β) ppm.

^{13}C NMR (125.77 MHz, MeOD): δ = 55.8 (O<u>C</u>H$_3$), 92.6 (C-8), 98.0 (C-6), 105.5 (C-4a), 107.3 (C-3), 116.0 (C-3',5'), 116.1 (C-α), 126.5 (C-1'), 129.7 (C-2',6'), 138.0 (C-β), 157.6 (C-8a), 159.2 (C-4'), 161.6 (C-5), 163.6 (C-2), 165.6 (C-7) and 182.6 (C=O) ppm.

5.2.4 Synthesis of 2-methylchromones

The route for the synthesis of 2-methylchromones consisted of a two-step sequence, starting from different acetophenones with sodium in dry ethyl acetate at room temperature, followed by cyclodehydrogenation in refluxing MeOH, in the presence of *p*-TSA.

2'-Hydroxy-6'-methoxy-acetophenone (**2**) (1.0 equiv, 0.500 g, 3.00 mmol) was added to a mixture of sodium (4.0 equiv, 0.276 g, 12.00 mmol) in 20.0 mL of dry AcOEt at room temperature for 18 h. The reaction mixture was then poured into iced water, acidified until pH = 5, and then dissolved in DCM. The reaction mixture was washed with water and the organic layer was dried over anhydrous sodium sulfate. At last, the solvent was evaporated. After that, the resulting crude (1.0 equiv, 0.803 g, 3.90 mmol) was dissolved in a minimum volume of MeOH and was added *p*-TSA (0.5 equiv, 0.371 g, 1.95 mmol). The reaction was left stirring at reflux for 27 h. The reaction mixture was washed with water, the organic layer was dried over anhydrous sodium sulfate, and the solvent evaporated to dryness to afford compound **13**.

5-Methoxy-2-methyl-4*H*-chromen-4-one (13)

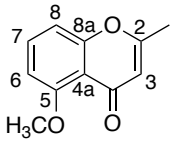

Compound **13** was obtained as an oil after thin layer chromatography with DCM. The overall yield of the synthesis was 15% (0.088 g).

^{1}H NMR (300.13 MHz, $CDCl_3$): δ = 2.31 (s, 3H, 2-C<u>H</u>$_3$), 3.97 (s, 3H, 5'-OC<u>H</u>$_3$), 6.08 (s, 1H, H-3), 6.78 (dd, 1H, *J* = 8.4, 1.0 Hz, H-6), 6.98 (dd, 1H, *J* = 8.4, 1.0 Hz, H-8), 7.51 (t, 1H, *J* = 8.4 Hz, H-7) ppm.

2'-Hydroxyacetophenone (**5**) (1.0 equiv, 44.0 mL, 3.67 mmol) was added to a mixture of sodium (4.0 equiv, 0.338 g, 14.68 mmol) in 20.0 mL of dry AcOEt at room temperature for 21 h. The reaction mixture was then poured into iced water, acidified until pH = 5, and then dissolved in AcOEt. The reaction mixture was washed with water and the organic layer was dried over anhydrous sodium sulfate. At last, the solvent was evaporated. After that, the resulting crude (1.0 equiv, 1.443 g, 8.10 mmol) was dissolved in a minimum volume of MeOH and was added *p*-TSA (0.5 equiv, 0.700 g, 4.10 mmol). The reaction was left stirring at reflux for 19 h. The reaction mixture was washed with water, the organic layer was dried over anhydrous sodium sulfate, and the solvent evaporated to dryness, resulting in compound **15**.

2-Methyl-4*H*-chromen-4-one (15)

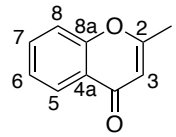

Compound **15** was obtained as an orange solid after column chromatography with chloroform/acetone 9:1 as eluent. The overall yield of the synthesis was 28% (0.162 g).

^{1}H NMR (300.13 MHz, $CDCl_3$): δ = 2.39 (s, 3H, 2-C$\underline{H}_3$), 6.18 (s, 1H, H-3), 7.37 (dd, 1H, *J* = 7.1, 1.1 Hz, H-8), 7.41 (dt, 1H, *J* = 8.2, 1.1 Hz, H-6), 7.65 (ddd, 1H, *J* = 8.2, 7.1, 1.7 Hz, H-7), 8.18 (dd, 1H, *J* = 8.2, 1.7 Hz, H-5) ppm.

1-(2-(Benzyloxy)-6-hydroxyphenyl)ethan-1-one (**16**) (1.0 equiv, 0.357 g, 1.47 mmol) was added to a mixture of sodium (4.0 equiv, 0.135 g, 5.88 mmol) in 20.0 mL of dry AcOEt at room temperature for 24 h. The reaction mixture was then poured into iced water, acidified until pH = 5, and then dissolved in AcOEt. The reaction mixture was washed with water and the organic layer was dried over anhydrous sodium sulfate. At last, the solvent was evaporated. After that, the resulting crude (1.0 equiv, 0.445 g, 1.66 mmol) was dissolved in a minimum volume of MeOH and was added *p*-TSA (0.5 equiv, 0.158 g, 0.83 mmol). The reaction was left stirring at reflux for 21 h. The reaction mixture was washed with water, the organic layer was dried over anhydrous sodium sulfate, and the solvent evaporated to dryness, to afford compound **18**.

5-Benzyloxy-2-methyl-4*H*-chromen-4-one (18)

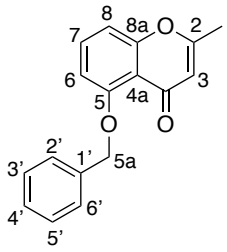

Compound **18** was obtained as a white solid after column chromatography with DCM. The overall yield of the synthesis was 9% (0.036 g).

^{1}H NMR (300.13 MHz, $CDCl_3$): δ = 2.32 (s, 3H, 2-C$\underline{H}_3$), 5.27 (s, 2H, 5a-C$\underline{H}_2$), 6.08 (s, 1H, H-3), 6.81 (dd, 1H, *J* = 8.4, 1.0 Hz, H-6), 6.98 (dd, 1H, *J* = 8.4, 1.0 Hz, H-8), 7.36-7.44 (m, 3H, H-3',4',5'), 7.47 (t, 1H, *J* = 8.4 Hz, H-7), 7.61 (dd, 2H, *J* = 7.4, 1.3 Hz, H-2',6') ppm.

1-[2,4-Bis(benzyloxy)-6-hydroxyphenyl]ethan-1-one (**19**) (1.0 equiv, 0.346 g, 0.99 mmol) was added to a mixture of sodium (4.0 equiv, 0.091 g, 3.96 mmol) in 15.0 mL of dry AcOEt at room temperature for 19 h. The reaction mixture was then poured into iced water, acidified until pH = 5, and then dissolved in AcOEt. The reaction mixture was washed with water and the organic layer was dried over anhydrous sodium sulfate. At last, the solvent was evaporated. After that, the resulting crude (1.0 equiv, 0.377 g, 0.97 mmol) was dissolved in a minimum volume of MeOH and was added *p*-TSA (0.5 equiv, 0.093 g, 0.49 mmol). The reaction was left stirring at reflux for 21 h. The reaction mixture was washed with water, the organic layer was dried over anhydrous sodium sulfate, and the solvent evaporated to dryness, giving compound **21**.

5,7-Bis(benzyloxy)-2-methyl-4*H*-chromen-4-one (21)

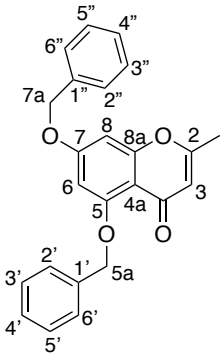

Compound **21** was obtained as a white solid after column chromatography with DCM. The overall yield of the synthesis was 18% (0.066 g).

^{1}H NMR (300.13 MHz, $CDCl_3$): δ = 2.27 (s, 3H, 2-C$\underline{H}_3$), 5.08 (s, 2H, 5a-C$\underline{H}_2$), 5.20 (s, 2H, 7a-C$\underline{H}_2$), 6.00 (s, 1H, H-3), 6.46 (dd, 1H, *J* = 2.3 Hz, H-6), 6.49 (dd, 1H, *J* = 2.3, H-8), 7.36-7.42 (m, 8H, H-3', 4', 5', 2'', 3'', 4'', 5'', 6''), 7.60 (dd, 2H, *J* = 7.4 Hz, H-2',6') ppm.

5.2.5 Synthesis of (*E*)-2-styrylchromones from 2-methylchromones

To a round-bottomed flask with 16.0 mL of ethanol and sodium (4.0 equiv, 0.043 g, 1.84 mmol), was added 5-methoxy-2-methylchromone (1.0 equiv, 0.088 g, 0.46 mmol). When the reaction turned dark orange/red, 3'-chlorobenzaldehyde (**25a**) (1.2 equiv, 0.078 g, 0.55 mmol) was added to the mixture. The reaction was left stirring overnight and then poured into iced water and acidified. The precipitate was dissolved in DCM and washed with water. The organic layer was dried with anhydrous sodium sulfate, and the solvent was evaporated to dryness, to afford compound **26a**.

(*E*)-5-Methoxy-2-(3-chlorostyryl)-4*H*-chromen-4-one (26a)

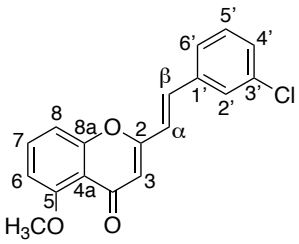

Compound **26a** was obtained as a white solid after thin layer chromatography with DCM/acetone 9.5:0.5 (0.074 g, 51%).

^{1}H NMR (300.13 MHz, $CDCl_3$): δ = 3.99 (s, 3H, 5-OC$\underline{H}_3$), 6.26 (s, 1H, H-3), 6.73 (d, 1H, *J* = 16.2 Hz, H-α), 6.82 (d, 1H, *J* = 8.4 Hz, H-6), 7.10 (dd, 1H, *J* = 8.4, 1.0 Hz, H-8), 7.34-7.36 (m, 2H, H-2', 5'), 7.45 (dt, 1H, *J* = 8.6, 1.7 Hz, H-4'), 7.48 (d, 1H, *J* = 16.2 Hz, H-β), 7.55-7.61 (m, 1H, H-6'), 7.57 (t, 1H, *J* = 8.4 Hz, H-7) ppm.

To a round-bottomed flask with 3.0 mL of ethanol and sodium (4.0 equiv, 0.061 g, 2.64 mmol), was added 5-methoxy-2-methylchromone (1.0 equiv, 0.125 g, 0.66 mmol). When the reaction turned dark orange/red, 3',4'-dichlorobenzaldehyde (**25b**) (1.5 equiv, 0.173 g, 0.99 mmol) were added to the mixture. The reaction was left stirring for 24 h and then poured into iced water and acidified. The precipitate was dissolved in DCM and washed with water. The organic layer was dried with anhydrous sodium sulfate, and the solvent was evaporated to dryness, affording compound **26b**.

(*E*)-5-Methoxy-2-(3,4-dichlorostyryl)-4*H*-chromen-4-one (26b)

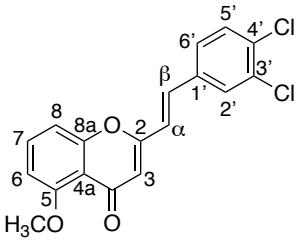

Compound **26b** was obtained as a light-yellow solid, after thin layer chromatography with DCM (0.138 g, 60%).

^{1}H NMR (300.13 MHz, $CDCl_3$): δ = 3.99 (s, 3H, 5-OC$\underline{H}_3$), 6.26 (s, 1H, H-3), 6.71 (d, 1H, *J* = 15.9 Hz, H-α), 6.82 (dd, 1H, *J* = 8.4, 1.0 Hz, H-6), 7.09 (dd, 1H, *J* = 8.4, 1.0 Hz, H-8), 7.40 (dd, 1H, *J* = 8.3, 2.2 Hz, H-6'), 7.44 (d, 1H, *J* = 15.9 Hz, H-β), 7.49 (d, 1H, *J* = 8.3 Hz, H-5'), 7.57 (t, 1H, *J* = 8.4 Hz, H-7), 7.65 (d, 1H, *J* = 2.2 Hz, H-2') ppm.

To a round-bottomed flask with 3.0 mL of ethanol of sodium (4.0 equiv, 0.048 g, 2.10 mmol), was added 5-methoxy-2-methylchromone (1.0 equiv, 0.100 g, 0.53 mmol). When the reaction turned dark orange/red, 2',6'-dichlorobenzaldehyde (**25c**) (1.5 equiv, 0.140 g, 0.80 mmol) were added to the mixture. The reaction was left stirring for 24 h and then poured into iced water and acidified. The precipitate was dissolved in DCM and washed with water. The organic layer was dried with anhydrous sodium sulfate, and the solvent was evaporated to dryness, to afford (*E*)-2-styrylchromone **26c**.

(*E*)-5-Methoxy-2-(2,6-dichlorostyryl)-4*H*-chromen-4-one (26c)

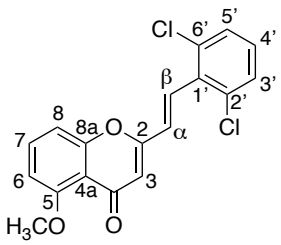

Compound **26c** was obtained as a light-yellow solid, after thin layer chromatography with DCM (0.089g, 48%).

^{1}H NMR (300.13 MHz, $CDCl_3$): δ = 4.00 (s, 3H, 5-OC$\underline{H}_3$), 6.28 (s, 1H, H-3), 6.82 (d, 1H, *J* = 8.4 Hz, H-6), 6.89 (d, 1H, *J* = 16.4 Hz, H-α), 7.13 (dd, 1H, *J* = 8.4, 0.8 Hz, H-8), 7.20 (t, 1H, *J* = 8.1 Hz, H-4'), 7.39 (d, 2H, *J* = 8.1 Hz, H-3',5'), 7.58 (t, 1H, *J* = 8.4 Hz, H-7), 7.63 (d, 1H, *J* = 16.4 Hz, H-β) ppm.

To a round-bottomed flask with 3.0 mL of ethanol and sodium (4.0 equiv, 0.052 g, 2.28 mmol), was added 5-methoxy-2-methylchromone (1.0 equiv, 0.108 g, 0.57 mmol). When the reaction turned dark orange/red, 2'-methoxybenzaldehyde (**25d**) (1.5 equiv, 0.100 mL, 0.86 mmol) was added to the mixture. The reaction was left stirring overnight and then poured into iced water and acidified. The precipitate was dissolved in DCM and washed with water. The organic layer was dried with anhydrous sodium sulfate, and the solvent was evaporated to dryness, affording compound **26d**.

(*E*)-5-Methoxy-2-(2-methoxystyryl)-4*H*-chromen-4-one (26d)

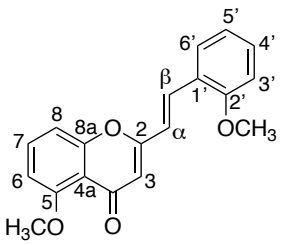

Compound **26d** was obtained as a light-yellow solid after thin layer chromatography with AcOEt/hexane 9:1 (0.101 g, 57%).

^{1}H NMR (300.13 MHz, $CDCl_3$): δ = 3.94 (s, 3H, 2'-OC<u>H</u>$_3$), 3.99 (s, 3H, 5-OC<u>H</u>$_3$), 6.25 (s, 1H, H-3), 6.80 (dd, 1H, *J* = 7.8, 1.0 Hz, H-3'), 6.82 (d, 1H, *J* = 16.3 Hz, H-α), 6.95 (dd, 1H, *J* = 8.4, 1.0 Hz, H-6), 7.00 (dt, 1H, *J* = 7.8, 1.0 Hz, H-5'), 7.13 (dd, 1H, *J* = 8.4, 1.0 Hz, H-8), 7.35 (dt, 1H, *J* = 7.8, 1.8, H-4'), 7.56 (t, 1H, *J* = 8.4 Hz, H-7), 7.57 (dd, 1H, *J* = 7.8, 1.8 Hz, H-6') ppm.

To a round-bottomed flask with 5.0 mL of ethanol and sodium (4.0 equiv, 0.101 g, 4.40 mmol), was added 5-methoxy-2-methylchromone (1.0 equiv, 0.200 g, 1.10 mmol). When the reaction turned dark orange/red, 3'-methoxybenzaldehyde (**25e**) (1.5 equiv, 0.20 mL, 1.65 mmol) were added to the mixture. The reaction was left stirring overnight and then poured into iced water and acidified. The precipitate was dissolved in DCM and washed with water. The organic layer was dried with anhydrous sodium sulfate, and the solvent was evaporated to dryness, to afford (*E*)-2-styrylchromone **26e**.

(*E*)-5-Methoxy-2-(3-methoxystyryl)-4*H*-chromen-4-one (26e)

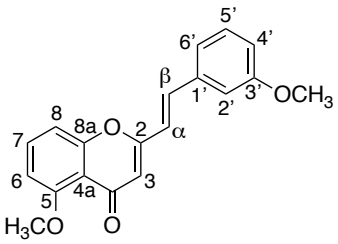

Compound **26e** was obtained as a yellow solid after thin layer chromatography with DCM (0.200 g, 59%).

M.p.: 123-125ºC.

^{1}H NMR (500.16 MHz, $CDCl_3$): δ = 3.87 (s, 3H, 3'-OC<u>H</u>$_3$), 4.00 (s, 3H, 5-OC<u>H</u>$_3$), 6.25 (s, 1H, H-3), 6.71 (d, 1H, *J* = 16.1 Hz, H-α), 6.81 (dd, 1H, *J* = 8.4, 1.0 Hz, H-6), 6.93 (ddt, 1H, *J* = 8.1, 2.2, 0.9 Hz, H-4'), 7.08 (t, 1H, *J* = 2.2 Hz, H-2'), 7.11 (dd, 1H, *J* = 8.4, 1.0 Hz, H-8), 7.17 (ddt, 1H, *J* = 8.1, 2.2, 0.9 Hz, H-6'), 7.33 (t, 1H, *J* = 8.1 Hz, H-5'), 7.51 (d, 1H, *J* = 16.1 Hz, H-β), 7.57 (t, 1H, *J* = 8.4 Hz, H-7) ppm.

^{13}C NMR (125.77 MHz, $CDCl_3$): δ = 55.4 (3'-O<u>C</u>H$_3$), 56.5 (5-O<u>C</u>H$_3$), 106.3 (C-6), 110.0 (C-8), 112.4 (C-3), 112.6 (C-2'), 114.7 (C-4a), 115.5 (C-4'), 120.2 (C-α), 120.3 (C-6'), 130.0 (C-5'), 133.7 (C-7), 136.3 (C-β), 136.5 (C-1'), 158.1 (C-8a), 159.5 (C-2), 159.8 (C-5), 160.0 (C-3'), 178.4 (C=O) ppm.

MS (ESI$^+$) m/z (%): 309.3 [(M+H)$^+$, 30], 331.2 [(M+Na)$^+$, 9], 639.0 [(2M+Na)$^+$, 100].

To a round-bottomed flask with 5.0 mL of ethanol and sodium (4.0 equiv, 0.101 g, 4.4 mmol), was added 5-methoxy-2-methylchromone (1.0 equiv, 0.200 g, 1.10 mmol). When the reaction turned dark orange/red, 3',4',5'-methoxybenzaldehyde (**25f**) (1.5 equiv, 0.20 mL, 1.65 mmol) were added to the mixture. The reaction was left stirring overnight and then poured into iced water and acidified. The precipitate was dissolved in DCM and washed with water. The organic layer was dried with

anhydrous sodium sulfate, and the solvent was evaporated to dryness, to afford (*E*)-2-styrylchromone **26f**.

(*E*)-5-Methoxy-2-(3,4,5-trimethoxystyryl)-4*H*-chromen-4-one (26f).

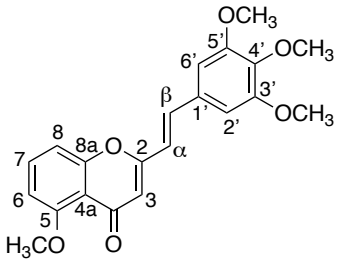

Compound **26f** was obtained as an orange-brick color solid, after crystallization with DCM (0.057 g, 76%).

^{1}H NMR (500.16 MHz, $CDCl_3$): δ = 3.90 (s, 3H, 4'-OC$\underline{H}_3$), 3.94 (s, 6H, 3'-OC$\underline{H}_3$, 5'-OC$\underline{H}_3$), 3.99 (s, 3H, 5-OC$\underline{H}_3$), 6.51 (s, 1H, H-3), 6.67 (s, 2H, H-2',6'), 6.78 (d, 1H, *J* = 8.2 Hz, H-6), 6.81 (d, 1H, *J* = 15.9 Hz, H-α), 7.14 (d, 1H, *J* = 8.2 Hz, H-8), 7.51 (d, 1H, *J* = 15.9 Hz, H-β), 7.65 (t, 1H, *J* = 8.2 Hz, H-7) ppm.

^{13}C NMR (125.77 MHz, $CDCl_3$): δ = 107.7 (C-8), 107.8 (C-3), 107.9 (C-2',6'), 110.6 (C-4a), 111.2 (C-6), 116.5 (C-α), 136.2 (C-7), 136.9 (C-1'), 139.5 (C-β), 156.2 (C-8a), 160.4 (C-5), 164.5 (C-2), 183.3 (C=O) ppm.

To a round-bottomed flask with 3.0 mL of ethanol and sodium (4.0 equiv, 0.048 g, 2.1 mmol), was added 2-methylchromone (1.0 equiv, 0.083 g, 0.52 mmol). When the reaction turned dark orange/red, 3'-methoxybenzaldehyde (**25e**) (1.5 equiv, 0.106 g, 0.78 mmol) were added to the mixture. The reaction was left stirring overnight and then poured into iced water and acidified. The precipitate was dissolved in DCM and washed with water. The organic layer was dried with anhydrous sodium sulfate, and the solvent was evaporated to dryness, affording compound **27a**.

(*E*)-2-(3-Methoxystyryl)-4*H*-chromen-4-one (27a)

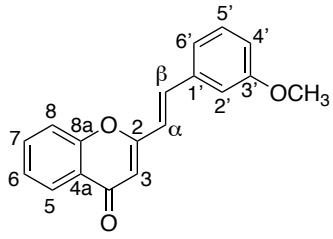

Compound **27a** was obtained as an orange brick color solid, after thin layer chromatography with DCM (0.080 g, 55%).

^{1}H NMR (300.13 MHz, $CDCl_3$): δ = 3.88 (s, 3H, 3'-OC$\underline{H}_3$), 6.34 (s, 1H, H-3), 6.79 (d, 1H, *J* = 16.1 Hz, H-α), 6.95 (ddd, 1H, *J* = 8.0, 2.0, 1.1 Hz, H-4'), 7.11 (t, 1H, *J* = 2.0 Hz, H-2'), 7.19 (ddd, 1H, *J* = 8.0, 2.0, 1.1 Hz, H-6'), 7.35 (t, 1H, *J* = 8.0 Hz, H-5'), 7.40 (ddd, 1H, *J* = 8.0, 7.1, 0.9 Hz, H-6), 7.54 (dd, 1H, *J* = 8.5, 0.9 Hz, H-8), 7.59 (d, 1H, *J* = 16.1 Hz, H-β), 7.69 (ddd, 1H, *J* = 8.5, 7.1, 1.6 Hz, H-7), 8.21 (dd, 1H, *J* = 8.0, 1.6 Hz, H-5) ppm.

5.2.6 Synthesis of hydroxylated (*E*)-2-styrylchromones by cleavage of the protecting methoxy groups

Compound (*E*)-5-methoxy-2-(3-chlorostyryl)-4*H*-chromen-4-one (**26a**) (1.0 equiv, 0.072 g, 0.23 mmol) was dissolved in 2.0 mL of dry DCM for a BBr_3-promoted cleavage reaction of the methoxy groups, with the addition of 2.5 equiv of BBr_3 1.0 M (0.58 mL, 0.58 mmol) at ~-70ºC. After

the addition of BBr_3, the reaction was left stirring at room temperature, for 1 h and 30 min. The reaction mixture was then poured into iced water, resulting in a precipitate which was filtered and recrystallized, affording compound **26'a**.

(*E*)-5-Hydroxy-2-(3-chlorostyryl)-4*H*-chromen-4-one (26'a)

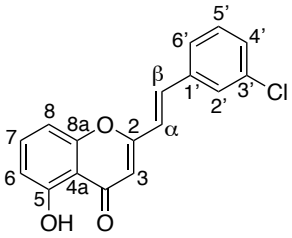

Compound **26'a** was obtained as a white solid after thin layer chromatography with DCM (0.066 g, 96%).

M.p.: 187-189ºC

^{1}H NMR (300.13 MHz, $CDCl_3$): δ = 6.27 (s, 1H, H-3), 6.77 (d, 1H, *J* = 15.9 Hz, H-α), 6.81 (dd, 1H, *J* = 8.4, 0.9 Hz, H-6), 6.97 (dd, 1H, *J* = 8.4, 0.9 Hz, H-8), 7.36-7.38 (m, 2H, H-2',5'), 7.45-7.48 (m, 1H, H-4'), 7.55 (t, 1H, *J* = 8.4 Hz, H-7), 7.56 (d, 1H, *J* = 15.9 Hz, H-β), 7.58-7.59 (m, 1H, H-6'), 12.54 (s, 1H, 5-O<u>H</u>) ppm.

^{13}C NMR (75.47 MHz, $CDCl_3$): δ = 107.0 (C-8), 109.8 (C-3), 111.2 (C-4a), 111.6 (C-6), 121.2 (C-α), 126.1 (C-4'), 127.7 (C-6'), 130.1 (C-5'), 130.4 (C-2'), 135.3 (C-3'), 135.7 (C-7), 136.5 (C-β), 136.7 (C-1'), 156.3 (C-8a), 161.0 (C-5), 162.3 (C-2), 183.7 (C=O) ppm.

MS (ESI$^+$) m/z (%): 299.1 [(M+H)$^+$, ^{35}Cl, 100], 301.2 [(M+H)$^+$, ^{37}Cl, 55], 620.1 [(2M+Na)$^+$, 29], 636.1 [(2M+K)$^+$, 10].

Compound (*E*)-2-(3,4-dichlorostyryl)-5-methoxy-4*H*-chromen-4-one (**26b**) (1.0 equiv, 0.129 g, 0.37 mmol) was dissolved in 2.0 mL of dry DCM for a BBr_3-promoted cleavage reaction of the methoxy groups, with the addition of 2.5 equiv of BBr_3 1.0 M (0.93 mL, 0.93 mmol) at ~-70ºC. After the addition of BBr_3, the reaction was left stirring, at room temperature, for 24 h. The reaction mixture was then poured into iced water, resulting in a precipitate which was filtered and recrystallized, to afford (*E*)-2-styrylchromone **26'b**.

(*E*)-5-Hydroxy-2-(3,4-dichlorostyryl)-4*H*-chromen-4-one (26'b)

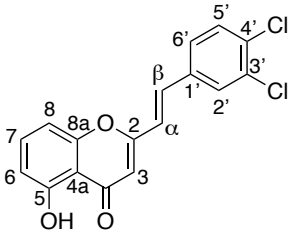

Compound **26'b** was obtained as a light-yellow solid, after recrystallization with DCM/Hexane (0.099 g, 80%).

M.p.: 225-227ºC

^{1}H NMR (500.16 MHz, $CDCl_3$): δ = 6.28 (s, 1H, H-3), 6.75 (d, 1H, *J* = 16.0 Hz, H-α), 6.81 (dd, 1H, *J* = 8.3, 0.9 Hz, H-6), 6.96 (dd, 1H, *J* = 8.3, 0.9 Hz, H-8), 7.42 (dd, 1H, *J* = 8.3, 2.1 Hz, H-6'), 7.51 (d, 1H, *J* = 8.3 Hz, H-5'), 7.52 (d, 1H, *J* = 16.0 Hz, H-β), 7.55 (t, 1H, *J* = 8.3 Hz, H-7), 7.68 (d, 1H, *J* = 2.1 Hz, H-2'), 12.51 (s, 1H, 5-O<u>H</u>) ppm.

^{13}C NMR (125.77 MHz, $CDCl_3$): δ = 107.0 (C-8), 110.0 (C-3), 111.2 (C-4a), 111.7 (C-6), 121.5 (C-α), 126.8 (C-6'), 129.5 (C-2'), 131.2 (C-5'), 133.6 (C-3'), 134.2 (C-4'), 134.9 (C-1'), 135.3 (C-β), 135.7 (C-7), 156.3 (C-8a), 161.0 (C-5), 162.1 (C-2), 183.7 (C=O) ppm.

MS (ESI$^+$) m/z (%): 333.2 [(M+H)$^+$, ^{35}Cl, 28], 335.2 [(M+H)$^+$, ^{35}Cl, ^{37}Cl, 21], 337.2 [(M+H)$^+$, ^{37}Cl, 13], 355.4 [(M+Na)$^+$, 22].

Compound (*E*)-5-methoxy-2-(2,6-dichlorostyryl)-4*H*-chromen-4-one (**26c**) (1.0 equiv, 0.089 g, 0.26 mmol) was dissolved in 3.0 mL of dry DCM for a BBr_3-promoted cleavage reaction of the methoxy groups, with the addition of 2.5 equiv of BBr_3 1.0 M (0.65 mL, 0.65 mmol) at ~-70ºC. After the addition of BBr_3, the reaction was left stirring, at room temperature, for 2 h. The reaction mixture was then poured into iced water, resulting in a precipitate which was filtered and recrystallized, giving compound **26'c**.

(*E*)-5-Hydroxy-2-(2,6-dichlorostyryl)-4*H*-chromen-4-one (26'c)

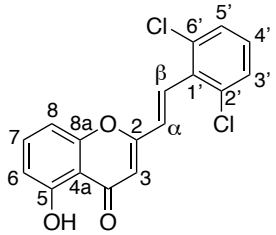

Compound **26'c** was obtained as a light-yellow solid, after crystallization with DCM/Hexane (0.074 g, 85%).

M.p.: 229-231ºC

^{1}H NMR (500.16 MHz, $CDCl_3$): δ = 6.30 (s, 1H, H-3), 6.82 (dd, 1H, *J* = 8.4, 0.9 Hz, H-6), 6.95 (d, 1H, *J* = 16.4 Hz, H-α), 7.00 (dd, 1H, *J* = 8.4, 0.9 Hz, H-8), 7.22 (t, 1H, *J* = 8.1 Hz, H-4'), 7.40 (d, 2H, *J* = 8.1 Hz, H-3',5'), 7.56 (t, 1H, *J* = 8.4 Hz, H-7), 7.72 (d, 1H, *J* = 16.4 Hz, H-β), 12.51 (s, 1H, 5-O<u>H</u>) ppm.

^{13}C NMR (125.77 MHz, $CDCl_3$): δ = 107.5 (C-8), 110.6 (C-3), 111.5 (C-4a), 111.9 (C-6), 128.5 (C-α), 129.4 (C-3',5'), 130.2 (C-4'), 131.9 (C-β), 132.6 (C-1'), 135.3 (C-2',6'), 136.0 (C-7), 156.7 (C-8a), 161.2 (C-5), 162.2 (C-2), 184.1 (C=O) ppm.

MS (ESI$^+$) m/z (%): 333.1 [(M+H)$^+$, ^{35}Cl, 100], 335.1 [(M+H)$^+$, ^{35}Cl, ^{37}Cl, 61], 337.1 [(M+H)$^+$, ^{37}Cl, 15], 703.1 [(2M+K)$^+$, 7].

Compound (*E*)-5-methoxy-2-(2-methoxystyryl)-4*H*-chromen-4-one (**26d**) (1.0 equiv, 0.101 g, 0.33 mmol) was dissolved in 4.0 mL of dry DCM for a BBr_3-promoted cleavage reaction of the methoxy groups, with the addition of 5.0 equiv of BBr_3 1.0 M (1.65 mL, 1.65 mmol) at ~-70ºC. After the addition of BBr_3, the reaction was left stirring, at room temperature, for 6 days. The reaction mixture was then poured into iced water, resulting in a precipitate which was filtered and recrystallized, achieving compound **26'd**.

(*E*)-5-Hydroxy-2-(2-hydroxystyryl)-4*H*-chromen-4-one (26'd)

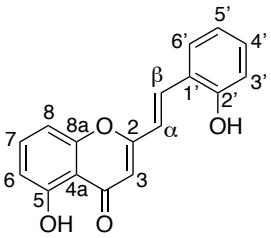

Compound **26'd** was obtained as a brown solid, after crystallization with DCM (0.049 g, 83%).

M.p.: 244-245ºC

^{1}H NMR (500.16 MHz, MeOD): δ = 6.33 (s, 1H, H-3), 6.77 (dd, 1H, *J* = 8.4, 1.0 Hz, H-6), 6.88 (dd, 1H, *J* = 7.9, 1.1 Hz, H-3'), 6.89 (ddd, 1H, *J* = 8.1, 7.4, 1.1 Hz, H-5'), 7.09 (dd, 1H, *J* = 8.4, 1.0 Hz, H-8), 7.12 (d, 1H, *J* = 16.2 Hz, H-α), 7.22 (ddd, 1H, *J* = 7.9, 7.4, 1.6 Hz, H-4'), 7.61 (dd, 1H, *J* = 8.1, 1.6 Hz, H-6'), 7.62 (t, 1H, *J* = 8.4 Hz, H-7), 8.01 (d, 1H, *J* = 16.2 Hz, H-β), 12.55 (s, 1H, 5-O<u>H</u>) ppm.

^{13}C NMR (125.77 MHz, MeOD): δ = 108.2 (C-8), 108.8 (C-3), 111.7 (C-4a), 112.1 (C-6), 117.1 (C-3'), 120.1 (C-α), 120.9 (C-5'), 123.2 (C-1'), 129.7 (C-6'), 132.5 (C-4'), 135.7 (C-β), 136.8 (C-7), 157.8 (C-8a), 158.3 (C-2'), 161.8 (C-5), 166.2 (C-2), 185.2 (C=O) ppm.

MS (ESI$^+$) m/z (%): 281.2 [(M+H)$^+$, 98].

Compound (*E*)-5-methoxy-2-(3-methoxystyryl)-4*H*-chromen-4-one (**26e**) (1.0 equiv, 0.200 g, 0.65 mmol) was dissolved in 6.0 mL of dry DCM for a BBr_3-promoted cleavage reaction of the methoxy groups, with the addition of 5.0 equiv of BBr_3 1.0 M (3.25 mL, 3.25 mmol) at ~-70ºC. After the addition of BBr_3, the reaction was left stirring, at room temperature, for 24 h. The reaction mixture was then poured into iced water, resulting in a precipitate which was filtered and recrystallized, to afford compound **26'e**.

(*E*)-5-Hydroxy-2-(3-hydroxystyryl)-4*H*-chromen-4-one (26'e)

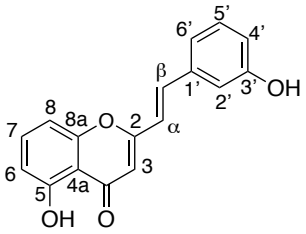

Compound **26'e** was obtained as a yellow solid, after crystallization with DCM (0.082 g, 45%).

Decomposition: 196-207ºC

^{1}H NMR (300.13 MHz, MeOD): δ = 6.38 (s, 1H, H-3), 6.78 (dd, 1H, *J* = 8.4, 0.9 Hz, H-6), 6.84 (ddt, 1H, *J* = 7.8, 2.3, 1.1 Hz, H-4'), 6.98 (d, 1H, *J* = 16.1 Hz, H-α), 7.09 (t, 1H, *J* = 2.3 Hz, H-2'), 7.10 (dd, 1H, *J* = 8.4, 0.9 Hz, H-8), 7.15 (d, 1H, *J* = 7.8 Hz, H-6'), 7.25 (t, 1H, *J* = 7.8 Hz, H-5'), 7.62 (t, 1H, *J* = 8.4 Hz, H-7), 7.65 (d, 1H, *J* = 16.1 Hz, H-β) ppm.

^{13}C NMR (75.47 MHz, MeOD): δ = 108.2 (C-8), 109.4 (C-3), 111.8 (C-4a), 112.2 (C-6), 115.2 (C-2'), 118.4 (C-4'), 120.5 (C-α), 120.7 (C-6'), 131.1 (C-5'), 136.9 (C-7), 137.7 (C-1'), 139.8 (C-β), 157.7 (C-8a), 159.1 (C-3'), 161.7 (C-5), 165.3 (C-2), 185.2 (C=O) ppm.

MS (ESI$^+$) m/z (%): 281.2 [(M+H)$^+$, 35], 303.2 [(M+Na)$^+$, 5], 319.2 [(M+K)$^+$, 7], 561.6 [(2M+H)$^+$, 11], 583.6 [(2M+Na)$^+$, 5].

Compound (*E*)-5-methoxy-2-(3,4,5-trimethoxystyryl)-4*H*-chromen-4-one (**26f**) (1.0 equiv, 0.090 g, 0.24 mmol) was dissolved in 3.0 mL of dry DCM for a BBr_3-promoted cleavage reaction of the methoxy groups, with the addition of 10.0 equiv of BBr_3 1.0 M (2.40 mL, 2.40 mmol) at ~-70ºC. After the addition of BBr_3, the reaction was left stirring, at room temperature, for 23 h. The reaction mixture was then poured into iced water, resulting in a precipitate which was filtered and recrystallized, affording (*E*)-2-styrylchromone **26'f**.

(*E*)-5-Hydroxy-2-(3,4,5-trihydroxystyryl)-4*H*-chromen-4-one (26'f)

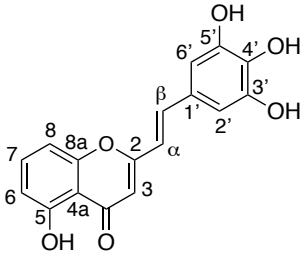

Compound **26'f** was obtained as an orange-brick color solid, after crystallization with DCM (0.057 g, 76%).

Decomposition: 242-337ºC

^{1}H NMR (500.16 MHz, $CDCl_3$): δ = 6.50 (s, 1H, H-3), 6.67 (s, 2H, H-2',6'), 6.78 (d, 1H, *J* = 8.2 Hz, H-6), 6.80 (d, 1H, *J* = 15.9 Hz, H-α), 7.14 (d, 1H, *J* = 8.2 Hz, H-8), 7.51 (d, 1H, *J* = 15.9 Hz, H-β), 7.64 (t, 1H, *J* = 8.2 Hz, H-7), 12.81 (s, 1H, 5-O<u>H</u>) ppm.

^{13}C NMR (125.77 MHz, $CDCl_3$): δ = 107.3 (C-8), 107.4 (C-3), 107.5 (C-2',6'), 110.2 (C-4a), 110.8 (C-6), 116.1 (C-α), 125.3 (C-1'), 135.7 (C-7), 136.5 (C-4'), 139.1 (C-β), 146.3 (C-3',5') ,155.8 (C-8a), 160.0 (C-5), 164.15 (C-2), 182.9 (C=O) ppm.

MS (ESI^+) m/z (%): 313.2 [$(M+H)^+$, 8], 663.7 [$(2M+K)^+$, 78].

Compound (*E*)-2-(3-methoxystyryl)-4*H*-chromen-4-one (**27a**) (1.0 equiv, 0.078 g, 0.28 mmol) was dissolved in 2.0 mL of dry DCM for a BBr_3-promoted cleavage reaction of the methoxy groups, with the addition of 2.5 equiv of BBr_3 1.0 M (0.70 mL, 0.70 mmol) at ~-70ºC. After the addition of BBr_3, the reaction was left stirring overnight, at room temperature. The reaction mixture was then poured into iced water, resulting in a precipitate which was filtered and recrystallized, to afford compound **27'a**.

(*E*)-2-(3-Hydroxystyryl)-4*H*-chromen-4-one (27'a)

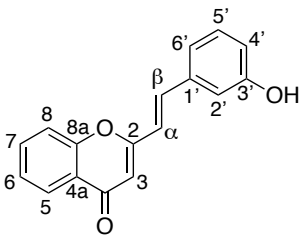

Compound **27'a** was obtained as a light-yellow solid, after recrystallization with DCM (0.0121 g, 16%).

M.p.: 187-189ºC

^{1}H NMR (500.16 MHz, $CDCl_3$): δ = 6.42 (s, 1H, H-3), 6.83 (d, 1H, *J* = 16.2 Hz, H-α), 6.86 (dd, 1H, *J* = 7.5 Hz, H-4'), 7.06 (dd, 1H, *J* = 7.5 Hz, H-6'), 7.09 (s, 1H, H-2'), 7.24 (t, 1H, *J* = 7.5 Hz, H-5'), 7.41 (t, 1H, *J* = 7.7 Hz, H-6), 7.55 (dd, 1H, *J* = 7.7 Hz, H-8), 7.58 (d, 1H, *J* = 16.2 Hz, H-β), 7.70 (ddd, 1H, *J* = 8.2, 7.7 Hz, H-7), 8.16 (dd, 1H, *J* = 7.7 Hz, H-5) ppm.

^{13}C NMR (125.77 MHz, $CDCl_3$): δ = 109.9 (C-3), 110.9 (C-4a), 113.8 (C-2'), 117.6 (C-4'), 118.0 (C-8), 120.0 (C-α), 120.3 (C-6'), 125.4 (C-6), 125.6 (C-5), 130.1 (C-5'), 134.3 (C-7), 136.3 (C-1'), 138.1 (C-β), 156.2 (C-8a), 157.4 (C-3'), 163.0 (C-2), 179.1 (C=O) ppm.
MS (ESI^+) m/z (%): 265.2 [$(M+H)^+$, 60], 287.1 [$(M+Na)^+$, 24].

5.3. Biological effects of (*E*)-2-styrylchromones in the oxidative burst of human monocytes

5.3.1 •NO scavenging assay

The scavenging of •NO by (*E*)-2-styrylchromones was evaluated based on the Griess *in chemico* method, a procedure already described and tested.[101,102] For the standard gallic acid were prepared seven dilutions in DMSO, between 0.006 µM and 0.195 µM, and for each compound were prepared eight dilutions also in DMSO, between 3.125 µM and 400.0 µM.

Into a 96-well plate were pipetted 100.0 µL of buffer (blank), standard (up to six different concentrations, in duplicate) or compound (up to eight different concentrations, in triplicate) and 100.0 µL of sodium nitroprusside (SNP) solution 1.0 mM. Then, the microplate was incubated under a fluorescent lamp for 15 min. After that time, were added 100.0 µL of the Griess reagent and 100.0 µL of phosphoric acid 5% to the third well of each compound, to make sure that the compounds' own color would not interfere. Lastly, the microplate was incubated in the dark, at room temperature, for 10 min. and then the absorbance was read at 562 nm, using the microplate reader.

5.3.2 Isolation of monocytes from human blood

Fresh human venous blood was collected, each day, antecubital venipuncture, from healthy volunteers, into four K3EDTA vacuum tubes (≈ 4.0 mL per tube). The cell types were separated according to their density, using two different solutions: histopaque 1119 (density of 1.119 g/mL) and histopaque 1077 (density of 1.077 g/mL), both at room temperature.[104] Approximately 3.0 mL of each solution were pipetted into four 15.0 mL polypropylene tubes (a material that prevents adhesion of the cells to the wall of the tube). Firstly, 3.0 mL of histopaque 1119 were pipetted into each tube and then 3.0 mL of histopaque 1077, considering that the pipetting of this last solution was done slowly and carefully to avoid the mixing of both solutions. Lastly, the blood was carefully layered on top of this discontinuous density gradient and the tubes were centrifuged at 980*g* for 30 min. at 20ºC, during which the cells were distributed along the tube, according to their density. The plasma was discarded and the agranulocytes and platelets layer was collected, using a *Pasteur* pipette, into centrifuge tubes with PBS buffer without Ca^{2+} and Mg^{2+} ions (≈ 10 mL) (this reduces the viscosity of the histopaque-monocyte suspension so that the cells can be centrifuged without the need for higher *g* forces). The tubes were then centrifuged at 890*g* for 5 min., at 4°C, to preserve the integrity of the cells. The resultant supernatant was discarded, and the monocytes pellet was resuspended in 1.25

mL of PBS without Ca^{2+} and Mg^{2+} ions, to wash the cells. The tubes were once again centrifuged in the aforementioned conditions, to preserve the integrity of the cells. Finally, the supernatant was aspirated and discarded, and the monocytes pellet was resuspended in Tris-Glucose buffer (1.26 mM $CaCl_2$, 5.37 mM KCl, 0.81 mM $MgSO_4$, 140.0 mM NaCl, 25.0 mM Trizma, pH = 7.4). In order to maintain the isolated monocytes' viability, the cells were kept in ice and under stirring in an orbital shaker, until use.[105,112]

5.3.3 Cell count and viability assessment

To perform the trypan blue dye exclusion method, 20.0 µL of freshly isolated human monocytes suspension and 20.0 µL of trypan blue (0.4%) were mixed in a microtube (cells dilution factor = 2). The mixture was then pipetted into a Neubauer chamber, and the monocytes were counted under an optical microscope.[107] Each study corresponded to, at least, two independent assays.

5.3.4 UV/Vis absorption and emission spectra of (*E*)-2-styrylchromones

For each (*E*)-2-styrylchromone were prepared sequential dilutions, in DMSO, with concentrations between 6.25 µM and 25.0 µM. Starting from the more concentrated solution to the less concentrated one, both absorption and emission spectra were obtained for all the compounds, using the spectrophotometer and the fluorimeter, respectively. Whenever a solution showed absorbance values higher than 0.100 nm, the spectra were obtained for the lower solution, until the concentration that did not exceed the 0.100 nm was found. According to each compound maximum wavelength, the chosen concentration was read in the fluorimeter, to make sure it would not also emit fluorescence.

5.3.5 Effects of (*E*)-2-styrylchromones on human monocytes cell death

In order to understand the level of toxicity of the nine (*E*)-2-styrylchromones under study against the oxidative burst caused by human monocytes and adequately select the maximum concentrations that can be tested in the following assay, it was carried out the Annexin V FITC binding and PI staining methods, according to Soares et al., with some modifications.[113]

Firstly, it was evaluated the effect of (*E*)-2-styrylchromones on human monocytes' viability. Accordingly, 225.0 µL of the cells' suspension (2.0 x 10^6 cells/mL), 12.5 µL of DMSO (the solvent used for the dilutions of the compounds in study) or 12.5 µL of each (*E*)-2-styrylchromone (in a range of concentrations established in **section 3.3.4**, which may be up to 25.0 µM) and 12.5 µL of TRIS-Glucose 5.5 mM buffer were incubated in a 48-well transparent polystyrene microplate, at 37ºC. After 2 h of incubation, the content of each well was collected into conical microtubes, which were then centrifuged at 400*g*, for 5 min., at 20°C. The resulting supernatants were discarded, and each pellet was resuspended in 500.0 µL of PBS. Subsequently, a second centrifugation was performed in the

same conditions as the previous one. Once again, the resulting supernatants were discarded and this time the pellets were resuspended in 100.0 µL of annexin buffer, 2.5 µL of annexin V FITC solution and 2.5 µL of PI solution (1.0 µg/mL). Once the stains were added, the microtubes were incubated during 15 min. in the dark, at room temperature. After this period, 500.0 µL of buffer were added and the fluorescence readings were taken in the flow cytometer. Fluorescence signals, for at least 10000 cells, were collected in logarithmic mode, followed in channel 1 (FL1-A) as well as in channel 3 (FL3-A) and the data was analyzed using C Flow (BD Accuri ®) software. Each study corresponded to, at least, three independent assays. The effects of each compound in monocytes' viability were expressed as the percentage of apoptosis and necrosis.

5.3.6 Evaluation of the inhibitory effect of (*E*)-2-styrylchromones against PMA-induced RS production by human monocytes

The inhibitory effects of (*E*)-2-styrylchromones in the oxidative burst in human monocytes were evaluated based on a method that mimics the production of reactive species, *in vitro*, a procedure already described and tested.[114]

Into a 96-well plate were pipetted 212.5 µL of the cells' suspension (2.0 x 10^6 cells/mL), 12.5 µL of each compound (up to five different concentrations) or DMSO (for the blank and control), 12.5 µL of dihydrorhodamine and, at last, 12.5 µL of PMA or Tris-Glucose buffer (for the blank). The kinetics study of the oxidation of DHR to rhodamine was performed at 37°C, in which the fluorescence signal was detected for 1 h and 40 min., at the emission wavelength of 528 nm with excitation at 485 nm, using the microplate reader.

Chapter 6 - References

References

(1) Popa-Wagner, A.; Mitran, S.; Sivanesan, S.; Chang, E.; Buga, A. M. ROS and Brain Diseases: The Good, the Bad, and the Ugly. *Oxid. Med. Cell. Longev.* **2013**, No. December. https://doi.org/10.1155/2013/963520.

(2) Sousa, A.; Lucas, M.; Ribeiro, D.; Correia, C. M.; Silva, V. L. M.; Silva, A. M. S.; Fernandes, E.; Freitas, M. Chalcones as Modulators of Neutrophil Oxidative Burst under Physiological and High Glucose Conditions. *J. Nat. Prod.* **2020**, *83* (10), 3131–3140. https://doi.org/10.1021/acs.jnatprod.0c00728.

(3) Berlett, B. S.; Stadtman, E. R. Protein Oxidation in Aging, Disease, and Oxidative Stress. *J. Biol. Chem.* **1997**, *272* (33), 20313–20316. https://doi.org/10.1074/jbc.272.33.20313.

(4) Salzano, S.; Checconi, P.; Hanschmann, E. M.; Lillig, C. H.; Bowler, L. D.; Chan, P.; Vaudry, D.; Mengozzi, M.; Coppo, L.; Sacre, S.; Atkuri, K. R.; Sahaf, B.; Herzenberg, L. A.; Herzenberg, L. A.; Mullen, L.; Ghezzi, P. Linkage of Inflammation and Oxidative Stress via Release of Glutathionylated Peroxiredoxin-2, Which Acts as a Danger Signal. *Proc. Natl. Acad. Sci. U. S. A.* **2014**, *111* (33), 12157–12162. https://doi.org/10.1073/pnas.1401712111.

(5) Anderson, M. T.; Staal, F. J. T.; Gitler, C.; Herzenberg, L. A.; Herzenberg, L. A. Separation of Oxidant-Initiated and Redox-Regulated Steps in the NF-KB Signal Transduction Pathway. *Proc. Natl. Acad. Sci. U. S. A.* **1994**, *91* (24), 11527–11531. https://doi.org/10.1073/pnas.91.24.11527.

(6) Flohé, L.; Brigelius-Flohé, R.; Saliou, C.; Traber, M. G.; Packer, L. Redox Regulation of NF-Kappa B Activation. *Free Radic. Biol. Med.* **1997**, *22* (6), 1115–1126. https://doi.org/10.1016/S0891-5849(96)00501-1.

(7) Collins, T. Acute and Chronic Inflammation. In *Robbins and Cotran Pathologic Basis of Disease*; **2009**, 50–88.

(8) Gallin, J. I.; Goldstein, I. M.; Snyderman, R. Inflammation: Basic Principles and Clinical Correlates. In *New Biological Books*; **1992**, 367.

(9) Takeuchi, O.; Akira, S. Pattern Recognition Receptors and Inflammation. *Cell* **2010**, *140* (6), 805–820. https://doi.org/10.1016/j.cell.2010.01.022.

(10) Lawrence, T.; Willoughby, D. A.; Gilroy, D. W. Anti-Inflammatory Lipid Mediators and Insights into the Resolution of Inflammation. *Nat. Rev. Immunol.* **2002**, *2* (10), 787–795. https://doi.org/10.1038/nri915.

(11) Perkins, J. A. Acute and Chronic Inflammation. In *Robbins and Cotran Pathologic Basis of Disease*; 2010; pp 43–77.

(12) Ribeiro, D.; Freitas, M.; Lima, J. L. F. C.; Fernandes, E. Proinflammatory Pathways: The Modulation by Flavonoids. *Med. Res. Rev.* **2015**, *35* (5), 877–936. https://doi.org/10.1002/med.21347.

(13) Hussain, T.; Tan, B.; Yin, Y.; Blachier, F.; Tossou, M. C. B.; Rahu, N. Oxidative Stress and Inflammation: What Polyphenols Can Do for Us? *Oxid. Med. Cell. Longev.* **2016**, *2016*. https://doi.org/10.1155/2016/7432797.

(14) Majno, G.; Joris, I. *Cells, Tissues and Disease*, 2nd ed.; **2004**.

(15) Medzhitov, R. Inflammation 2010: New Adventures of an Old Flame. *Cell* **2010**, *140* (6), 771–776. https://doi.org/10.1016/j.cell.2010.03.006.

(16) Rosales, C.; Uribe-Querol, E. Phagocytosis: A Fundamental Process in Immunity. *Biomed Res. Int.* **2017**, *2017*, 1–18. https://doi.org/10.1155/2017/9042851.

(17) Tauber, A. I. Metchnikoff and the Phagocytosis Theory. *Nat. Rev. Mol. Cell Biol.* **2003**, *4* (11), 897–901.

(18) Linthout, S. Van; Miteva, K.; Tschöpe, C. Crosstalk between Fibroblasts and Inflammatory Cells. *Cardiovasc. Res.* **2014**, *102* (2), 258–269. https://doi.org/10.1093/cvr/cvu062.

(19) van Furth, R.; Beekhuizen, H. Monocytes. In *Encyclopedia of Immunology (Second Edition)*; Delves, P. J., Ed.; Elsevier: Oxford, **1998**, 1750–1754. https://doi.org/https://doi.org/10.1006/rwei.1999.0443.

(20) Ziegler-Heitbrock, L.; Ancuta, P.; Crowe, S.; Dalod, M.; Grau, V.; Hart, D. N.; Leenen, P. J. M.; Liu, Y. J.; MacPherson, G.; Randolph, G. J.; Scherberich, J.; Schmitz, J.; Shortman, K.; Sozzani, S.; Strobl, H.; Zembala, M.; Austyn, J. M.; Lutz, M. B. Nomenclature of Monocytes and Dendritic Cells in Blood. *Blood* **2010**, *116* (16), 5–7. https://doi.org/10.1182/blood-2010-02-258558.

(21) Wrigley, B. J.; Lip, G. Y. H.; Shantsila, E. The Role of Monocytes and Inflammation in the Pathophysiology of Heart Failure. *Eur. J. Heart Fail.* **2011**, *13* (11), 1161–1171. https://doi.org/10.1093/eurjhf/hfr122.

(22) Geissmann, F.; Jung, S.; Littman, D. R. Blood Monocytes Consist of Two Principal Subsets with Distinct Migratory Properties. *Immunity* **2003**, *19* (1), 71–82. https://doi.org/https://doi.org/10.1016/S1074-7613(03)00174-2.

(23) Mirjam, K.; Broos, C. E. *Immunological Manifestations in Sarcoidosis*; Elsevier Inc., **2019**, *3*. https://doi.org/10.1016/b978-0-323-54429-0.00003-3.

(24) Tesfaigzi, Y.; Daheshia, M. CD14. In *Encyclopedia of Respiratory Medicine*; Laurent, G. J., Shapiro, S. D., Eds.; Academic Press: Oxford, **2006**, 343–347. https://doi.org/https://doi.org/10.1016/B0-12-370879-6/00063-6.

(25) Naeim, F.; Nagesh Rao, P.; Song, S. X.; Phan, R. T. Chapter 2 - Principles of Immunophenotyping. In *Atlas of Hematopathology (Second Edition)*; Naeim, F., Nagesh Rao, P., Song, S. X., Phan, R. T., Eds.; Academic Press, **2018**, 29–56. https://doi.org/https://doi.org/10.1016/B978-0-12-809843-1.00002-4.

(26) Nimmerjahn, F.; Ravetch, J. V. Fc$γ$Rs in Health and Disease. In *Negative Co-Receptors and Ligands*; Ahmed, R., Honjo, T., Eds.; Springer Berlin Heidelberg: Berlin, Heidelberg; **2011**, 105–125. https://doi.org/10.1007/82_2010_86.

(27) Rosales, C.; Uribe-Querol, E. Fc Receptors: Cell Activators of Antibody Functions. *Adv. Biosci. Biotechnol.* **2013**, *4* (4), 21–33. https://doi.org/10.4236/abb.2013.44a004.

(28) Daëron, M. Fc Receptor Biology. *Annu. Rev. Immunol.* **1997**, *15* (1), 203–234. https://doi.org/10.1146/annurev.immunol.15.1.203.

(29) Ravetch, J. V; Bolland, S. IgG Fc Receptors. *Annu. Rev. Immunol.* **2001**, *19* (1), 275–290. https://doi.org/10.1146/annurev.immunol.19.1.275.

(30) Kratofil, R. M.; Kubes, P.; Deniset, J. F. Monocyte Conversion during Inflammation and Injury. *Arterioscler. Thromb. Vasc. Biol.* **2017**, *37* (1), 35–42. https://doi.org/10.1161/ATVBAHA.116.308198.

(31) Jakubzick, C. V; Randolph, G. J.; Henson, P. M. Monocyte Differentiation and Antigen-Presenting Functions. *Nat. Rev. Immunol.* **2017**, *17* (6), 349–362. https://doi.org/10.1038/nri.2017.28.

(32) van Furth, R.; Cohn, Z. A. The Origin and Kinetics of Mononuclear Phagocytes. *J. Exp. Med.* **1968**, *128* (3), 415–435. https://doi.org/10.1084/jem.128.3.415.

(33) Cathcart, M. K. Regulation of Superoxide Anion Production by NADPH Oxidase in Monocytes/Macrophages: Contributions to Atherosclerosis. *Arterioscler. Thromb. Vasc. Biol.* **2004**, *24* (1), 23–28. https://doi.org/10.1161/01.ATV.0000097769.47306.12.

(34) Ley, K.; Laudanna, C.; Cybulsky, M. I.; Nourshargh, S. Getting to the Site of Inflammation: The Leukocyte Adhesion Cascade Updated. *Nat. Rev. Immunol.* **2007**, *7* (9), 678–689. https://doi.org/10.1038/nri2156.

(35) Jones, D. P.; True, H. D.; Patel, J. Leukocyte Trafficking in Cardiovascular Disease: Insights from Experimental Models. *Mediators Inflamm.* **2017**, *2017*, 1–9. https://doi.org/10.1155/2017/9746169.

(36) Webster, S. J.; Daigneault, M.; Bewley, M. A.; Preston, J. A.; Marriott, H. M.; Walmsley, S. R.; Read, R. C.; Whyte, M. K. B.; Dockrell, D. H. Distinct Cell Death Programs in Monocytes Regulate Innate Responses Following Challenge with Common Causes of Invasive Bacterial Disease. *J. Immunol.* **2010**, *185* (5), 2968–2979. https://doi.org/10.4049/jimmunol.1000805.

(37) Rivas-Arancibia, S; Gallego-Ríos, C.; Gomez-Crisostomo, N.; Ferreira-Garciduenas E., Briseño, D. F.; Navarro, L. and Rodríguez-Martínez, E. Oxidative Stress and Neurodegenerative Disease. In *Neurodegenerative Diseases: Processes, Prevention, Protection and Monitoring*; Chuen-Chung Chang, R., Ed.; **2011**, 53–88.

(38) Giles, G. I.; Jacob, C. Reactive Sulfur Species: An Emerging Concept in Oxidative Stress. *Biol. Chem.* **2005**, *383* (3–4), 375–388. https://doi.org/10.1515/BC.2002.042.

(39) Asmat, U.; Abad, K.; Ismail, K. Diabetes Mellitus and Oxidative Stress-A Concise Review. *Saudi Pharm. J. SPJ Off. Publ. Saudi Pharm. Soc.* **2016**, *24* (5), 547–553. https://doi.org/10.1016/j.jsps.2015.03.013.

(40) Halliwell, B.; Gutteridge, J. M. C. Oxygen: Boon yet Bane-Introducing Oxygen Toxicity and Reactive Species. In *Free Radicals in Biology and Medicine*; **2015**, 20.

(41) Bienert, G. P.; Schjoerring, J. K.; Jahn, T. P. Membrane Transport of Hydrogen Peroxide. *Biochim. Biophys. Acta. Biomembr.* **2006**, *1758* (8), 994–1003. https://doi.org/10.1016/j.bbamem.2006.02.015.

(42) Finkel, T. Oxidant Signals and Oxidative Stress. *Curr. Opin. Cell Biol.* **2003**, *15* (2), 247–254. https://doi.org/10.1016/S0955-0674(03)00002-4.

(43) Smythies, J. The Neurotoxicity of Glutamate, Dopamine, Iron and Reactive Oxygen Species: Functional Interrelationships in Health and Disease: A Review — Discussion. *Neurotox. Res.* **1999**, *1* (1), 27–39. https://doi.org/10.1007/bf03033337.

(44) Stone, J. R.; and Yang, S. Hydrogen Peroxide: A Signaling Messenger. *Antioxid. Redox Signal.* **2006**, *8* (3–4), 243–270. https://doi.org/10.1089/ars.2006.8.243.

(45) Darley-usmar, V.; White, R. Physiological Society Symposium : Impaired Endothelial and Smooth Muscle Cell Function in Oxidative Stress Reaction of Nitric Oxide With Superoxide : *Exp. Physiol.* **1997**, *13*, 305–316.

(46) Halliwell, B.; Whiteman, M. Measuring Reactive Species and Oxidative Damage in Vivo and in Cell Culture: How Should You Do It and What Do the Results Mean? *Br. J. Pharmacol.* **2004**, *142* (2), 231–255. https://doi.org/10.1038/sj.bjp.0705776.

(47) Reuter, S.; Gupta, S. C.; Chaturvedi, M. M.; Aggarwal, B. B. Oxidative Stress, Inflammation, and Cancer: How Are They Linked? *Free Radic. Biol. Med.* **2010**, *49* (11), 1603–1616. https://doi.org/10.1016/j.freeradbiomed.2010.09.006.

(48) Schulz, J. B.; Lindenau, J.; Seyfried, J. . D. J. Glutathione, Oxidative Stress and Neurodegeneration. *Eur J Biochem.* **2000**, *267* (16), 4904–4911.

(49) Rains, J. L.; Jain, S. K. Oxidative Stress, Insulin Signaling, and Diabetes. *Free Radic. Biol. Med.* **2011**, *50* (5), 567–575. https://doi.org/10.1016/j.freeradbiomed.2010.12.006.

(50) Kirkham, P. A.; Caramori, G.; Casolari, P.; Papi, A. A.; Edwards, M.; Shamji, B.; Triantaphyllopoulos, K.; Hussain, F.; Pinart, M.; Khan, Y.; Heinemann, L.; Stevens, L.; Yeadon, M.; Barnes, P. J.; Chung, K. F.; Adcock, I. M. Oxidative Stress-Induced Antibodies to Carbonyl-Modified Protein Correlate with Severity of Chronic Obstructive Pulmonary Disease. *Am. J. Respir. Crit. Care Med.* **2011**, *184* (7), 796–802. https://doi.org/10.1164/rccm.201010-1605OC.

(51) Badran, M.; Ayas, N.; Laher, I. Cardiovascular Complications of Sleep Apnea: Role of Oxidative Stress. *Oxid. Med. Cell. Longev.* **2014**, *2014*, 1–10. https://doi.org/10.1155/2014/985258.

(52) Halliwell, B. Oxidative Stress and Neurodegeneration: Where Are We Now? *J. Neurochem.* **2006**, *97* (6), 1634–1658. https://doi.org/10.1111/j.1471-4159.2006.03907.x.

(53) Andersen, J. K. Oxidative Stress in Neurodegeneration: Cause or Consequence? *Nat Med* **2004**, *10*, S18-25. https://doi.org/10.1038/nrn1434.

(54) Ali Qureshi, G.; Hasan Parvez, S. Oxidative Stress and Neurodegenerative Disorders. In *Oxidative Stress and Neurodegenerative Disorders*; **2007**, *1–31*, 1–757. https://doi.org/10.1016/B978-0-444-52809-4.X5140-0.

(55) Gomes, A.; Fernandes, E.; Silva, A. M. S.; Santos, C. M. M.; Pinto, D. C. G. A.; Cavaleiro, J. A. S.; Lima, J. L. F. C. 2-Styrylchromones: Novel Strong Scavengers of Reactive Oxygen and Nitrogen Species. *Bioorg. Med. Chem.* **2007**, *15* (18), 6027–6036. https://doi.org/10.1016/j.bmc.2007.06.046.

(56) Birben, E.; Sahiner, U. M.; Sackesen, C.; Erzurum, S.; Kalayci, O. Oxidative Stress and Antioxidant Defense. *World Allergy Organ. J.* **2012**, *5* (1), 9–19. https://doi.org/10.1097/WOX.0b013e3182439613.

(57) McCord, J. M.; Fridovich, I. The Utility of Superoxide Dismutase in Studying Free Radical Reactions. I. Radicals Generated by the Interaction of Sulfite, Dimethyl Sulfoxide, and Oxygen. *J. Biol. Chem.* **1969**, *244* (22), 6056–6063. https://doi.org/10.1016/S0021-9258(18)63505-7.

(58) Freitas, M.; Lima, J. L. F. C.; Fernandes, E. Optical Probes for Detection and Quantification of Neutrophils' Oxidative Burst. A Review. *Anal. Chim. Acta* **2009**, *649* (1), 8–23. https://doi.org/10.1016/j.aca.2009.06.063.

(59) Grisham, M. B.; Jourd'heuil, D.; Wink, D. A. I. Physiological Chemistry of Nitric Oxide and Its Metabolites: Implications in Inflammation. *Am. J. Physiol. Gastrointest. Liver Physiol.* **1999**, *276* (2 39-2), 315–321. https://doi.org/10.1152/ajpgi.1999.276.2.g315.

(60) Valko, M.; Leibfritz, D.; Moncol, J.; Cronin, M. T. D.; Mazur, M.; Telser, J. Free Radicals and Antioxidants in Normal Physiological Functions and Human Disease. *Int. J. Biochem. Cell Biol.* **2007**, *39* (1), 44–84. https://doi.org/10.1016/j.biocel.2006.07.001.

(61) Zhao, X.; Carnevale, K. A.; Cathcart, M. K. Human Monocytes Use Rac1, Not Rac2, in the NADPH Oxidase Complex*. *J. Biol. Chem.* **2003**, *278* (42), 40788–40792. https://doi.org/https://doi.org/10.1074/jbc.M302208200.

(62) Dinarello, C. A. Anti-Inflammatory Agents: Present and Future. *Cell* **2010**, *140* (6), 935–950. https://doi.org/10.1016/j.cell.2010.02.043.

(63) Rainsford, K. D. Anti-Inflammatory Drugs in the 21st Century. In *Inflammation in the Pathogenesis of Chronic Diseases: The COX-2 Controversy*; Harris, R. E., Bittman, R., Dasgupta, D., Engelhardt, H., Flohe, L., Herrmann, H., Holzenburg, A., Nasheuer, H.-P., Rottem, S., Wyss, M., Zwickl, P., Eds.; Springer Netherlands: Dordrecht, **2007**, 3–27. https://doi.org/10.1007/1-4020-5688-5_1.

(64) Andrianova, N. V.; Zorov, D. B.; Plotnikov, E. Y. Targeting Inflammation and Oxidative Stress as a Therapy for Ischemic Kidney Injury. *Biochem.* **2020**, *85* (12–13), 1591–1602. https://doi.org/10.1134/S0006297920120111.

(65) Jean, T.; Bodinier, M. C. Mediators Involved in Inflammation: Effects of Daflon 500 Mg on Their Release. *Angiology.* **1994**, *45*, 554–559.

(66) Scalbert, A.; Manach, C.; Morand, C.; Rémésy, C.; Jiménez, L. Dietary Polyphenols and the Prevention of Diseases. *Crit. Rev. Food Sci. Nutr.* **2005**, *45* (4), 287–306. https://doi.org/10.1080/1040869059096.

(67) Spencer, J. P. E.; Abd El Mohsen, M. M.; Minihane, A. M.; Mathers, J. C. Biomarkers of the Intake of Dietary Polyphenols: Strengths, Limitations and Application in Nutrition Research. *Br. J. Nutr.* **2008**, *99* (1), 12–22. https://doi.org/10.1017/S0007114507798938.

(68) Kim, Y. S.; Young, M. R.; Bobe, G.; Colburn, N. H.; Milner, J. A. Bioactive Food Components, Inflammatory Targets, and Cancer Prevention. *Cancer Prev. Res.* **2009**, *2* (3), 200–208. https://doi.org/10.1158/1940-6207.CAPR-08-0141.

(69) Keri, R. S.; Budagumpi, S.; Pai, R. K.; Balakrishna, R. G. Chromones as a Privileged Scaffold in Drug Discovery: A Review. *Eur. J. Med. Chem.* **2014**, *78*, 340–374. https://doi.org/10.1016/j.ejmech.2014.03.047.

(70) Gaspar, A.; Matos, M. J.; Garrido, J.; Uriarte, E.; Borges, F. Chromone: A Valid Scaffold in Medicinal Chemistry. *Chem. Rev.* **2014**, *114* (9), 4960–4992. https://doi.org/10.1021/cr400265z.

(71) Sharma, S. K.; Kumar, S.; Chand, K.; Kathuria, A.; Gupta, A.; Jain, R. An Update on Natural Occurrence and Biological Activity of Chromones. *Curr. Med. Chem.* **2011**, *18* (25), 3825–3852. https://doi.org/10.2174/092986711803414359.

(72) Pawar, S. P.; Kondhare, D. D.; Zubaidha, P. K. Synthesis and Evaluation of Antioxidant Activity of 2-Styrylchromones. *Med. Chem. Res.* **2013**, *22* (2), 753–757. https://doi.org/10.1007/s00044-012-0069-z.

(73) Rocha-Pereira, J.; Cunha, R.; Pinto, D. C. G. A.; Silva, A. M. S.; Nascimento, M. S. J. (E)-2-Styrylchromones as Potential Anti-Norovirus Agents. *Bioorg. Med. Chem.* **2010**, *18* (12), 4195–4201. https://doi.org/10.1016/j.bmc.2010.05.006.

(74) Martens, S.; Mithöfer, A. Flavones and Flavone Synthases. *Phytochemistry* **2005**, *66* (20), 2399–2407. https://doi.org/10.1016/j.phytochem.2005.07.013.

(75) Lin, C.; Lu, P. J.; Yang, C. N.; Hulme, C.; Shaw, A. Y. Structure-Activity Relationship Study of Growth Inhibitory 2-Styrylchromones against Carcinoma Cells. *Med. Chem. Res.* **2013**, *22* (5), 2385–2394. https://doi.org/10.1007/s00044-012-0232-6.

(76) Gomes, A.; Neuwirth, O.; Freitas, M.; Couto, D.; Ribeiro, D.; Figueiredo, A. G. P. R.; Silva, A. M. S.; Seixas, R. S. G. R.; Pinto, D. C. G. A.; Tomé, A. C.; Cavaleiro, J. A. S.; Fernandes, E.; Lima, J. L. F. C. Synthesis and Antioxidant Properties of New Chromone Derivatives. *Bioorg. Med. Chem.* **2009**, *17* (20), 7218–7226. https://doi.org/10.1016/j.bmc.2009.08.056.

(77) Simon, L. In Vitro Cytotoxicity and Antioxidant Evaluation of 7-Amino-2-Styrylchromone Derivatives. *Asian J. Pharm. Clin. Res.* **2017**, *10* (11), 152–156. https://doi.org/10.22159/ajpcr.2017.v10i11.20587.

(78) Sousa, J. L. C.; Proença, C.; Freitas, M.; Fernandes, E.; Silva, A. M. S. New Polyhydroxylated Flavon-3-ols and 3-Hydroxy-2-Styrylchromones: Synthesis and ROS/RNS Scavenging Activities. *Eur. J. Med. Chem.* **2016**, *119*, 250–259. https://doi.org/10.1016/j.ejmech.2016.04.057.

(79) Fernandes, E.; Carvalho, M.; Carvalho, F.; Silva, A. M. S.; Santos, C. M. M.; Pinto, D. C. G. A.; Cavaleiro, J. A. S.; Maria, D. L. B. Hepatoprotective Activity of Polyhydroxylated 2-Styrylchromones against Tert-Butylhydroperoxide Induced Toxicity in Freshly Isolated Rat Hepatocytes. *Arch. Toxicol.* **2003**, *77* (9), 500–505. https://doi.org/10.1007/s00204-003-0480-9.

(80) Filipe, P.; Silva, A. M. S.; Morlière, P.; Brito, C. M.; Patterson, L. K.; Hug, G. L.; Silva, J. N.; Cavaleiro, J. A. S.; Mazière, J. C.; Freitas, J. P.; Santus, R. Polyhydroxylated 2-Styrylchromones as Potent Antioxidants. *Biochem. Pharmacol.* **2004**, *67* (12), 2207–2218. https://doi.org/10.1016/j.bcp.2004.02.030.

(81) Gomes, A.; Capela, J.; Ribeiro, D.; Freitas, M.; Silva, A.; Pinto, D.; Santos, C.; Cavaleiro, J.; Lima, J.; Fernandes, E. Inhibition of NF-KB Activation and Cytokines Production in THP-1 Monocytes by 2-Styrylchromones. *Med. Chem.* **2015**, *11* (6), 560–566. https://doi.org/10.2174/1573406411666150209114702.

(82) Jung, H. J.; Jung, H. A.; Min, B. S.; Choi, J. S. Anticholinesterase and β-Site Amyloid Precursor Protein Cleaving Enzyme 1 Inhibitory Compounds from the Heartwood of Juniperus Chinensis. *Chem. Pharm. Bull.* **2015**, *63* (11), 955–960. https://doi.org/10.1248/cpb.c15-00504.

(83) Ono, M.; Maya, Y.; Haratake, M.; Nakayama, M. Synthesis and Characterization of Styrylchromone Derivatives as β-Amyloid Imaging Agents. *Bioorg. Med. Chem.* **2007**, *15* (1), 444–450. https://doi.org/10.1016/j.bmc.2006.09.044.

(84) Yoon, J. S.; Lee, M. K.; Sung, S. H.; Kim, Y. C. Neuroprotective 2-(2-Phenylethyl)Chromones of Imperata Cylindrica. *J. Nat. Prod.* **2006**, *69* (2), 290–291. https://doi.org/10.1021/np0503808.

(85) Chaniad, P.; Wattanapiromsakul, C.; Pianwanit, S.; Tewtrakul, S. Anti-HIV-1 Integrase Compounds from Dioscorea Bulbifera and Molecular Docking Study. *Pharm. Biol.* **2016**, *54* (6), 1077–1085. https://doi.org/10.3109/13880209.2015.1103272.

(86) Wu, J. H.; Wang, X. H.; Yi, Y. H.; Lee, K. H. Anti-AIDS Agents 54. A Potent Anti-HIV Chalcone and Flavonoids from Genus Desmos. *Bioorg. Med. Chem. Lett.* **2003**, *13* (10), 1813–1815. https://doi.org/10.1016/S0960-894X(03)00197-5.

(87) Desideri, N.; Conti, C.; Mastromarino, P.; Mastropaolo, F. Synthesis and Anti-Rhinovirus Activity of 2-Styrylchromones. *Antivir. Chem. Chemother.* **2000**, *11* (6), 373–381. https://doi.org/10.1177/095632020001100604.

(88) Conti, C.; Mastromarino, P.; Goldoni, P.; Portalone, G.; Desideri, N. Synthesis and Anti-Rhinovirus Properties of Fluoro-Substituted Flavonoids. *Antivir. Chem. Chemother.* **2005**, *16* (4), 267–276. https://doi.org/10.1177/095632020501600406.

(89) Desideri, N.; Mastromarino, P.; Conti, C. Synthesis and Evaluation of Antirhinovirus Activity of 3-Hydroxy and 3-Methoxy 2-Styrylchromones. *Antivir. Chem. Chemother.* **2003**, *14* (4), 195–203. https://doi.org/10.1177/095632020301400404.

(90) Shaw, A. Y.; Chang, C. Y.; Liau, H. H.; Lu, P. J.; Chen, H. L.; Yang, C. N.; Li, H. Y. Synthesis of 2-Styrylchromones as a Novel Class of Antiproliferative Agents Targeting Carcinoma Cells. *Eur. J. Med. Chem.* **2009**, *44* (6), 2552–2562. https://doi.org/10.1016/j.ejmech.2009.01.034.

(91) Marinho, J.; Pedro, M.; Pinto, D. C. G. A.; Silva, A. M. S.; Cavaleiro, J. A. S.; Sunkel, C. E.; Nascimento, M. S. J. 4′-Methoxy-2-Styrylchromone a Novel Microtubule-Stabilizing Antimitotic Agent. *Biochem. Pharmacol.* **2008**, *75* (4), 826–835. https://doi.org/10.1016/j.bcp.2007.10.014.

(92) Peixoto, F.; Barros, A. I. R. N. A.; Silva, A. M. S. Interactions of a New 2-Styrylchromone with Mitochondrial Oxidative Phosphorylation. *J. Biochem. Mol. Toxicol.* **2002**, *16* (5), 220–226. https://doi.org/10.1002/jbt.10042.

(93) Momoi, K.; Sugita, Y.; Ishihara, M.; Satoh, K.; Kikuchi, H.; Hashimoto, K.; Yokoe, I.; Nishikawa, H.; Fijisawa, S.; Sakagami, H. Cytotoxic Activity of Styrylchromones against Human Tumor Cell Lines. *In Vivo (Brooklyn).* **2005**, *19* (1), 157–164. PMID: 15796168.

(94) Doria, G.; Romeo, C.; Forgione, A.; Sberze, P.; Tibolla, N.; Corno, M. L.; Cruzzola, G.; Cadelli, G. Antiallergic Agents. III: Substituted Trans-2-Ethenyl-4-Oxo-4H-1-Benzopyran-6-Carboxylic Acids. *Eur. J. Med. Chem.* **1979**, *14* (4), 347–351.

(95) Santos, C. M. M.; Silva, A. M. S. An Overview of 2-Styrylchromones: Natural Occurrence, Synthesis, Reactivity and Biological Properties. *Eur. J. Org. Chem.* **2017**, *2017* (22), 3115–3133. https://doi.org/10.1002/ejoc.201700003.

(96) Fernandes, E.; Carvalho, F.; Silva, A. M. S.; Santos, C. M. M.; Pinto, D. C. G. A.; Cavaleiro, J. A. S.; Bastos, M. D. L. 2-Styrylchromones as Novel Inhibitors of Xanthine Oxidase. A Structure-Activity Study. *J. Enzyme Inhib. Med. Chem.* **2002**, *17* (1), 45–48. https://doi.org/10.1080/14756360290019944.

(97) Karton, Y.; Jiang, J. L.; Ji, X. D.; Melman, N.; Olah, M. E.; Stiles, G. L.; Jacobson, K. A. Synthesis and Biological Activities of Flavonoid Derivatives as A3 Adenosine Receptor Antagonists. *J. Med. Chem.* **1996**, *39* (12), 2293–2301. https://doi.org/10.1021/jm950923i.

(98) Gerwick, W. H.; Lopez, A.; Van Duyne, G. D.; Clardy, J.; Ortiz, W.; Baez, A. Hormothamnione, a Novel Cytotoxic Styrylchromone from the Marine Cyanophyte Hormothamnion Enteromorphoides Grunow. *Tetrahedron Lett.* **1986**, *27* (18), 1979–1982.

(99) Gerwick, W. H. 6-Desmethoxyhotmothamnione, a New Cytotoxic Styrylchromone from the Marine Cryptophyte Chrysophaeum Taylori. *J. Nat. Prod.* **1989**, *52* (2), 252–256. https://doi.org/10.1021/np50062a005.

(100) Yang, C. H.; Yang, Y.; Liu, J. H. Platachromone A-D: Cytotoxic 2-Styrylchromones from the Bark of Platanus Acerifolia (Aiton) Willd. *Phytochem. Lett.* **2013**, *6* (3), 387–391. https://doi.org/10.1016/j.phytol.2013.05.003.

(101) Hazra, B.; Biswas, S.; Mandal, N. Antioxidant and Free Radical Scavenging Activity of Spondias Pinnata. *BMC Complement. Altern. Med.* **2008**, *8* (1), 63. https://doi.org/10.1186/1472-6882-8-63.

(102) Garratt C, D. *The Quantitative Analysis of Drugs*; Chapman and Hall ltd: Japan; Vol. 3. https://doi.org/10.1111/j.2042-7158.1964.tb07408.x.

(103) Ishak, B. Spectra of Atoms and Molecules (3rd Edition), by Peter F. Bernath. *Contemp. Phys.* **2017**, *58* (2), 201–202. https://doi.org/10.1080/00107514.2017.1291731.

(104) Bland, E. J.; Keshavarz, T.; Bucke, C. To Assess Polysaccharides as Immunomodulating Agents. **2001**, *19*, 125–131. https://doi.org/10.1385/MB:19:2:125.

(105) Costa, D.; Marques, A. P.; Reis, R. L.; Lima, J. L. F. C.; Fernandes, E. Inhibition of Human Neutrophil Oxidative Burst by Pyrazolone Derivatives. *Free Radic. Biol. Med.* **2006**, *40* (4), 632–640. https://doi.org/10.1016/j.freeradbiomed.2005.09.017.

(106) Farah, M. E.; Maia, M.; Penha, F. M.; Rodrigues, E. B. CHAPTER 48 - The Use of Vital Dyes during Vitreoretinal Surgery – Chromovitrectomy. In *Retinal Pharmacotherapy*; Nguyen, Q. D., Rodrigues, E. B., Farah, M. E., Mieler, W. F., Eds.; W.B. Saunders: Edinburgh, **2010**, 331–335. https://doi.org/https://doi.org/10.1016/B978-1-4377-0603-1.00053-3.

(107) Strober, W. Trypan Blue Exclusion Test of Cell Viability. *Curr. Protoc. Immunol.* **1997**, *21* (1), A.3B.1-A.3B.2. https://doi.org/https://doi.org/10.1002/0471142735.ima03bs21.

(108) Vermes, I.; Haanen, C.; Steffens-Nakken, H.; Reutellingsperger, C. A Novel Assay for Apoptosis Flow Cytometric Detection of Phosphatidylserine Expression on Early Apoptotic Cells Using Fluorescein Labelled Annexin V. *J. Immunol. Methods* **1995**, *184* (1), 39–51. https://doi.org/https://doi.org/10.1016/0022-1759(95)00072-I.

(109) Koopman, G.; Reutelingsperger, C. P.; Kuijten, G. A.; Keehnen, R. M.; Pals, S. T.; van Oers, M. H. Annexin V for Flow Cytometric Detection of Phosphatidylserine Expression on B Cells Undergoing Apoptosis. *Blood* **1994**, *84* (5), 1415–1420. PMID: 8068938.

(110) Crowley, L. C.; Marfell, B. J.; Scott, A. P.; Waterhouse, N. J. Quantitation of Apoptosis and Necrosis by Annexin V Binding, Propidium Iodide Uptake, and Flow Cytometry. *Cold Spring Harb. Protoc.* **2016**, *2016* (11), 953–957. https://doi.org/10.1101/pdb.prot087288.

(111) Darzynkiewicz, Z.; Bruno, S.; Del Bino, G.; Gorczyca, W.; Hotz, M. A.; Lassota, P.; Traganos, F. Features of Apoptotic Cells Measured by Flow Cytometry. *Cytometry* **1992**, *13* (8), 795–808. https://doi.org/https://doi.org/10.1002/cyto.990130802.

(112) Freitas, M.; Porto, G.; Lima, J. L. F. C.; Fernandes, E. Isolation and Activation of Human Neutrophils in Vitro. The Importance of the Anticoagulant Used during Blood Collection. *Clin. Biochem.* **2008**, *41* (7–8), 570–575. https://doi.org/10.1016/j.clinbiochem.2007.12.021.

(113) Soares, T.; Ribeiro, D.; Proença, C.; Chisté, R. C.; Fernandes, E.; Freitas, M. Size-Dependent Cytotoxicity of Silver Nanoparticles in Human Neutrophils Assessed by Multiple Analytical Approaches. *Life Sci.* **2016**, *145*, 247–254. https://doi.org/10.1016/j.lfs.2015.12.046.

(114) Ponath, V.; Kaina, B. Death of Monocytes through Oxidative Burst of Macrophages and Neutrophils: Killing in Trans. *PLoS One* **2017**, *12* (1), 1–20. https://doi.org/10.1371/journal.pone.0170347.